Nonlinearity

LONDON MATHEMATICAL SOCIETY EST. 1865

IOP Publishing

PAPER • **OPEN ACCESS**

Monge–Ampère geometry and vortices

To cite this article: Lewis Napper *et al* 2024 *Nonlinearity* **37** 045012

OPEN ACCESS
IOP Publishing | London Mathematical Society Nonlinearity
Nonlinearity **37** (2024) 045012 (55pp) https://doi.org/10.1088/1361-6544/ad2a8b

Monge–Ampère geometry and vortices

Lewis Napper[1], **Ian Roulstone**[1,*], **Vladimir Rubtsov**[2] **and Martin Wolf**[1]

[1] School of Mathematics and Physics, University of Surrey, Guildford GU2 7XH, United Kingdom
[2] University of Angers, CNRS, LAREMA, SFR MATHSTIC, F-49000 Angers, France

E-mail: i.roulstone@surrey.ac.uk, lewis.napper@surrey.ac.uk, volodya@univ-angers.fr and m.wolf@surrey.ac.uk

Received 31 March 2023; revised 19 January 2024
Accepted for publication 19 February 2024
Published 12 March 2024

Recommended by Dr Richard Montgomery

Abstract

We introduce a new approach to Monge–Ampère geometry based on techniques from higher symplectic geometry. Our work is motivated by the application of Monge–Ampère geometry to the Poisson equation for the pressure that arises for incompressible Navier–Stokes flows. Whilst this equation constitutes an elliptic problem for the pressure, it can also be viewed as a non-linear partial differential equation connecting the pressure, the vorticity, and the rate-of-strain. As such, it is a key diagnostic relation in the quest to understand the formation of vortices in turbulent flows. We study this equation via an associated (higher) Lagrangian submanifold in the cotangent bundle to the configuration space of the fluid. Using our definition of a (higher) Monge–Ampère structure, we study an associated metric on the cotangent bundle together with its pull-back to the (higher) Lagrangian submanifold. The signatures of these metrics are dictated by the relationship between vorticity and rate-of-strain, and their scalar curvatures can be interpreted in a physical context in terms of the accumulation of vorticity, strain, and their gradients. We show explicity, in the case of two-dimensional flows, how topological information can be derived from the Monge–Ampère geometry of the Lagrangian submanifold. We also demonstrate how certain solutions to the three-dimensional incompressible Navier–Stokes equations, such as Hill's spherical vortex and an integrable case

* Author to whom any correspondence should be addressed.

of Arnol'd–Beltrami–Childress flow, have symmetries that facilitate a formulation of these solutions from the perspective of (higher) symplectic reduction.

Keywords: Monge–Ampere equations, Navier–Stokes equations, Lagrangian submanifolds, symplectic reduction, (pseudo-) Riemannian geometry, higher symplectic geometry, vortex topology

Mathematics Subject Classification numbers: 76D05, 53B30, 53B35, 53D05, 53D20, 53D12

Contents

1. Introduction 3
   1.1. Organisation of the paper 6
2. Fluid flows and Monge–Ampère geometry 7
   2.1. Incompressible fluid flows 7
      2.1.1. Navier–Stokes equations 7
      2.1.2. Pressure constraint 8
   2.2. Geometric properties of fluids in two dimensions 10
      2.2.1. Monge–Ampère structures 10
      2.2.2. Monge–Ampère geometry of two-dimensional fluid flows 10
      2.2.3. Almost (para-)Hermitian structure 11
      2.2.4. Pull-back metric 12
      2.2.5. Local Gauß–Bonnet theorem 13
      2.2.6. Christoffel symbols and curvatures 13
   2.3. Examples in two dimensions 15
      2.3.1. Preliminaries 15
      2.3.2. Larchevêque's criterion and uniform vorticity and strain 16
      2.3.3. Flow with bifurcations 17
      2.3.4. Legendre duals 18
      2.3.5. Flow with bifurcations and Legendre duality 19
      2.3.6. Taylor–Green vortex 20
3. Geometric properties of fluids in three dimensions 22
   3.1. Two-dimensional case revisited 23
      3.1.1. Monge–Ampère structure 23
      3.1.2. Almost (para-)Hermitian structure 24
   3.2. Higher symplectic manifolds 25
      3.2.1. Higher symplectic vector spaces 25
      3.2.2. Higher symplectic manifolds 26
   3.3. Higher Monge–Ampère geometry of three-dimensional fluid flows 26
      3.3.1. Higher Monge–Ampère structure 26
      3.3.2. Almost (para-)Hermitian structure 27
      3.3.3. Curvature 28
      3.3.4. Pull-back metric 29
      3.3.5. Helicity 29
   3.4. Examples in three dimensions 30
      3.4.1. Preliminaries 30
      3.4.2. Burgers' vortex 30
   3.5. Higher symplectic reductions 31

3.5.1. Setting for dimensional reduction 32
3.5.2. Symplectic reduction of the higher Monge–Ampère structure 34
3.5.3. Higher symplectic reduction of the higher Monge–Ampère structure 35
3.6. Examples of higher symplectic reductions 37
3.6.1. Arnol'd–Beltrami–Childress flow 37
3.6.2. Hicks–Moffatt vortex 39
4. Summary and conclusions 45
Data availability statement 46
Acknowledgments 46
Appendix A. Lagrangian submanifolds 46
Appendix B. Non-degenerate Monge–Ampère structures 48
Appendix C. Connections and curvatures 48
C.1. Pull-back metric in two dimensions 49
C.1.1. Connection 49
C.1.2. Curvature 49
C.2. Phase space curvature 50
C.2.1. Vielbein formalism 50
C.2.2. Connection 51
C.2.3. Curvature 52
References 53

1. Introduction

The anatomy and dynamics of vortices are subjects of fundamental importance in the study of the incompressible Euler and Navier–Stokes equations in two and three dimensions. According to the incompressible Navier–Stokes equations on a three-dimensional Euclidean domain, the evolution of the vorticity, $\boldsymbol{\zeta} := \boldsymbol{\nabla} \times \boldsymbol{v}$, is given by

$$\frac{\mathrm{D}\boldsymbol{\zeta}}{\mathrm{D}t} \;=\; \boldsymbol{\sigma} + \nu\Delta\boldsymbol{\zeta} \quad \text{with} \quad \frac{\mathrm{D}}{\mathrm{D}t} \;:=\; \frac{\partial}{\partial t} + \boldsymbol{v}\cdot\boldsymbol{\nabla}\,, \tag{1.1}$$

where $\boldsymbol{v}$ is the fluid velocity, $\boldsymbol{\sigma} := (\boldsymbol{\zeta}\cdot\boldsymbol{\nabla})\boldsymbol{v}$ is the vortex-stetching vector, Δ is the Laplacian, and ν is the viscosity. The equation for divergence-free flow is

$$\nabla\cdot\boldsymbol{v} \;=\; 0\,. \tag{1.2}$$

When the flow is inviscid, $\nu = 0$, we obtain the Euler equations. In two dimensions, the vortex-stretching vector is identically zero, and the vorticity is a materially conserved scalar field when the flow is inviscid.

The vortex-stretching vector $\boldsymbol{\sigma}$ can be written in terms of the rate-of-strain matrix, S, which is the symmetric part of the velocity-gradient matrix, as follows

$$\boldsymbol{\sigma} \;=\; S\boldsymbol{\zeta}\,. \tag{1.3}$$

The magnitude and direction of vorticity are critical features in studies of turbulent flows in three dimensions. If, for the moment, we focus on inviscid flows in three dimensions, then using (1.1) and the Euler equation relating flow velocity and the pressure gradient

$$\frac{\mathrm{D}\boldsymbol{v}}{\mathrm{D}t} \;=\; -\boldsymbol{\nabla}p\,, \tag{1.4}$$

where p is pressure, it can be shown (see e.g. [1]) that the vortex-stretching vector evolves according to

$$\frac{\mathrm{D}\boldsymbol{\sigma}}{\mathrm{D}t} = -P\boldsymbol{\zeta}\,, \tag{1.5}$$

where P is the Hessian of the pressure. Upon taking the divergence of (1.4) and using (1.2), the rate-of-strain, the vorticity, and the pressure field are related by

$$\mathrm{tr}\,(P) = \Delta p = \frac{1}{2}\zeta^2 - \mathrm{tr}\left(S^2\right)\,. \tag{1.6}$$

This equation holds for the incompressible Euler and Navier–Stokes equations in both two and three dimensions. In the standard literature, (1.6) is recognised as the Poisson equation for the pressure, and depends on time only as a parameter. Consequently, the time evolution of Δp will depend on whether we are considering the Euler or the Navier–Stokes equations.

Equation (1.6) has been employed in studies of the accumulation of vorticity and of the plausible conditions under which such accumulations may be considered to be 'a vortex'. From (1.6) it follows that, when vorticity dominates over strain, then $\Delta p > 0$, and conversely, when strain dominates over vorticity, $\Delta p < 0$. In two dimensions, the vorticity is a scalar field, the rate-of-strain matrix has only two independent components (due to incompressibility) and therefore (1.6) is a useful diagnostic relation involving the velocity gradients and the pressure field, as studied in [2–4]. In three dimensions, although the components of vorticity and strain can interact in more complicated ways to determine the sign of the Laplacian of the pressure, (1.6) has still been widely used in studies that address the enduring question as to what a vortex is; see e.g. [5, 6].

Equation (1.6), or rather its reformulation on an arbitrary Riemannian manifold, is a focal point of this paper. In particular, [2–4] studied this equation in the context of incompressible flows on a two-dimensional Euclidean domain, whereupon the velocity can be expressed in terms of the derivatives of a stream function. Using such a representation of the velocity field, the right-hand side of (1.6) becomes proportional to the determinant of the Hessian of the stream function. Consequently, the Gaußian curvature of the stream function is related to the sign of the Laplacian of pressure. When vorticity dominates over strain, the stream function, viewed as a graph in Euclidean space, has positive Gaußian curvature, and it has negative Gaußian curvature when strain dominates. By introducing the stream function, (1.6) can then be viewed as a non-linear Monge–Ampère equation for this function, assuming Δp is known and time, t, is considered a parameter. When $\Delta p > 0$, this equation is elliptic; conversely, when $\Delta p < 0$, the equation is hyperbolic (we shall return to these points in greater detail later in this paper).

The appearance of a Monge–Ampère equation for two-dimensional incompressible flows led [7] to study this problem from the point of view of the Monge–Ampère geometry of [8]. In this context, one considers a pair of differential two-forms, (ω, α), on T^*M, where M is the configuration space of the fluid, ω is the symplectic form, and α is called the Monge–Ampère form, which encodes (1.6). This pair of forms satisfies a non-degeneracy condition, and such a pair is called a Monge–Ampère structure. With this geometric picture in mind, the conditions for ellipticity and hyperbolicity noted by [2–4] then translate, via the Monge–Ampère structure, into almost (para-)complex structures on T^*M which, in fact, extend to almost quaternionic (para-)Hermitian structures [7, 9].

When incompressible flows in three dimensions are considered in terms of (1.6), the absence of a stream function prohibits a generalisation of the classification of flows in terms

of an elliptic or hyperbolic Monge–Ampère equation [2, 3]. Nevertheless, [10] showed how, on a three-dimensional Euclidean domain, (1.6) can still be described using a suitably-defined Monge–Ampère structure. This construction facilitated a generalisation of the criteria derived by [2–4] to three-dimensional incompressible flows. In this present paper, we shall show how these earlier results can be reformulated and unified by combining the ideas of Monge–Ampère geometry with that of the higher symplectic geometry of [11–13], thereby providing a generalisation of this approach to incompressible flows on arbitrary Riemannian manifolds of arbitrary dimensions.

Concretely, when classifying Monge–Ampère equations in two or three independent variables, [14] introduced a certain Riemannian or Kleinian metric on T^*M, whose signature has been related to the elliptic or hyperbolic nature of the underlying Monge–Ampère equation. In view of this, one makes use of generalised solutions to the Monge–Ampère equation associated with a Monge–Ampère structure (ω, α), which are Lagrangian submanifolds of T^*M on which α vanishes. The notion of a generalised solution to a partial differential equation was first introduced in [15–17] and corresponds to admitting solutions that are multivalued or are not globally defined. In this context, classical (global, single valued) solutions to a Monge–Ampère equation are described precisely by the graphs of differentials of functions. We shall adopt this view of generalised solutions when extending the aforementioned ideas to higher-dimensional incompressible flows. In particular, beginning from a (higher) Monge–Ampère structure, now a specific pair of differential m-forms on T^*M in the m-dimensional case, we construct a metric on T^*M. Moreover, it will be useful to study its pull-back to a certain (higher) Lagrangian submanifold of T^*M, noting that the submanifold is of the same dimension as the configuration space of the fluid.

A physical motivation for considering the pull-back metric is as follows. In [1], it was noted that (1.6) locally holds the key to the formation of vortical structures through the sign of Δp. The equation also plays a role in Navier–Stokes turbulence calculations in which vorticity tends to accumulate on 'thin sets' – quasi-two-dimensional sheets that roll up into one-dimensional tubes [18]. The topology of vortex tubes can become highly complicated, but they are ubiquitous features of turbulent flows and have been dubbed 'the sinews of turbulence' in [19]. Extracting topological information from the underlying partial differential equation of the Navier–Stokes equations is an enduring problem: for a review, see [20]. Using the pull-back metric described above, we demonstrate, explicitly in the case of two-dimensional incompressible flows, that a topological invariant can be associated with the Lagrangian submanifold L defined by (1.6). Since L is two-dimensional in this case, when the pull-back metric is Riemannian we can use the Gauß–Bonnet theorem to calculate an Euler number. We find that the curvature of L is related to the physical properties of the flow in terms of gradients of vorticity and strain.

We go on to show that certain solutions to the three-dimensional Navier–Stokes equations, such as Burgers' vortex, Hill's spherical vortex, and an integrable Arnol'd–Beltrami–Childress flow, possess symmetries that facilitate Hamiltonian reductions to two-dimensional problems. These results extend those presented in [9]; in particular we show how such solutions can be studied from the point of view of the higher symplectic reduction of [21]. As somewhat of an aside for this paper, we note that helicity is described readily using the component parts of the Monge–Ampère geometry developed herein. Further investigations using helicity or other invariants (e.g. Maslov index) to study the topology of three-dimensional flows, within the framework of our Monge–Ampère geometry, is a topic for future research.

1.1. Organisation of the paper

In section 2.1, we present the Navier–Stokes equations in a covariant framework, where the configuration space is an arbitrary Riemannian manifold M. Whilst this introduces some additional structure, the majority of our results are couched in a covariant language and it is therefore consistent to allow for arbitrary background geometries. Furthermore, the Poisson equation for the pressure involves additional curvature terms when written for an arbitrary M.

Focusing on two-dimensional incompressible flows, in section 2.2 we introduce the machinery of Monge–Ampère geometry and Monge–Ampère structures, following the geometric approach as described, for example, by [8]. This allows us to formulate the Monge–Ampère equation arising in the Poisson equation for the pressure, revisiting some of the results of [7]. However, in addition, we describe the role of the metric structure that arises on T^*M, as well as its pull-back to the Lagrangian submanifold L. We then use the pull-back metric on L to show how the Gauß–Bonnet theorem, together with conditions on the projection $L \to M$, enable us to define the Euler number for 'a vortex'.

Examples are then given in section 2.3, in order to illustrate the application of the foregoing theory. These examples include a flow with topological bifurcations and the Taylor–Green vortex in two dimensions. Naturally, it is possible to find solutions to (1.6) that are not solutions to the full dynamical equations. However, our focus for now is to take the view that the geometry developed herein gives us the possibility to characterise the physical features of given solutions, rather than to explore how the Monge–Ampère structure might facilitate the search for new solutions.

In section 3, we move on to consider (1.6) for flows in three dimensions. Concretely, we first revisit, in section 3.1, the two-dimensional case and note that another Monge–Ampère structure can be defined using a different choice of symplectic structure. This choice is characterised by a duality (with respect to the metric on the configuration manifold, M), which in two-dimensions simply provides an alternative formulation to the one used before. However, in three dimensions, the duality leads to a higher Monge–Ampère type structure defined in terms of a pair of differential three-forms, and this naturally encodes an equation such as (1.6), even though there is no longer an underlying Monge–Ampère equation in a single dependent variable. In section 3.2, we introduce the relevant concepts from higher symplectic geometry, in which the symplectic form is superseded by a closed, non-degenerate differential form of degree higher than two.

In section 3.3, we explicitly set out the Monge–Ampère geometry of three-dimensional flow, thereby extending the results of [9]. We explain how the curvature of L can be related, once again, to gradients of vorticity and strain. However, because the higher Lagrangian submanifold is now three-dimensional, we can no longer use the Gauß–Bonnet theorem to quantify the topology of vortices. Instead, we remark that helicity, a much-studied invariant of incompressible flows in three dimensions, can be formulated in terms of the geometric objects we have introduced. In principle, the resulting formulation can be applied to the Navier–Stokes equations in arbitrary dimensions.

We then illustrate the foregoing theory with examples in section 3.4. We begin by writing out the form of the pull-back metric in terms of vorticity and rate-of-strain, via the velocity gradient matrix, and then discuss an example based on Burgers' vortex. This canonical model of a vortex tube has been studied from the point-of-view of Monge–Ampère geometry in [9], where symplectic reduction was employed to illuminate the symmetry of the model, which is characterised physically by uniformity along the axis of rotation.

Inspired by this approach to solutions to the three-dimensional Navier–Stokes equations with symmetry, we introduce, in section 3.5, a higher symplectic reduction of the phase space

and apply this to an integrable example of the Arnol'd–Beltrami–Childress flows, and to Hill's spherical vortex (a special case of the Hicks–Moffatt vortex), in section 3.6.

Finally, in section 4, we summarise and draw conclusions.

2. Fluid flows and Monge–Ampère geometry

2.1. Incompressible fluid flows

To set the stage, let us summarise some facts about incompressible fluid flows. We shall be somewhat more general in that we allow the domain of the fluid flow to be a Riemannian manifold. This is because the equation (1.6) for the Laplacian of the pressure will be modified by a term depending on the Ricci curvature tensor of the underlying domain.

2.1.1. Navier–Stokes equations. Consider an m-dimensional oriented Riemannian manifold[3] M with metric $\mathring{g}$. Let 'd' be the exterior derivative on M and '$\star_{\mathring{g}}$' be the Hodge star with respect to the metric $\mathring{g}$. Furthermore, let the codifferential acting on differential p-forms $\Omega^p(M)$ and the Hodge Laplacian be given by

$$\mathring{\delta} \;:=\; (-1)^{m(p-1)+1}\star_{\mathring{g}}\mathrm{d}\star_{\mathring{g}} \quad\text{and}\quad \mathring{\Delta}_{\mathrm{H}} \;:=\; \mathring{\delta}\mathrm{d}+\mathrm{d}\mathring{\delta}\,, \tag{2.1}$$

respectively. Set

$$|\rho|^2 \;:=\; \frac{\rho\wedge\star_{\mathring{g}}\rho}{\mathrm{vol}_M} \tag{2.2}$$

for all $\rho\in\Omega^p(M)$, with 'vol_M' the volume form on M induced by $\mathring{g}$.

In the following, M is taken to be the domain of the fluid flow in which we are interested, and the fluid flow is described by a one-parameter family of differential one-forms $v\in\Omega^1(M)$ on M, parametrised by $t\in\mathbb{R}$, known as the velocity (co-)vector field. The incompressible Navier–Stokes equations is a system consisting of a flow equation for v,

$$\frac{\partial v}{\partial t} \;=\; -(-1)^m\star_{\mathring{g}}(v\wedge\star_{\mathring{g}}\mathrm{d}v)-\frac{1}{2}\mathrm{d}|v|^2-\mathrm{d}p-\nu\mathring{\Delta}_{\mathrm{H}}v\,, \tag{2.3a}$$

together with the divergence-free constraint

$$\mathring{\delta}v \;=\; 0\,. \tag{2.3b}$$

Here, $p\in\mathscr{C}^\infty(M)$ is known as the pressure field and $\nu\in\mathbb{R}$ as the viscosity, respectively.

If we coordinatise M by x^i for $i,j,\ldots=1,\ldots,m$, then, with $v=v_i\mathrm{d}x^i$ and $v_i=v_i(t,x^1,\ldots,x^m)$, the equations (2.3*a*) become

$$\frac{\partial v^i}{\partial t} \;=\; -v^j\mathring{\nabla}_j v^i-\partial^i p+\nu\left(\mathring{\Delta}_{\mathrm{B}}v^i-\mathring{R}^{ij}v_j\right) \tag{2.4a}$$

and

$$\mathring{\nabla}_i v^i \;=\; 0\,, \tag{2.4b}$$

[3] We shall always assume that our manifolds are equipped with a good cover, by which we mean a covering by open and contractible sets. Likewise, we shall always work in the induced topologies.

where $\mathring{\nabla}_i$ is the Levi–Civita connection for the metric $\mathring{g}_{ij}$ with Christoffel symbols denoted by $\mathring{\Gamma}_{ij}{}^k$. Furthermore, the components of the associated Ricci tensor and Riemann curvature tensor are given by

$$\mathring{R}_{ij} := \mathring{R}_{kij}{}^k \quad \text{and} \quad \mathring{R}_{ijk}{}^l := \partial_i \mathring{\Gamma}_{jk}{}^l - \partial_j \mathring{\Gamma}_{ik}{}^l - \mathring{\Gamma}_{ik}{}^m \mathring{\Gamma}_{jm}{}^l + \mathring{\Gamma}_{jk}{}^m \mathring{\Gamma}_{im}{}^l , \tag{2.5}$$

respectively. Letting $\mathring{g}^{ij}$ be the inverse of $\mathring{g}_{ij}$, the Beltrami Laplacian is given by

$$\mathring{\Delta}_{\mathrm{B}} := \mathring{g}^{ij} \mathring{\nabla}_i \mathring{\nabla}_j = \mathring{\nabla}^i \mathring{\nabla}_i . \tag{2.6}$$

Indices are raised and lowered using $\mathring{g}^{ij}$ and $\mathring{g}_{ij}$ respectively and we always use Einstein's summation convention. In deriving (2.4*a*), we have used the standard Weitzenböck formula

$$(\mathring{\Delta}_{\mathrm{H}} \rho)_{i_1 \cdots i_p} = -\mathring{\Delta}_{\mathrm{B}} \rho_{i_1 \cdots i_p} + p \mathring{R}_{j[i_1} \rho^j{}_{i_2 \cdots i_p]} + \frac{1}{2} p(p-1) \mathring{R}_{jk[i_1 i_2} \rho^{jk}{}_{i_3 \cdots i_p]} \tag{2.7}$$

for a differential p-form $\rho = \frac{1}{p!} \rho_{i_1 \cdots i_p} \mathrm{d}x^{i_1} \wedge \ldots \wedge \mathrm{d}x^{i_p}$ on M that relates (2.1) and (2.6). Here and in the following, parentheses (respectively, square brackets) denote normalised symmetrisation (respectively, anti-symmetrisation) of the enclosed indices.

Evidently, when M is $\mathbb{R}^m$ with the standard Euclidean metric $\delta_{ij} = 1$ for $i = j$ and zero otherwise, the equations (2.4*a*) reduce to the more familiar equations

$$\frac{\partial v^i}{\partial t} = -v^j \partial_j v^i - \partial^i p + \nu \Delta v^i \tag{2.8a}$$

and

$$\partial_i v^i = 0 , \tag{2.8b}$$

where now $\Delta := \partial^i \partial_i$ is the standard Euclidean Laplacian.

2.1.2. Pressure constraint. Upon applying the codifferential to (2.3*a*) and using the divergence-free constraint (2.3*b*), we obtain the so-called pressure equation

$$\mathring{\Delta}_{\mathrm{H}} p = -|\mathrm{d}v|^2 + \star_{\mathring{g}} \left(v \wedge \star_{\mathring{g}} \mathring{\Delta}_{\mathrm{H}} v \right) - \frac{1}{2} \mathring{\Delta}_{\mathrm{H}} |v|^2 . \tag{2.9}$$

In local coordinates, this becomes

$$\mathring{\Delta}_{\mathrm{B}} p = -\left(\mathring{\nabla}_i v_j \right) \left(\mathring{\nabla}^j v^i \right) - v^i v^j \mathring{R}_{ij} , \tag{2.10}$$

where we have again used the Weitzenböck formula (2.7).

Upon setting

$$\zeta_{ij} := \mathring{\nabla}_{[i} v_{j]} = \partial_{[i} v_{j]} \quad \text{and} \quad S_{ij} := \mathring{\nabla}_{(i} v_{j)} , \tag{2.11}$$

which are called the vorticity two-form and the rate-of-strain tensor, respectively, the pressure equation (2.10) can be written in a more standard form as

$$\mathring{\Delta}_{\mathrm{B}} p = \zeta_{ij} \zeta^{ij} - S_{ij} S^{ij} - v^i v^j \mathring{R}_{ij} . \tag{2.12}$$

By definition, the rate-of-strain tensor vanishes if any only if the velocity vector field is a Killing vector field.

Furthermore, because of the Poincaré lemma, on an open and contractible[4] set $U \subseteq M$, the divergence-free constraint (2.3*b*) can always be solved as

$$v = \star_{\mathring{g}} \mathrm{d}\psi \quad \text{for} \quad \psi \in \Omega^{m-2}(U) \quad \Longleftrightarrow \quad v^i = \frac{\sqrt{\det(\mathring{g})}}{(m-2)!} \varepsilon^{i_1 \cdots i_{m-1} i} \partial_{i_1} \psi_{i_2 \cdots i_{m-1}} \,, \tag{2.13}$$

where $\varepsilon_{i_1 \cdots i_m}$ is the Levi-Civita symbol with $\varepsilon_{1 \cdots m} = 1$; note that $\varepsilon^{1 \cdots m} = \frac{1}{\det(\mathring{g})} \varepsilon_{1 \cdots m}$. Upon substituting this expression into (2.10), we obtain a Monge–Ampère-type equation for ψ. For $m = 2$, ψ is known as the stream function, and we obtain a Monge–Ampère equation in a familiar setting. Generally, we may refer to $\psi \in \Omega^{m-2}(U)$ as the stream $(m-2)$-form.

Remark 2.1. The viscosity term in the Navier–Stokes equations (2.3*a*) may be modified as

$$\frac{\partial v}{\partial t} = -(-1)^m \star_{\mathring{g}} (v \wedge \star_{\mathring{g}} \mathrm{d}v) - \frac{1}{2} \mathrm{d}|v|^2 - \mathrm{d}p - \nu \left[\mathring{\Delta}_{\mathrm{H}} v + c \, \mathring{\mathsf{Ric}}(v) \right] \,, \tag{2.14}$$

where $c \in \mathbb{R}$ and $\mathring{\mathsf{Ric}}(\rho) := \mathring{R}_i{}^j \rho_j \mathrm{d}x^i$ for any $\rho \in \Omega^1(M)$. Evidently, in the flat case, the extra term vanishes and this modified equation again reduces to the standard equation (2.8*a*). The coordinate version (2.4*a*) then becomes

$$\frac{\partial v^i}{\partial t} = -v^j \mathring{\nabla}_j v^i - \partial^i p + \nu \left[\mathring{\Delta}_{\mathrm{B}} v^i - (c+1) \mathring{R}^{ij} v_j \right] \,. \tag{2.15}$$

When $c = 0$, we return to the situation given by (2.3*a*), and this version of the Navier–Stokes equations was perhaps first studied in the seminal work [22] and more recently in e.g. [23, 24]. The case $c = -1$ was discussed in e.g. [25] and the case $c = -2$ in e.g. [22, 26, 27] and the references therein. For instance, under the assumption of the divergence-free constraint (2.4*b*), when $c = -2$ and with S_{ij} the rate-of-strain tensor (2.11), it can straightforwardly be seen that the viscosity term can be rewritten as

$$\mathring{\Delta}_{\mathrm{B}} v^i + \mathring{R}^{ij} v_j = 2 \mathring{\nabla}_j S^{ij} \,. \tag{2.16}$$

Hence, in this case, for velocity fields that preserve the metric (i.e. that are Killing), the viscosity term drops out from the Navier–Stokes equations. Generally, with the c-term switched on, the pressure equation (2.10) takes the form

$$\mathring{\Delta}_{\mathrm{B}} p = -\left(\mathring{\nabla}_i v_j \right) \left(\mathring{\nabla}^j v^i \right) - v^i v^j \mathring{R}_{ij} - \nu c \left(\mathring{R}_{ij} S^{ij} + \frac{1}{2} v^i \partial_i \mathring{R} \right) \,, \tag{2.17}$$

where $\mathring{R} := \mathring{g}^{ij} \mathring{R}_{ij}$ is the curvature scalar and we have used the well-known identity

$$\mathring{\nabla}^i \left(\mathring{R}_{ij} - \frac{1}{2} \mathring{g}_{ij} \mathring{R} \right) = 0 \,. \tag{2.18}$$

Henceforth, we shall always assume that $c = 0$. Our results and conclusions remain unchanged, and all of the formulæ can easily be adjusted to accommodate the c-term.

[4] In the following, we declare a neighbourhood (of a point) to be an open and contractible set.

2.2. Geometric properties of fluids in two dimensions

One of the enduring challenges of fluid mechanics is to understand the topology of vortices. However, no systematic method has been developed to extract topological information from the partial differential equations governing the flow. To this end, we now make some observations about how Monge–Ampère geometry might provide new insights by focusing on incompressible flows in two spatial dimensions. We start off by recalling some of the key aspects of Monge–Ampère geometry. See also appendix B. We shall be rather brief and only list the relevant material for our discussion, and we refer the interested reader to the text book [8] for more details.

2.2.1. Monge–Ampère structures. Let us consider the cotangent bundle $\pi : T^*M \to M$ of an m-dimensional manifold M, which we coordinatise by (x^i, q_i) with x^i local coordinates on M as before and q_i local fibre coordinates. Then, T^*M comes with a canonical symplectic structure ω which in local coordinates is $\omega = \mathrm{d}q_i \wedge \mathrm{d}x^i$. Following [14] (see also [28]) a differential m-form $\alpha \in \Omega^m(T^*M)$ is called ω-effective whenever $\omega \wedge \alpha = 0$. Furthermore, the pair (ω, α), with α an ω-effective m-form, will be called a Monge–Ampère structure [29]. In this context, we shall refer to α as the Monge–Ampère form. We draw attention to the purpose of the requirement that the Monge–Ampère form α is ω-effective. This constraint removes redundancy that would occur if α were an arbitrary differential m-form, two of which produce the same Monge–Ampère equation if and only if their difference is a differential form which is not ω-effective [14, 28]. Theorem B.1 then tells us that the ω-effective piece of a differential m-form uniquely determines the Monge–Ampère equation.

A generalised solution for a Monge–Ampère structure (ω, α) is a Lagrangian submanifold $\iota : L \hookrightarrow T^*M$ with respect to ω, that is, $\iota^*\omega = 0$ and $\dim(L) = \dim(M)$, for which, in addition, we have $\iota^*\alpha = 0$. In particular, the section $\mathrm{d}\psi : M \to T^*M$ associated with the function $\psi \in \mathscr{C}^\infty(M)$ and locally given by $x^i \mapsto (x^i, q_i) = (x^i, \partial_i\psi)$ defines a Lagrangian submanifold $L_M := \mathrm{d}\psi(M)$. Additionally, the requirement that a generalised solution satisfies $\iota^*\alpha = 0$ then reads $(\mathrm{d}\psi)^*\alpha = 0$, which in turn yields a Monge–Ampère equation for ψ. In this case, the functions $\psi \in \mathscr{C}^\infty(M)$ satisfying the Monge–Ampère equation and the corresponding generalised solutions described by $\mathrm{d}\psi$ are both referred to as classical solutions. We shall call Monge–Ampère structures (ω, α) and (ω, α') symplectically equivalent whenever there is a symplectomorphism $\Phi \in \mathscr{C}^\infty(T^*M)$ such that $\alpha' = \Phi^*\alpha$.

Moreover, as explained in appendix A, a Lagrangian submanifold L is locally a section $\mathrm{d}\psi : U \to T^*M$ for some $\psi \in \mathscr{C}^\infty(U)$ and $U \subseteq M$ open and contractible if and only if the map $\pi|_L := \pi \circ \iota : L \to M$ is a local diffeomorphism. In this case, we may take x^i as local coordinates on L and we have $\iota : x^i \mapsto (x^i, q_i) = (x^i, \partial_i\psi)$. However, an arbitrary generalised solution may exhibit singular behaviour where the projection $\pi|_L$ fails to be an immersion [30–32] and L is not locally described by the coordinates x^i. Recent work [33] studying the semi-geostrophic equations has shown that such projection singularities may be related to the degeneracy of a specific metric on L. In order to isolate behaviour of L which is due to the variation of vorticity and strain, hereafter we predominantly consider solutions which are (locally) described by a section.

2.2.2. Monge–Ampère geometry of two-dimensional fluid flows. Let us now specialise to incompressible fluid flows in $m = 2$ dimensions. In this case, the components (2.5) of the Ricci and Riemann curvature tensors simplify to

$$\mathring{R}_{ij} \;=\; \frac{\mathring{R}}{2}\mathring{g}_{ij} \quad \text{and} \quad \mathring{R}_{ijk}{}^{l} \;=\; \mathring{R}\mathring{g}_{k[j}\delta_{i]}{}^{l} \tag{2.19}$$

respectively, where $\mathring{R}$ is the curvature scalar. Furthermore, we denote by $\mathsf{Hess}(\psi)$ the Hessian of a function $\psi \in \mathscr{C}^{\infty}(M)$. Explicitly, in local coordinates, it reads as $\mathsf{Hess}(\psi) = (\mathring{\nabla}_i\partial_j\psi) = (\mathring{\nabla}_j\partial_i\psi)$. In this case, (2.13) yields

$$v^i \;=\; -\sqrt{\det(\mathring{g})}\varepsilon^{ij}\partial_j\psi\,, \tag{2.20}$$

and the pressure equation (2.10), on an open and contractible set $U \subseteq M$, becomes

$$\frac{1}{2}\mathring{\Delta}_{\mathrm{B}}p \;=\; \det\left(\mathring{g}^{-1}\mathsf{Hess}\,(\psi)\right) - \frac{\mathring{R}}{4}|\mathrm{d}\psi|^2 \quad\Longleftrightarrow\quad \frac{1}{2}\mathring{\nabla}^i\partial_i p \;=\; \det\left(\mathring{\nabla}^i\partial_j\psi\right) - \frac{\mathring{R}}{4}\left(\mathring{\nabla}^i\psi\right)(\partial_i\psi)\,. \tag{2.21}$$

This can be understood as a Monge–Ampère equation for the stream function and hence for the velocity field. The vorticity two-form (2.11) can be written as

$$\zeta_{ij} \;=\; \frac{1}{2}\sqrt{\det(\mathring{g})}\,\varepsilon_{ij}\,\zeta \quad \text{with} \quad \zeta \;:=\; \mathring{\Delta}_{\mathrm{B}}\psi \quad\Longrightarrow\quad \zeta_{ij}\zeta^{ij} \;=\; \frac{1}{2}\zeta^2\,. \tag{2.22}$$

Importantly, the pressure equation (2.21) arises from a Monge–Ampère structure on T^*M. Indeed, upon fixing the notation

$$\hat{f} \;:=\; \frac{1}{2}\mathring{\Delta}_{\mathrm{B}}p + \frac{\mathring{R}}{4}|q|^2 \quad \text{and} \quad \mathring{\nabla}q_i \;:=\; \mathrm{d}q_i - \mathrm{d}x^j\mathring{\Gamma}_{ji}{}^{k}q_k\,, \tag{2.23a}$$

with $\mathring{\Gamma}_{ij}{}^{k}$ the Christoffel symbols for $\mathring{g}_{ij}$, it is readily checked that the differential forms[5]

$$\begin{aligned} \omega \;&:=\; \mathring{\nabla}q_i \wedge \mathrm{d}x^i\,, \\ \alpha \;&:=\; \frac{\sqrt{\det(\mathring{g})}}{2}\left[\varepsilon^{ij}\mathring{\nabla}q_i \wedge \mathring{\nabla}q_j - \hat{f}\varepsilon_{ij}\mathrm{d}x^i \wedge \mathrm{d}x^j\right] \end{aligned} \tag{2.23b}$$

on T^*M form a Monge–Ampère structure on T^*M. For Lagrangian submanifolds $\iota : L \hookrightarrow T^*M$ which are locally $\mathrm{d}\psi : U \to T^*M$ for some $\psi \in \mathscr{C}^{\infty}(U)$ with $U \subseteq M$ open and contractible, whilst $\iota^*\omega = 0$ is automatic, the condition $\iota^*\alpha = 0$ is equivalent to ψ satisfying the Monge–Ampère equation (2.21). In conclusion, the Monge–Ampère equation (2.21) arises from the Monge–Ampère structure (2.23*b*).

Note that α is non-degenerate if and only if $\hat{f} \neq 0$, and it is shown in section 3 that α is closed. We also note that pulling back α via $v = \star_{\mathring{g}}\mathrm{d}\psi$ again yields (2.21); this observation shall inform the alternative Monge–Ampère structure chosen in section 3, which naturally generalises to higher dimensions.

2.2.3. Almost (para-)Hermitian structure. Next, following [14],[6] we associate with the Monge–Ampère structure (2.23*b*) an endomorphism $\hat{J}$ of the tangent bundle of T^*M defined by

[5] Note that $\mathring{\nabla}q_i \wedge \mathrm{d}x^i = \mathrm{d}q_i \wedge \mathrm{d}x^i$.

[6] see also (B.2).

$$\frac{\alpha}{\sqrt{|\hat{f}|}} =: \hat{J} \lrcorner \omega \tag{2.24}$$

with $\hat{f}$ as defined in (2.23*b*) and under the assumption that $\hat{f}$ does not vanish. By virtue of the results of [14], $\hat{J}$ is an almost complex structure on T^*M when $\hat{f} > 0$ (in which case the Monge–Ampère equation (2.21) is elliptic) and an almost para-complex structure on T^*M when $\hat{f} < 0$ (in which case the Monge–Ampère equation (2.21) is hyperbolic). As can be checked following the arguments of [8, 14, 34], this structure is integrable if and only if $\hat{f}$ is constant[7].

Furthermore, as discussed in appendix B, we can always find a differential two-form $\hat{K}$ which is of type $(1,1)$ with respect to $\hat{J}$, such that $\hat{K} \wedge \omega = 0$, $\hat{K} \wedge (\hat{J} \lrcorner \omega) = 0$, and $\hat{K} \wedge \hat{K} \neq 0$. Explicitly, we may take

$$\hat{K} := -\sqrt{|\hat{f}|}\, \mathring{\nabla} q_i \wedge \star_{\hat{g}} \mathrm{d}x^i \,. \tag{2.25}$$

Since $\hat{K}(\hat{J}X, Y) = -\hat{K}(X, \hat{J}Y)$ for all $X, Y \in \mathfrak{X}(T^*M)$, we are naturally led to the almost (para-)Hermitian metric $\hat{g}(X,Y) := \hat{K}(X, \hat{J}Y)$ on T^*M for all $X, Y \in \mathfrak{X}(T^*M)$, which is explicitly given by

$$\hat{g} = \frac{1}{2}\hat{f}\mathring{g}_{ij}\mathrm{d}x^i \odot \mathrm{d}x^j + \frac{1}{2}\mathring{g}^{ij}\mathring{\nabla} q_i \odot \mathring{\nabla} q_j \,. \tag{2.26}$$

Evidently, in the elliptic case, when $\hat{f} > 0$, the metric $\hat{g}$ is Riemannian, whilst in the hyperbolic case, when $\hat{f} < 0$, the metric is Kleinian.

2.2.4. Pull-back metric. It is easily seen that the pull-back $g := \iota^* \hat{g}$ of (2.26) to the Lagrangian submanifold $\iota : L \hookrightarrow T^*M$ via $\mathrm{d}\psi$ is

$$g = \frac{1}{2} g_{ij} \mathrm{d}x^i \odot \mathrm{d}x^j \quad \text{with} \quad g_{ij} := \zeta \mathring{\nabla}_i \partial_j \psi \,, \tag{2.27}$$

where we have used that

$$f := \iota^* \hat{f} = \frac{1}{2}\mathring{\Delta}_{\mathrm{B}} p + \frac{\mathring{R}}{4}|\mathrm{d}\psi|^2 = \det\left(\mathring{\nabla}^i \partial_j \psi\right) \tag{2.28}$$

by (2.21) and substituted (2.22). Clearly, in regions where the vorticity vanishes, this metric vanishes as well. When both $\mathrm{tr}(\mathring{g}^{ik} g_{kj}) > 0$ and $\det(\mathring{g}^{ik} g_{kj}) > 0$, it follows that g is Riemannian. The former condition is always satisfied since $\mathrm{tr}(\mathring{g}^{ik} g_{kj}) = \zeta^2$, and the latter is satisfied if and only if $f > 0$. Similarly, when $f < 0$, g is Kleinian. Hence, the signature of g is independent of the sign of the vorticity (2.22) and only depends on the sign of f.

Upon comparing (2.12) and (2.28), we find that $f = \frac{1}{2}(\zeta_{ij}\zeta^{ij} - S_{ij}S^{ij})$ with the indices on ζ_{ij} and S_{ij} raised with the background metric. Hence, when $f > 0$ and the metric g is Riemannian, vorticity dominates, yet when $f < 0$ and g is Kleinian, strain dominates. This statement covariantly extends the pressure criterion for a vortex, as given in [2, 3], to an arbitrary Riemannian background manifold, while accounting for the underlying curvature. The standard criterion are recovered on a flat background.

Now that we have criterion for testing the dominance of vorticity and strain of a flow on a Riemannian manifold, we discuss how to obtain topological information about the flow.

[7] This then necessarily means that the curvature of M vanishes, i.e. M is flat.

2.2.5. Local Gauß–Bonnet theorem. Let L be a Lagrangian submanifold of T^*M, which is locally described by sections $\mathrm{d}\psi_U : U \to T^*M$, with $U \subseteq M$ open and contractible, and $\psi_U \in \mathscr{C}^\infty(U)$ the stream function on U. Furthermore, let $\Sigma \subseteq U$ be a compact region in U, on which $f > 0$. We can then define the compact region $L_\Sigma \subseteq L$ by $L_\Sigma := \mathrm{d}\psi_U(\Sigma)$. It is now natural to consider the question of how we might use the local Gauß–Bonnet theorem to relate the geometry of L_Σ to its topology, as given by the Euler characteristic $\chi(L_\Sigma)$. For the reader's convenience, let us state this theorem, see e.g. [35, theorem 4.2] for details.

Theorem 2.2. *Let Σ be a two-dimensional, compact, oriented Riemannian manifold with metric g. Suppose that Σ has a boundary composed of disjoint, simple, closed, piecewise regular, piecewise arc-length parametrised curves γ_α, that is, $\partial\Sigma = \bigcup_\alpha \gamma_\alpha$. Let R be the curvature scalar of the Levi-Civita connection of g, vol_Σ the volume form on Σ, and κ the geodesic curvature. Furthermore, let φ_β be the exterior angles at the non-smooth points of the boundary $\partial\Sigma$. Then, the Euler number $\chi(\Sigma)$ of Σ is given by*

$$\frac{1}{2}\int_\Sigma vol_\Sigma R + \sum_\alpha \int_{\gamma_\alpha} \mathrm{d}s\, \kappa(\gamma_\alpha(s)) + \sum_\beta \varphi_\beta \;=\; 2\pi\chi(\Sigma)\ . \tag{2.29}$$

Let $\Sigma \subseteq U \subseteq M$ be as above. Then, $\chi(\Sigma) = \chi(L_\Sigma)$, since $\pi|_L$ is now a diffeomorphism. For instance, if such Σ is bounded by a simple, closed curve such as closed, isovortical contour, or a closed stream-line, then Σ is homeomorphic to a disc and so, $\chi(L_\Sigma) = 1$.

2.2.6. Christoffel symbols and curvatures. Let us now give some of the formulæ needed when evaluating (2.29). In particular, we introduce the notation

$$\psi_{i_1\cdots i_n} \;:=\; \mathring{\nabla}_{(i_1}\cdots\mathring{\nabla}_{i_{n-1}}\partial_{i_n)}\psi\ . \tag{2.30}$$

A quick calculation shows that $\psi_{i_1\cdots i_n}$ can be expressed in terms of the components of the rate-of-strain tensor and the vorticity two-form, see (2.11) and (2.22), as

$$\psi_{i_1\cdots i_n} \;=\; -\sqrt{\det(\mathring{g})}\,\mathring{g}^{jk}\varepsilon_{j(i_1}\mathring{\nabla}_{i_2}\cdots\mathring{\nabla}_{i_{n-1}}S_{i_n)k} + \frac{1}{2}\mathring{g}_{(i_1i_2}\mathring{\nabla}_{i_3}\cdots\mathring{\nabla}_{i_{n-1}}\partial_{i_n)}\zeta \tag{2.31}$$

for $n > 1$. Then, using (2.22), we can write the metric (2.27) as $g_{ij} = \zeta\tilde{g}_{ij}$ with $\tilde{g}_{ij} := \psi_{ij}$. Hence, due to its conformal nature, the Christoffel symbols $\Gamma_{ij}{}^k$ of g_{ij} take the form

$$\Gamma_{ij}{}^k \;=\; \tilde{\Gamma}_{ij}{}^k + \partial_{(i}\delta_{j)}{}^k\log(|\zeta|) - \frac{1}{2}\tilde{g}_{ij}\tilde{g}^{kl}\partial_l\log(|\zeta|)\ , \tag{2.32a}$$

where $\tilde{g}^{ij}$ denotes the inverse of $\tilde{g}_{ij}$, and the $\tilde{\Gamma}_{ij}{}^k$ are the Christoffel symbols of the Hessian metric $\tilde{g}_{ij}$,

$$\tilde{\Gamma}_{ij}{}^k \;=\; \mathring{\Gamma}_{ij}{}^k + \frac{1}{2}\Upsilon_{ijl}\tilde{g}^{lk} \quad\text{with}\quad \Upsilon_{ijk} \;:=\; \psi_{ijk} + \frac{4}{3}\psi_l\mathring{R}_{k(ij)}{}^l\ . \tag{2.32b}$$

Consequently, the curvature scalar R of g_{ij} is given by

$$R \;=\; \frac{1}{\zeta}\left\{\tilde{R} - \frac{1}{\sqrt{|\det(\tilde{g})|}}\partial_i\left[\sqrt{|\det(\tilde{g})|}\,\tilde{g}^{ij}\partial_j\log(|\zeta|)\right]\right\}, \tag{2.33a}$$

where $\tilde{R}$ is the curvature scalar for $\tilde{g}_{ij}$,

$$\begin{aligned}\tilde{R} \;=\; & \frac{1}{2}\tilde{g}^{ij}\mathring{g}_{ij}\mathring{R} - \frac{1}{4}\tilde{g}^{ij}\tilde{g}^{kl}\tilde{g}^{mn}(\Upsilon_{ijm}\Upsilon_{kln} - \Upsilon_{ikm}\Upsilon_{jln}) \\ & + \frac{2}{3}\tilde{g}^{ij}\tilde{g}^{kl}[\psi_{mn}(\delta_i^m\mathring{R}_{j(kl)}{}^n - \delta_j^m\mathring{R}_{l(ik)}{}^n) + \psi_m(\mathring{\nabla}_i\mathring{R}_{j(kl)}{}^m - \mathring{\nabla}_j\mathring{R}_{l(ik)}{}^m)]\,,\end{aligned} \tag{2.33b}$$

see appendix C.1 for details. Importantly, no fourth-order derivatives of the stream function appear, and in that sense, the curvature scalar of the pull-back metric (2.27) is generated by gradients of vorticity and strain, see (2.31). In addition, ψ_i occurs without any further derivatives, hence the curvature scalar depends also on the components of velocity directly.

Furthermore, given an arc-length parametrised curve $\gamma : s \to (y^1(s), y^2(s))$ in two dimensions, we may use Beltrami's formula

$$\kappa(\gamma(s)) \;=\; \sqrt{|\det(g(y(s)))|}\,\varepsilon_{ij}\dot{y}^i(s)[\ddot{y}^j(s) + \Gamma_{kl}{}^j(y(s))\dot{y}^k(s)\dot{y}^l(s)]\,, \tag{2.34}$$

for the geodesic curvature κ at a point $\gamma(s)$ of the curve. Here, the superposed dots indicate derivatives with respect to the arc-length parameter s.

Let us return to our previous example, where $\Sigma \subseteq U \subseteq M$ with $f > 0$ and a boundary given by a simple, regular, closed curve $c : \mathbb{R} \to U$. As $\mathrm{d}\psi_U$ is a diffeomorphism on U, it follows that the boundary of $L_\Sigma := \mathrm{d}\psi_U(\Sigma)$ is given by $\gamma := \mathrm{d}\psi_U \circ c : \mathbb{R} \to L$, which is also a simple, regular, closed curve and may be assumed to be arclength-parametrised without loss of generality. Consequently, (2.29) evaluates to

$$\int_\gamma \mathrm{d}s\,\kappa(\gamma(s)) \;=\; 2\pi - \frac{1}{2}\int_{L_\Sigma}\mathrm{vol}_{L_\Sigma}\,R\,, \tag{2.35}$$

on L_Σ, where R is given by (2.33a). That is, the mean curvature of the boundary is determined by the average curvature of the interior. Noting (2.33a), (2.33b) and (2.34), we remark that at a formal qualitative level, the local Gauß–Bonnet relation (2.35) is a statement to the effect that[8]

$$\begin{aligned}&\text{mean curvature of the boundary of } L_\Sigma \\ &\quad = 2\pi - \text{mean gradients of vorticity and strain}\,.\end{aligned} \tag{2.36}$$

In this sense, we can use Monge–Ampère geometry, when $f > 0$, to assign a topological invariant to a 'vortex' described by L_Σ — the image of the graph of the gradient of the stream function, over a compact region of M bounded by some closed stream-line. Whilst the framework described here is an elaborate mechanism for determining the Euler number of a vortex patch, it illuminates a relationship between vortex topology and the physical phenomena, such as the gradients of vorticity and strain, that determine certain topological properties of the flow via the topology of L and the diffeomorphic nature of the projection $\pi|_L$. When $\pi|_L$ fails to be a diffeomorphism, then singular behaviour may be anticipated (note the recent work by some of the authors in [33] focuses on this problem in the context of the semi-geostrophic equations of meteorological flows). When the pull-back metric (2.27) is Kleinian, the Gauß–Bonnet theorem can be extended to such cases, under certain conditions pertaining to the boundary ∂L_Σ — e.g. it should have no null segments—however, the link between topology as quantified by the Euler characteristic and the Gauß–Bonnet theorem becomes tenuous [36, 37].

[8] Recall here that the boundary of L_Σ is given by the image of the boundary of Σ, that is, the image of the closed stream-line bounding a candidate vortex in M, under $\mathrm{d}\psi_U$.

2.3. Examples in two dimensions

We now consider some classical examples of flows on $\mathbb{R}^2$ with metric $\mathring{g}_{ij} = \delta_{ij}$. As noted in section 1, a solution for (1.6) is not necessarily one for the Navier–Stokes equations, and our first two examples fall into this category. However, they illustrate how the topology of flows can change with time and it is useful to view such phenomena from the point of view of Monge–Ampère geometry. The second example can be turned into a solution to the Navier–Stokes equations by adding higher-order terms [38], yet the basic topological features on which we focus (as did [38]) are most clearly illustrated in the form presented below. Our final example, the Taylor–Green vortex, is a solution to Navier–Stokes equations.

2.3.1. Preliminaries. For convenience, let us summarise the relevant simplified formulæ first, adopting the notation $x := x^1$ and $y := x^2$. Working with a flat background metric, $\mathring{R} = 0$, and so we find for $\hat{f}$ given in (2.23*b*) and f given below (2.27) that

$$\hat{f} \;=\; \frac{1}{2}\Delta p \;=\; \partial_x^2\psi\,\partial_y^2\psi - (\partial_x\partial_y\psi)^2 = f \quad \text{with} \quad \Delta \;:=\; \partial_x^2 + \partial_y^2 \,. \tag{2.37}$$

Hence, the metric (2.26) on $T^*\mathbb{R}^2$ takes the form

$$\hat{g} \;=\; \begin{pmatrix} f\mathbb{1}_2 & 0 \\ 0 & \mathbb{1}_2 \end{pmatrix} \tag{2.38}$$

with its signature dictated by the sign of f. This is singular if and only if $f = 0$, and the corresponding curvature scalar (3.22) becomes

$$\hat{R} \;=\; \frac{1}{f^3}\left(\partial_x f\partial_x f + \partial_y f\partial_y f - f\Delta f\right) . \tag{2.39}$$

Thus, at a stationary point of f, the sign of $\hat{R}$ is determined by the sign of Δf. Consequently, when f accumulates and has a local maximum, $\Delta f < 0$ and $\hat{R} > 0$.

The vorticity (2.22) is simply $\zeta = \Delta\psi$ for the stream function $\psi = \psi(x,y)$, so the pull-back metric (2.27) becomes

$$g \;=\; \zeta\begin{pmatrix} \partial_x^2\psi & \partial_x\partial_y\psi \\ \partial_x\partial_y\psi & \partial_y^2\psi \end{pmatrix} \;=\; \frac{\zeta}{2}\begin{pmatrix} \zeta + 2S_{xy} & -2S_{xx} \\ -2S_{xx} & \zeta - 2S_{xy} \end{pmatrix}, \tag{2.40}$$

where $S_{xx} = -S_{yy}$ and S_{xy} are the components of rate-of-strain tensor (2.11), describing a shearing deformation at an angle of $\frac{1}{2}\arctan\left(\frac{S_{xy}}{S_{xx}}\right)$, without overall dilation, since our flow is divergence-free [39, 40]. We note that g is singular when the vorticity vanishes, in addition to when the Hessian part of the metric is singular, that is, where $f = 0$. We shall discuss these points in due course. We also note that when f depends on time t, then the metric (2.38) will depend on t as a parameter. The same is true for (2.40) via the time-dependence of vorticity and rate-of-strain. The one-parameter family of metrics (2.38) and (2.40) will thus evolve according to either the Euler or the Navier–Stokes equations.

Another rotational invariant of the velocity-gradient matrix

$$A \;:=\; \begin{pmatrix} -\partial_x\partial_y\psi & -\partial_y^2\psi \\ \partial_x^2\psi & \partial_x\partial_y\psi \end{pmatrix}, \tag{2.41}$$

the resultant deformation D_{R} [39], occurs in the expression for the eigenvalues of (2.40),

$$E_{\pm} \;=\; \frac{1}{2}\left(\zeta^2 \pm |\zeta| D_{\mathrm{R}}\right) \quad \text{with} \quad D_{\mathrm{R}}^2 \;:=\; 4\left(\partial_x\partial_y\psi\right)^2 + \left(\partial_x^2\psi - \partial_y^2\psi\right)^2 . \tag{2.42}$$

Note that $D_{\mathrm{R}}^2 = \zeta^2 - 4f$, so the eigenvalues take the same sign for $f > 0$ and opposite sign for $f < 0$, provided they are both non-zero. Finally, the curvature scalars (2.33*a*) reduce to

$$R \;=\; \frac{1}{\zeta}\left\{\tilde{R} - \frac{1}{\sqrt{|\det(\tilde{g})|}}\partial_i\left[\sqrt{|\det(\tilde{g})|}\,\tilde{g}^{ij}\partial_j \log\left(|\zeta|\right)\right]\right\}, \tag{2.43a}$$

where

$$\tilde{g}^{-1} \;=\; \frac{1}{f}\begin{pmatrix} \partial_y^2\psi & -\partial_x\partial_y\psi \\ -\partial_x\partial_y\psi & \partial_x^2\psi \end{pmatrix} \tag{2.43b}$$

and

$$\tilde{R} \;=\; -\frac{1}{4}\tilde{g}^{ij}\tilde{g}^{kl}\tilde{g}^{mn}\left(\partial_i\partial_j\partial_m\psi\,\partial_k\partial_l\partial_n\psi - \partial_i\partial_k\partial_m\psi\,\partial_j\partial_l\partial_n\psi\right) . \tag{2.43c}$$

As shown in (2.40), the pull-back metric can be considered a function of vorticity and rate-of-strain, and the curvature of that metric therefore involves derivatives of these quantities. In turbulent flows, fine-scale structure (such as vortex filaments) could imply large gradients of vorticity and rate-of-strain, which in turn could present challenges in calculating such gradients in numerical simulations. However, as we shall illustrate in the following section, when the metric structure degenerates and/or the scalar curvature becomes singular, then these geometric features are associated with topological changes in the fluid flow.

2.3.2. Larchevêque's criterion and uniform vorticity and strain. In [2, 3] it is noted that the stream function is uniquely defined on a simply connected domain Σ bounded by a closed streamline when $\Delta p > 0$ and $\psi|_{\partial\Sigma}$ is known. For example, consider the stream function

$$\psi(t,x,y) \;:=\; \frac{1}{2}\left[a(t)x^2 + b(t)y^2\right] , \tag{2.44}$$

where a and b are functions of time t alone. The Laplacian of the pressure is $\Delta p = 2f = 2ab$, hence when a and b have the same sign, $f > 0$, vorticity dominates, and the metric $\hat{g}$ given by (2.38) is Riemannian. Similarly, when a and b have different signs, $f < 0$, strain dominates, and the metric $\hat{g}$ is Kleinian. Additionally, the metric is globally singular when a or b vanish, that is, when $f = 0$.

The vorticity is simply $\zeta = a + b$ and the pull-back metric (2.40) becomes

$$g \;=\; (a+b)\begin{pmatrix} a & 0 \\ 0 & b \end{pmatrix} . \tag{2.45}$$

Like $\hat{g}$, its pull-back is Riemannian when $f > 0$, Kleinian when $f < 0$, and singular when $f = 0$, with the following exception: the pull-back metric is also singular when the vorticity vanishes, that is, where $a = -b$. In line with Larchevêque, this additional singularity falls outside of Riemannian regions, hence the sign of vorticity remains constant where $f > 0$.

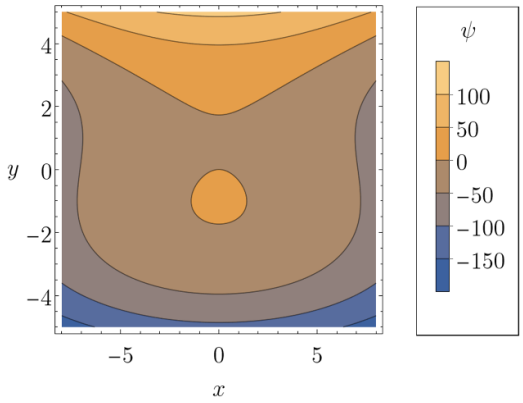

Figure 1. Plot of the streamlines for stream function (2.46) with $t=-1$. The streamlines around the elliptic point $(0,-1)$ form closed contours, whilst those near the hyperbolic point $(0,1)$ diverge.

2.3.3. Flow with bifurcations. In the following example, discussed in [38] in connection with topological fluid dynamics, the occurrence of singularities in the Monge–Ampère geometry can be associated with important features, such as bifurcations, in the fluid flow.

In particular, following [38], we consider the stream function

$$\psi(t,x,y) \;:=\; -x^2+3yt+y^3\,, \tag{2.46}$$

shown in figure 1, where time, t, is a parameter. Using (2.46), the Poisson equation for the pressure takes the explicit form

$$\partial_x^2\psi\partial_y^2\psi-(\partial_x\partial_y\psi)^2 \;=\; -12y \;=f\,, \tag{2.47}$$

which we can view as a variable-coefficient Monge–Ampère equation for ψ. This equation is elliptic when $y<0$, hyperbolic when $y>0$, and it degenerates to parabolic form on $y=0$.

The equations for the flow are

$$\dot{x} \;=\; -\partial_y\psi \;=\; -3\left(t+y^2\right) \quad\text{and}\quad \dot{y} \;=\; \partial_x\psi \;=\; -2x\,, \tag{2.48}$$

where the superposed dot indicates the derivative with respect to t. When $t>0$ there are no real fixed points[9] (defined by $\dot{x}=\dot{y}=0$) and when $t=0$ the level set $\psi=0$ has a cusp singularity at the origin. When $t<0$, the fixed points are located at $(0,\pm\sqrt{-t})$; the fixed point at $(0,\sqrt{-t})$ is hyperbolic, hence streamlines in a neighbourhood of this fixed point tend to diverge, whilst the fixed point at $(0,-\sqrt{-t})$ is elliptic, indicating that the flow in a neighbourhood around this fixed point tends to swirl. This shows that for values of t at which there are fixed points, the elliptic fixed point lies in the region where vorticity dominates, whilst the hyperbolic fixed point resides where strain dominates. Note that f is time-independent, so these regions remain coherent in time, regardless of the fixed points.

[9] The stability matrix $A^i{}_j$ with $\delta\dot{x}^i=A^i{}_j\delta x^j$ is the velocity-gradient matrix $A^i{}_j:=\partial_j v^i$ which, upon recalling (2.13), is related to the Hessian of the stream function by means of $A^i{}_j=\varepsilon^{ik}\partial_j\partial_k\psi$. It has eigenvalues $\pm\sqrt{-f}$ which are thus purely imaginary when $f>0$.

In terms of the Monge–Ampère geometry introduced thus far, the metric $\hat{g}$ on $T^*\mathbb{R}^2$ is given by (2.38). The corresponding curvature scalar (2.39) is given by

$$\hat{R} \;=\; -\frac{1}{12y^3}\,. \tag{2.49}$$

Note that f vanishes at $y=0$ and hence the metric $\hat{g}$ is singular. Furthermore, the signs of $\hat{R}$ and f coincide. More generally, for $y<0$, we have $f>0$ and vorticity dominates in this region, where the metric (2.38) is Riemannian with positive curvature scalar. For $y>0$, it follows that $f<0$ and strain dominates, with (2.38) becoming Kleinian with negative curvature scalar. Furthermore, the vorticity is $\zeta=2(3y-1)$, hence the pull-back metric (2.40) is

$$g \;=\; 4\,(1-3y)\begin{pmatrix}1 & 0\\ 0 & -3y\end{pmatrix}. \tag{2.50}$$

Evidently, the metric is Riemannian for $y<0$ and singular when $y=0$ or $y=\frac{1}{3}$. The former singularity corresponds to where $f=0$, with the latter occurring precisely where the vorticity vanishes. Using (2.40), the components of strain are given by $S_{xx}=S_{yy}=0$ and $S_{xy}=-3y-1$, describing shearing at an angle $\frac{\pi}{4}$ to the coordinate axes, near hyperbolic fixed points, in regions where strain dominates. The corresponding curvature scalars (2.43*a*) are

$$R \;=\; \frac{1-9y}{8y^2\,(1-3y)^3} \quad\text{and}\quad \tilde{R} \;=\; 0\,. \tag{2.51}$$

This, in turn, shows that the metric singularities $y=0$ and $y=\frac{1}{3}$ are, in fact, singularities of the scalar curvature, which is invariant under changes of coordinates on M.

The picture emerging here has some interesting features. Recall the definitions of classical and generalised solutions from section 2.2. Then, commencing with (2.46), we note that L is a classical solution. However, as just indicated, the metric and curvature of L have singularities, which are related to the points at which the flow changes from elliptic to hyperbolic, and where vorticity vanishes. We shall show next that we can describe this singular behaviour in terms of a generalised solution to the Legendre-dual problem.

2.3.4. Legendre duals. Consider a domain Σ of the flow, with $L_\Sigma := \mathrm{d}\psi(\Sigma) = \{(x,y;\partial_x\psi,\partial_y\psi)\,|\,(x,y)\in\Sigma\}$ the corresponding region in the Lagrangian submanifold L described locally by $\mathrm{d}\psi$. Then, locally on this domain, $\pi|_L$ is the identity and is hence non-singular. In [41] it is shown that

$$x'(t) \;=\; \frac{\partial\psi(t,x,y)}{\partial x} \;=\; v \quad\text{and}\quad y'(t) \;=\; \frac{\partial\psi(t,x,y)}{\partial y} \;=\; -u\,. \tag{2.52}$$

is a local inversion and one can define the Legendre transformation [42]

$$\psi'(t,x',y') \;:=\; x'x+y'y-\psi(t,x,y) \tag{2.53}$$

when $f\notin\{0,\infty\}$, where finiteness of f follows from the non-singular nature of the projection $\pi|_L$. Here, x' and y' are the local coordinates on the Legendre-dual space and ψ' is known as the Legendre-dual (stream-)function. Furthermore, in this setting we may also define the map

$\tilde{\pi}|_L : (x,y) \mapsto (\partial_x\psi, \partial_y\psi) = (x',y')$[10], with determinant f. Hence, $f \neq 0$ precisely when $\tilde{\pi}|_L$ is non-singular, corresponding to when (2.52) is a local inversion.

It follows that the map $\tilde{\pi}|_L$ is singular precisely when f vanishes and (2.52) is not invertible, in which case ψ and ψ' have different regularity. In particular, if ψ is a classical solution to (2.21), the Legendre-dual ψ' generates a generalised solution to the dual Monge–Ampère equation, with singular behaviour where $f = 0$. The dual Monge–Ampère equation is given by

$$f(t,x(x',y'),y(x',y')) \;=\; \frac{1}{\det\left(\mathsf{Hess}\left(\psi'(t,x',y')\right)\right)}\,. \tag{2.54}$$

Consequently, vanishing f corresponds to $\det(\mathsf{Hess}(\psi'(t,x',y')))$ blowing up. As f is finite, it follows that $\det(\mathsf{Hess}(\psi'(x',y'))) \neq 0$. The Legendrian dual to the Hessian part of the metric (2.27) is

$$\tilde{g}' \;=\; \frac{1}{2}\psi'_{ij}\mathrm{d}x'^i \odot \mathrm{d}x'^j\,, \tag{2.55}$$

where $(x'^i) = (x',y')$ and $\det(\tilde{g}') = \frac{1}{f}$. It follows that $\tilde{g}'$ is non-degenerate, however, it does blow up when $f = 0$. The accompanying vorticity conformal factor ζ has the Legendrian dual

$$\zeta' \;=\; f\Delta'\psi'\,, \tag{2.56}$$

with Δ' the Laplacian with respect to (x',y'). From this, it follows that $g' = \zeta'\tilde{g}'$ may in-fact be singular when $f = 0$ or $\Delta'\psi' = 0$. The curvature scalar associated to g' is given by (2.43*a*), with objects replaced by their primed Legendre dual as appropriate and

$$g'^{-1} \;=\; \frac{f}{(\Delta'\psi')}^2 \begin{pmatrix} \partial^2_{y'}\psi' & -\partial_{x'}\partial_{y'}\psi' \\ -\partial_{x'}\partial_{y'}\psi' & \partial^2_{x'}\psi' \end{pmatrix}. \tag{2.57}$$

Thus, singularities of $\tilde{g}$ in the (x,y) coordinates do not occur in $\tilde{g}'$ in the (x',y') coordinates and are instead transferred to the projection $\tilde{\pi}|_L$ and the dual solution ψ', via the Legendre transformation. By restricting our domain Σ such that f has constant sign, we can impose that the Legendre transformation is well defined and both $\tilde{\pi}|_L$ and $\tilde{g}$ are non-singular.

2.3.5. Flow with bifurcations and Legendre duality. Returning to the stream function (2.46), we obtain for (2.53)

$$\psi'(t,x',y') \;= -\frac{1}{4}x'^2 \pm \frac{2}{3\sqrt{3}}\left(y' - 3t\right)^{\frac{3}{2}}\,, \tag{2.58a}$$

with

$$x' \;=\; \dot{y} \;=\; -2x \quad \text{and} \quad y' \;=\; -\dot{x} \;=\; 3y^2 + 3t\,, \tag{2.58b}$$

and

$$x \;=\; -\frac{1}{2}x' \;=\; \frac{\partial\psi'}{\partial x'} \quad \text{and} \quad y \;=\; \pm\sqrt{\frac{1}{3}\left(y' - 3t\right)} \;=\; \frac{\partial\psi'}{\partial y'}\,, \tag{2.58c}$$

[10] Note that $\tilde{\pi}|_L = \tilde{\pi} \circ \iota$ with $\tilde{\pi} : (x,y,p,q) \mapsto (p,q)$ defined on $T^*\mathbb{R}^2$. Furthermore, we use that $\pi|_L$ is locally a diffeomorphism to coordinatise L by (x,y) from M.

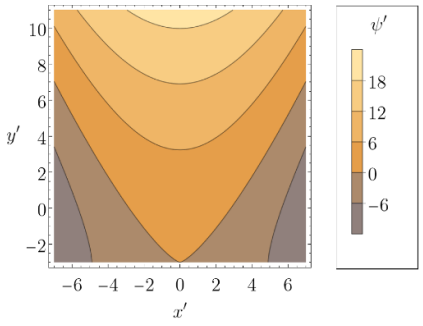

(a) Contour plot for the upper sheet of the function (2.58a). There is a hyperbolic point at $(0, 3t)$.

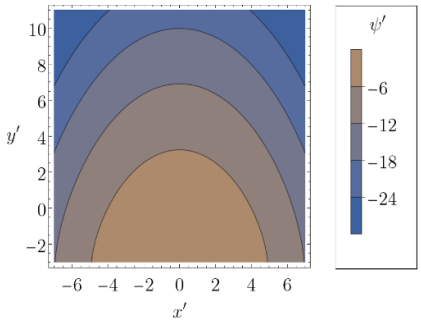

(b) Contour plot for the lower sheet of the function (2.58a). There is an elliptic point at $(0, 3t)$.

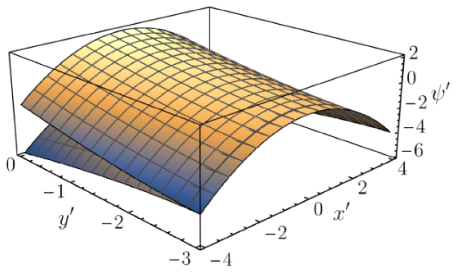

(c) A plot of the two sheets of the function (2.58a), with a fold singularity appearing along the line $y' = -3$, where the two sheets meet.

Figure 2. A selection of plots of the Legendre-dual stream function (2.58*a*), at time $t = -1$. The multivalued behaviour of ψ' is associated with the corresponding Lagrangian submanifold $\iota : L \hookrightarrow T^*\mathbb{R}^2$ being a generalised solution to (2.54).

respectively. As ψ is a classical solution to our Monge–Ampère equation, it follows that $\pi|_L$ is the identity on $\mathbb{R}^2$. However, ψ' is only defined for $y' - 3t \geqslant 0$ and is multivalued on momentum space, except where $y' - 3t = 0$; plots of the two sheets are shown in figure 2.

As the Jacobian of the projection $\tilde{\pi}|_L : (x, y) \mapsto (\partial_x\psi, \partial_y\psi)$ is precisely the Hessian, it follows that both $\tilde{\pi}|_L$ and the local inversion (2.52) are singular where the Hessian is degenerate, that is, where $f = 0 = y' - 3t$. Restricting to a domain Σ on which the sign of f is constant then amounts to choosing a sheet of ψ'.

2.3.6. Taylor–Green vortex. In two dimensions, the stream function of the Taylor–Green vortex [43] takes the form

$$\psi(t, x, y) := -F(t)\cos(ax)\cos(by) \tag{2.59}$$

where F is a function of time t alone and $a, b \in \mathbb{R}$ are some parameters. See figure 3(a).

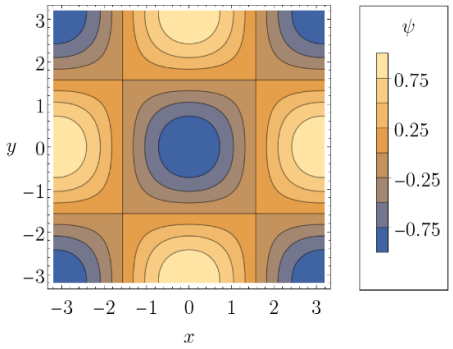

(a) Plot of the streamlines of the stream function (2.59). The domain is partitioned the domain into squares of side length π, across which the sign of the stream function alternates.

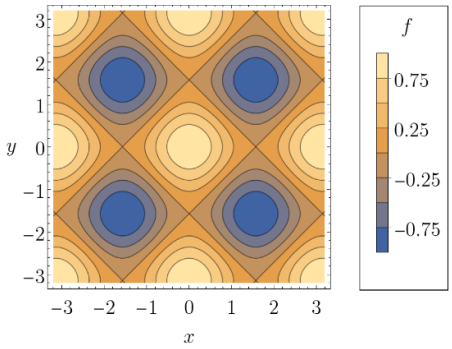

(b) Contour plot of $f = \frac{1}{2}a^2b^2F^2[\cos(2ax) + \cos(2by)]$. The domain is partitioned into rhombi, with positive/negative regions around elliptic/hyperbolic fixed points.

Figure 3. Plots of the iso-lines of the stream function and half the Laplacian of pressure for the Taylor–Green vortex with parameters $a = b = 1$ and $F(t) \equiv 1$, which shall be used for the remainder of the plots for this example. Streamlines corresponding to values of sufficiently large magnitude are closed contours contained in regions of positive f, where vorticity dominates. The vorticity is proportional to the stream function, $\zeta = -(a^2 + b^2)\psi$.

Hence, for (2.59), we have $f = \frac{1}{2}a^2b^2F^2[\cos(2ax) + \cos(2by)]$, so the metric is again (2.38), and the curvature scalar (2.39) is simply given by

$$\hat{R} \;=\; \frac{8\left(a^2+b^2\right)\left[1+\cos\left(2ax\right)\cos\left(2by\right)\right]}{a^2b^2F^2\left[\cos\left(2ax\right)+\cos\left(2by\right)\right]^3}\,. \tag{2.60}$$

See figure 4(a). Consequently, when $\cos(2ax) + \cos(2by) > 0$, the metric is Riemannian with a positive curvature scalar and vorticity dominates. When $\cos(2ax) + \cos(2by) < 0$ the metric is Kleinian with negative curvature scalar, and strain dominates. The signs of f and $\hat{R}$ coincide. Both the metric and curvature scalar are singular when $abF = 0$ and along the lines $y = \frac{a}{b}x + \frac{\pi}{2b}(2n+1)$ for all $n \in \mathbb{Z}$ (when $\cos(2ax) + \cos(2by) = 0$), corresponding to where $f = 0$.

Furthermore, the vorticity is given by $\zeta = (a^2 + b^2)F\cos(ax)\cos(by)$ so that the pull-back metric (2.40) becomes

$$g \;=\; \frac{\left(a^2+b^2\right)F^2}{4}\begin{pmatrix} a^2\left[1+\cos\left(2ax\right)\right]\left[1+\cos\left(2by\right)\right] & -ab\sin\left(2ax\right)\sin\left(2by\right) \\ -ab\sin\left(2ax\right)\sin\left(2by\right) & b^2\left[1+\cos\left(2ax\right)\right]\left[1+\cos\left(2by\right)\right] \end{pmatrix}. \tag{2.61}$$

Its eigenvalues (2.42) are

$$E_\pm \;=\; \frac{F^2\left(a^2+b^2\right)}{4}\left[2\left(a^2+b^2\right)\cos^2\left(ax\right)\cos^2\left(by\right) \pm \left|\cos\left(ax\right)\cos\left(by\right)\right|\sqrt{\tilde{E}}\right] \tag{2.62a}$$

with

$$\tilde{E} \;:=\; \left(a^4 - 6a^2b^2 + b^4\right)\left[\cos\left(2ax\right)+\cos\left(2by\right)\right] + \left(a^2+b^2\right)^2\left[1+\cos\left(2ax\right)\cos\left(2by\right)\right]\,. \tag{2.62b}$$

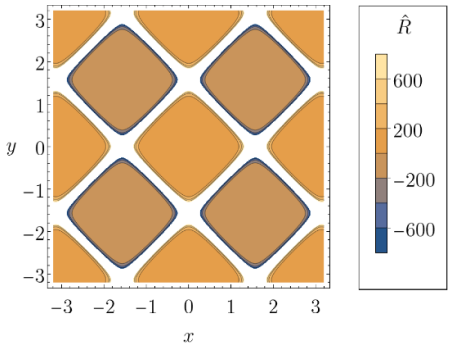

(a) Contour plot for the curvature scalar $\hat{R}$ on $T^*\mathbb{R}^2$. This is singular at $y = x + \frac{\pi}{2}(2n+1)$ for all $n \in \mathbb{Z}$, which is where f vanishes.

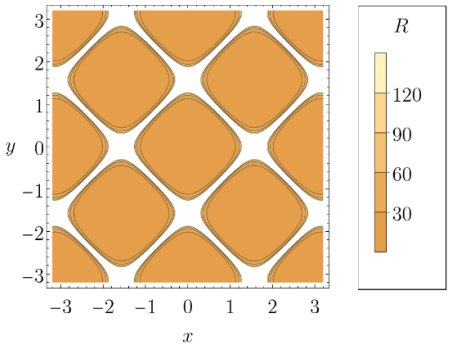

(b) Contour plot for the curvature scalar R. This is everywhere positive yet small away from the singularities given by $y = x + \frac{\pi}{2}(2n+1)$ for all $n \in \mathbb{Z}$.

Figure 4. Contour plots of the curvatures (2.60) and (2.63) respectively, for the Taylor Green vortex with parameters $a = b = 1$ and $F(t) \equiv 1$.

See figure 5. The corresponding curvature scalars (2.43*a*) are

$$R = \frac{8}{F^2\,(a^2+b^2)\,[\cos(2ax)+\cos(2by)]^2} \quad \text{and} \quad \tilde{R} = 0\,. \tag{2.63}$$

The curvature scalar R is singular along the same curves as $\hat{R}$ but is otherwise everywhere positive. See figure 4(b) Evidently, E_+ is everywhere non-negative, so the signature of the metric (2.61) is determined by the sign of E_-. It is clear from figure 5(b) that, when $\cos(2ax) + \cos(2by) \gtrless 0$, we have $E_- \gtrless 0$ and the metric g is Riemannian/Kleinian with vorticity/strain dominating. Also, $E_- = 0$ when $\cos(2ax) + \cos(2by) = 0$ and we note from (2.63) that the scalar curvature is singular at these points too. The vorticity changes sign as the contours $x = \frac{\pi}{2a}(2n+1)$ or $y = \frac{\pi}{2b}(2n+1)$ are crossed, and the metric (2.61) is Kleinian on both sides; this is consistent with the observations that the vorticity has constant sign in Riemannian regions, where it also dominates [3].

3. Geometric properties of fluids in three dimensions

Having discussed two-dimensional fluid flows, we now consider flows in three (or even higher) dimensions. Here, the situation is much more involved, since in the general case the flow is not described by a stream function[11]. Hence, the pressure equation (2.10) cannot be converted into a Monge–Ampère equation. Nevertheless, one can formulate the flow in terms of differential forms, as we shall now explain. To do this, we first revisit the formulation we have just used for two-dimensional flows, and note that an alternative description naturally presents itself. Whilst this alternative view makes little difference to the geometric picture in two dimensions, we

[11] We shall consider some examples of three-dimensional flows with symmetries, which can be described in terms of a stream function, such as Hill's spherical vortex.

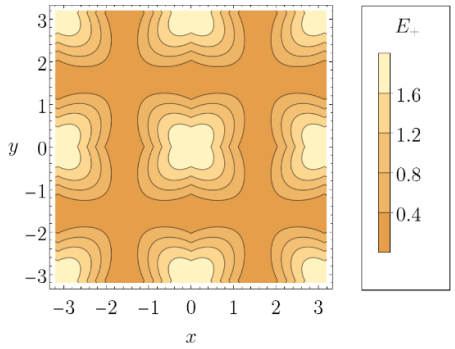

(a) Contour plot for the eigenvalue E_+. This eigenvalue is non-negative on the domain and vanishes along $x = \frac{\pi}{2}(2n+1)$ or $y = \frac{\pi}{2}(2n+1)$ for all $n \in \mathbb{Z}$.

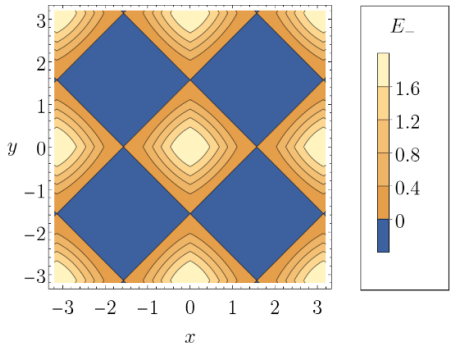

(b) Contour plot for the eigenvalue E_-. This eigenvalue is non-positive within the dark blue regions, but also vanishes at points within these domains.

Figure 5. Plots of the eigenvalues (2.62*a*) of the pull-back metric (2.61) for the Taylor–Green vortex with parameters $a = b = 1$ and $F(t) \equiv 1$.

show that it provides a mechanism to unify what could otherwise be quite different geometric descriptions of two-dimensional and three-dimensional flows, as was described in [9].

3.1. Two-dimensional case revisited

3.1.1. Monge–Ampère structure. In section 2.2, we have seen that the Monge–Ampère structure (2.23*b*) encodes incompressible fluids on a two-dimensional Riemannian manifold $(M, \mathring{g})$. As before, let (x^i, q_i) be local coordinates on T^*M. Instead of using the standard symplectic structure (2.23*b*) on T^*M, we now propose taking the 'dual' form

$$\varpi \;:=\; \mathring{\nabla} q_i \wedge \star_{\mathring{g}} \mathrm{d}x^i \,, \tag{3.1}$$

that is, (2.25) without the pre-factor. Evidently, ϖ is non-degenerate[12] and it is also closed as a consequence of

$$\mathrm{d}\left(\mathring{\nabla} q_i\right) \;=\; \frac{1}{2}\mathrm{d}x^l \wedge \mathrm{d}x^k \mathring{R}_{kli}{}^j q_j + \mathrm{d}x^j \mathring{\Gamma}_{ji}{}^k \wedge \mathring{\nabla} q_k \tag{3.2a}$$

and

$$\mathrm{d}\star_{\mathring{g}} \mathrm{d}x^i \;=\; -\mathring{g}^{jk}\mathring{\Gamma}_{jk}{}^i \,\mathrm{vol}_M \quad \text{with} \quad \mathrm{vol}_M \;:=\; \frac{\sqrt{\det(\mathring{g})}}{2}\varepsilon_{ij}\mathrm{d}x^i \wedge \mathrm{d}x^j \,. \tag{3.2b}$$

Hence, (3.1) defines a symplectic structure. It is then easily seen that, when $\iota : L \hookrightarrow T^*M$ is given by

$$\iota : x^i \;\mapsto\; \left(x^i, q_i\right) \;:=\; \left(x^i, v_i(x)\right) \,, \tag{3.3}$$

[12] We have already seen this in our discussion around (2.25).

where $v_i = v_i(x)$ are the components of the velocity (co-)vector field, the condition $\iota^*\varpi = 0$ is equivalent to requiring the divergence-free constraint (2.4*b*). Thus, we again obtain a Lagrangian submanifold L of T^*M, and this time L encodes the divergence-free constraint.

Moreover, using $\star_{\mathring{g}}(\mathrm{d}x^i \wedge \mathrm{d}x^j) = \sqrt{\det(\mathring{g})}\varepsilon^{ij}$ and the volume form (3.2*b*) on M, we may rewrite the Monge–Ampère form α defined in (2.23*b*) as

$$\alpha \;=\; \frac{1}{2}\mathring{\nabla}q_i \wedge \mathring{\nabla}q_j \wedge \star_{\mathring{g}}\left(\mathrm{d}x^i \wedge \mathrm{d}x^j\right) - \hat{f}\mathrm{vol}_M \,. \tag{3.4}$$

Again, using (3.2*a*) together with

$$\mathrm{d}\star_{\mathring{g}}(\mathrm{d}x^i \wedge \mathrm{d}x^j) \;=\; 2\mathring{g}^{kl}\mathring{\Gamma}_{kl}{}^{[i}\star_{\mathring{g}}\mathrm{d}x^{j]} + 2\mathring{g}^{k[i}\mathring{\Gamma}_{kl}{}^{j]}\star_{\mathring{g}}\mathrm{d}x^l \tag{3.5a}$$

and

$$\mathrm{d}x^k \wedge \star_{\mathring{g}}(\mathrm{d}x^i \wedge \mathrm{d}x^j) \;=\; -2\mathring{g}^{k[i}\star_{\mathring{g}}\mathrm{d}x^{j]} \tag{3.5b}$$

it is not too difficult to see that α is closed. In addition, the requirement that the pull-back of α under (3.3) vanishes is directly equivalent to the pressure equation (2.10), provided that we simultaneously demand that $\iota^*\varpi = 0$. Notice that we also have $\alpha \wedge \varpi = 0$ so that the pair (ϖ, α) is again a Monge–Ampère structure.

3.1.2. Almost (para-)Hermitian structure. We may now follow our discussion in section 2.2 and define an endomorphism $\hat{\mathcal{J}}$ of the tangent bundle of T^*M by

$$\frac{\alpha}{\sqrt{|\hat{f}|}} \;=:\; \hat{\mathcal{J}} \lrcorner \varpi \tag{3.6}$$

under the assumption that $\hat{f}$ does not vanish. As before, $\hat{\mathcal{J}}$ is an almost complex structure when $\hat{f} > 0$, an almost para-complex structure when $\hat{f} < 0$, and integrable if and only if $\hat{f}$ is constant. As in section 2.2, we can always find a differential two-form $\hat{\mathcal{K}}$ of type $(1,1)$ with respect to $\hat{\mathcal{J}}$ such that $\hat{\mathcal{K}} \wedge \varpi = 0$, $\hat{\mathcal{K}} \wedge (\hat{\mathcal{J}} \lrcorner \varpi) = 0$, and $\hat{\mathcal{K}} \wedge \hat{\mathcal{K}} \neq 0$. In particular, we choose

$$\hat{\mathcal{K}} \;:=\; \sqrt{|\hat{f}|}\,\mathring{\nabla}q_i \wedge \mathrm{d}x^i \,, \tag{3.7}$$

that is, the standard symplectic structure (2.23*b*) times the same function as in (2.25). Importantly, the compatibility of $\hat{\mathcal{K}}$ and $\hat{\mathcal{J}}$ again yields the metric (2.26). It should be noted that the pull-back of the standard symplectic structure $\omega = \mathring{\nabla}q_i \wedge \mathrm{d}x^i$ from (2.23*b*) under (3.3) is $\iota^*\omega = \mathrm{d}v$ and thus, this vanishes if and only if the vorticity (2.11) is zero.

Remark 3.1. In conclusion, the Monge–Ampère structure (ϖ, α), with ϖ defined by (3.1) and α written as (3.4), represents alternative means to describe two-dimensional incompressible fluids. Whilst the Monge–Ampère structure (2.23*b*) yields manifestly the description of the fluid flow in terms of a stream function, the advantage of this alternative Monge–Ampère structure is that with this choice[13], we can straightforwardly generalise our treatment to fluid

[13] The triple of differential two-forms α, $\mathring{\nabla}q_i \wedge \mathrm{d}x^i$, and $\mathring{\nabla}q_i \wedge \star_{\mathring{g}}\mathrm{d}x^i$ define for $\hat{f} > 0$ what is known as an almost quaternionic Hermitian structure on T^*M and for $\hat{f} < 0$ an almost quaternionic para-Hermitian structure, respectively, with the two choices of Monge–Ampère structure we have presented corresponding to picking specific points in the moduli space of such structures.

flows in any dimension. Essentially, this is due to the fact that the conditions $\iota^*\varpi = 0$ and $\iota^*\alpha = 0$ with ι given by (3.3) (with $i = 1,\dots,m$) are equivalent to the divergence-free constraint and the pressure equation in any dimension. However, in $m > 2$ dimensions, we leave the realm of symplectic geometry as we shall explain shortly.

Remark 3.2. At this stage, it is worth noting how our above choices deviate from constructions used in previous works. It is clear that (3.1) and (3.4) are a covariantisation of the Monge–Ampère structure in [9, 10], with (3.6) the corresponding almost (para-)complex structure. However, we are free to make a choice of differential two-form in (3.7), which corresponds to a choice of almost (para)-Hermitian metric on T^*M. In particular, [9] works with the non-degenerate bilinear form

$$g_\alpha(X,Y) := \frac{[(X\lrcorner\alpha)\wedge(Y\lrcorner\varpi)+(Y\lrcorner\alpha)\wedge(X\lrcorner\varpi)]\wedge\mathrm{vol}_M}{\frac{1}{2}\varpi^2} \tag{3.8}$$

for all $X, Y \in \mathfrak{X}(T^*M)$. As discussed in [44, 45], the third differential two-form may be defined by[14] $\sqrt{|\hat{f}|}\,g_\alpha(\hat{\mathcal{J}}X,Y)$ for all $X, Y \in \mathfrak{X}(T^*M)$ in this case. The pull-back of g_α via (3.3) is then simply the Hessian of ψ without vorticity as a conformal factor, in contrast to (2.27), where the vorticity is made manifest. Whilst the presence of the vorticity prefactor is clearly significant in our context, our choice is far from ad-hoc, as it arises perhaps even more naturally from the underlying geometry than (3.8). Note also that the metric (3.8) has been linked in [46] to a metric occurring in the theory of optimal mass transport in which optimal maps are characterised by volume-maximising Lagrangian submanifolds.

3.2. Higher symplectic manifolds

The appropriate notion for our purposes is that of higher symplectic geometry. Here, we shall be rather brief and merely summarise some of the key facts that are needed for our subsequent discussion. For more details, we refer the interested reader to [11–13].

3.2.1. Higher symplectic vector spaces. To begin with, let V be a real vector space and $\varpi \in \bigwedge^{k+1} V^*$ a $(k+1)$-form. Then, ϖ is called non-degenerate if and only if the contraction map $V \to \bigwedge^k V^*$, given by $v \mapsto v\lrcorner\varpi$ for all $v \in V$, is injective. Generally, the contraction map is not surjective; for $k = 1$, however, injectivity implies surjectivity by the rank–nullity theorem, and we obtain the identification $V \cong V^*$ in this case. We call the pair (V,ϖ) with $\varpi \in \bigwedge^{k+1} V^*$ non-degenerate a k-plectic vector space. When $k = 1$, we recover the standard case of a symplectic vector space.

Furthermore, for $U \subseteq V$ a vector subspace of V, we define the ℓth orthogonal complement $U^{\perp,\ell}$ for $\ell = 1,\dots,k$ with respect to ϖ by

$$U^{\perp,\ell} := \{v \in V \,|\, v\lrcorner u_1 \dots \lrcorner u_\ell \lrcorner \varpi = 0 \text{ for all } u_1,\dots u_\ell \in U\}\ . \tag{3.9}$$

Whenever $U = U^{\perp,\ell}$ for some $\ell = 1,\dots,k$, we call the vector subspace U an ℓ-Lagrangian subspace of V. For $k = 1$, there are only 1-Lagrangian subspaces (or simply Lagrangian subspaces), and they all have the same dimension $\frac{1}{2}\dim(V)$. For $k > 1$, ℓ-Lagrangian subspaces may have different dimensions.

[14] Whilst we present these expressions in our notation, the literature only treats the Euclidean case.

3.2.2. Higher symplectic manifolds. Let M be a manifold and $\varpi \in \Omega^{k+1}(M)$ a differential $(k+1)$-form which is point-wise non-degenerate. Suppose also that ϖ is closed. Such a manifold is called a k-plectic manifold, and in this case ϖ is referred to as a k-plectic structure. A diffeomorphism on M that preserves ϖ is called a k-plectomorphism. Furthermore, a submanifold $L \hookrightarrow M$ is called an ℓ-Lagrangian submanifold of M if and only if $TL = TL^{\perp,\ell}$ for some $\ell = 1,\dots,k$. Here, we have used the obvious notation

$$TL^{\perp,\ell} := \bigcup_{p\in L}\left\{(p,X_p)\,|\,X_p \in (T_pL)^{\perp,\ell}\right\} . \tag{3.10}$$

3.3. Higher Monge–Ampère geometry of three-dimensional fluid flows

Having introduced the notion of k-plectic manifolds, we can now make precise the description of higher-dimensional incompressible fluid flows.

3.3.1. Higher Monge–Ampère structure. In $m = 3$ dimensions, the components (2.5) of the Riemann and Ricci curvature tensors are related by the identity

$$\mathring{R}_{ijk}{}^{l} = 2\mathring{R}^{l}{}_{[i}\mathring{g}_{j]k} - 2\left(\mathring{R}_{k[i} - \frac{1}{2}\mathring{R}\mathring{g}_{k[i}\right)\delta_{j]}{}^{l} , \tag{3.11}$$

where $\mathring{R}$ is the curvature scalar. Upon following our above discussion and setting

$$\hat{f} := \frac{1}{2}\left(\mathring{\Delta}_{\mathrm{B}}p + \mathring{R}^{ij}q_iq_j\right) , \tag{3.12a}$$

we consider the pair of differential three-forms

$$\begin{aligned} \varpi &:= \mathring{\nabla}q_i \wedge \star_{\mathring{g}}\mathrm{d}x^i , \\ \alpha &:= \frac{1}{2}\mathring{\nabla}q_i \wedge \mathring{\nabla}q_j \wedge \star_{\mathring{g}}\left(\mathrm{d}x^i \wedge \mathrm{d}x^j\right) - \hat{f}\mathrm{vol}_M \end{aligned} \tag{3.12b}$$

on T^*M, where the volume form on M is now given by

$$\mathrm{vol}_M := \frac{\sqrt{\det(\mathring{g})}}{3!}\varepsilon_{ijk}\mathrm{d}x^i \wedge \mathrm{d}x^j \wedge \mathrm{d}x^k . \tag{3.12c}$$

Again, ϖ is non-degenerate and closed by virtue of (3.2*a*) and so, ϖ defines a two-plectic structure on T^*M. The submanifold $\iota : L \hookrightarrow T^*M$ defined by $\iota^*\varpi = 0$ with ι given by (3.3) with $i = 1,2,3$ is a three-dimensional two-Lagrangian submanifold of the two-plectic manifold (T^*M,ϖ). As discussed above, the conditions $\iota^*\varpi = 0$ and $\iota^*\alpha = 0$ are equivalent to the divergence-free constraint (2.4*b*) and the pressure equation (2.10), respectively. Furthermore, by virtue of (3.2*a*) and (3.5*a*), α is closed. It is also non-degenerate, so (T^*M,α) defines a two-plectic manifold. Note that (3.12*b*) can be understood as a covariantisation of what was given previously in [9, 10]. Note also that, for

$$\omega = \mathring{\nabla}q_i \wedge \mathrm{d}x^i \tag{3.13}$$

the standard symplectic structure on T^*M, $\varpi \wedge \omega = 0$ and $\alpha \wedge \omega = 0$, so ϖ and α are both Monge–Ampère forms for ω.

Importantly, the formulation (3.12*b*) makes it transparent that this construction works in any dimension $m>1$. Indeed, we simply need to take the appropriate volume form in α and the function $\hat{f}$ is the same in any dimension. The pull-backs $\iota^*\varpi=0$ and $\iota^*\alpha=0$ then yield the divergence-free constraint and the pressure equation. Furthermore, ϖ is $(m-1)$-plectic, and it defines an m-dimensional $(m-1)$-Lagrangian submanifold for general m. However, in general, whilst α is $(m-1)$-plectic, it may not define an m-dimensional $(m-1)$-Lagrangian submanifold. It should also be noted that $\alpha\wedge\varpi$ vanishes if and only if $m\neq 3$.

3.3.2. Almost (para-)Hermitian structure. Next, we wish to generalise the relation (3.6). To this end, we use the results of [47]. In particular, we note that the there is a isomorphism $\Omega^5(T^*M)\cong\mathfrak{X}(T^*M)\otimes\Omega^6(T^*M)$ that is induced by the natural exterior product pairing $\Omega^1(T^*M)\otimes\Omega^5(T^*M)\to\Omega^6(T^*M)$[15]. Consequently, upon letting ω be the standard symplectic structure on T^*M as in (3.13) and ε be the poly-vector field dual to the Liouville volume form $\frac{1}{3!}\omega^3$ on T^*M, that is, $\varepsilon\lrcorner\frac{1}{3!}\omega^3=1$, we may associate with the differential three-form α defined in (3.12*b*) the endomorphism

$$\hat{\mathcal{J}}X \;:=\; -\frac{1}{2\sqrt{|\hat{f}|}}\,\varepsilon\lrcorner(\alpha\wedge X\lrcorner\alpha)\quad\text{for all}\quad X\,\in\,\mathfrak{X}(T^*M) \tag{3.14}$$

under the assumption that $\hat{f}$ does not vanish. It then follows that $\hat{\mathcal{J}}$ is an almost complex structure on T^*M when $\hat{f}>0$ and an almost para-complex structure when $\hat{f}<0$. Since α is closed and can also be taken as the imaginary part of a holomorphic top form with respect to (3.14), this choice of endomorphism, in fact, defines what is known as a nearly (para-) Calabi–Yau structure [48, 49].

Furthermore, the differential two-form $\hat{\mathcal{K}}$ defined in (3.7), now with i running from one to three, together with (3.14), satisfies $\hat{\mathcal{K}}(\hat{\mathcal{J}}X,Y)=-\hat{\mathcal{K}}(X,\hat{\mathcal{J}}Y)$ for all $X,Y\in\mathfrak{X}(T^*M)$. Consequently, we can define an almost (para-)Hermitian metric $\hat{g}$ on T^*M with respect to (3.14) by setting $\hat{g}(X,Y):=\hat{\mathcal{K}}(X,\hat{\mathcal{J}}Y)$ for all $X,Y\in\mathfrak{X}(T^*M)$. Explicitly,

$$\hat{g}\;=\;\frac{1}{2}\hat{f}\mathring{g}_{ij}\mathrm{d}x^i\odot\mathrm{d}x^j+\frac{1}{2}\mathring{g}^{ij}\mathring{\nabla}q_i\odot\mathring{\nabla}q_j\,. \tag{3.15}$$

Evidently, this metric is the direct generalisation of (2.26), and it is essentially a covariantisation that follows from a bilinear form introduced in [14] (see also [10]). This thus makes $\hat{\mathcal{K}}$ of type $(1,1)$ with respect to (3.14). This also justifies using the same letter $\hat{\mathcal{J}}$ in the definition (3.14) as it is a direct generalisation of (3.6).

Remark 3.3. We can make the relationship between (3.6) and (3.14) more explicit. To make a notational distinction between the dimensions $m=2$ and $m=3$, we shall write $(M^m,\mathring{g}_m)$ as well as ϖ_m and α_m for (3.12*b*), $\hat{\mathcal{J}}_m$ for (3.6) and (3.14), and ω_m for the standard symplectic structure. In addition, we let ε_m be the poly-vector field dual to Liouville volume form on T^*M^m with respect to ω_m.

Firstly, it is not too difficult to see that (3.6) can be rewritten as

$$\hat{\mathcal{J}}_2X\;=\;\frac{1}{\sqrt{|\hat{f}|}}\,\varepsilon_2\lrcorner(\varpi_2\wedge X\lrcorner\alpha_2)\quad\text{for all}\quad X\,\in\,\mathfrak{X}\left(T^*M^2\right)\,. \tag{3.16}$$

[15] Explicitly, $\phi:\Omega^5(T^*M)\to\mathfrak{X}(T^*M)\otimes\Omega^6(T^*M)$ is given by $\phi(\rho)(\lambda,X_1,\ldots,X_6):=X_1\lrcorner\ldots\lrcorner X_6\lrcorner(\rho\wedge\lambda)$ for all $\rho\in\Omega^5(T^*M)$, $\lambda\in\Omega^1(T^*M)$, and $X_1,\ldots,X_6\in\mathfrak{X}(T^*M)$.

Note that $\omega_2 \wedge \omega_2 = \varpi_2 \wedge \varpi_2$ and so, ε_2 is also dual to the Liouville volume form with respect to ϖ_2. Next, let us assume that M^3 factorises as $M^3 = M^2 \times N$ with N a one-dimensional manifold, and we take

$$\mathring{g}_3 \;=\; \mathring{g}_2 + \mathrm{d}x^3 \otimes \mathrm{d}x^3 \;, \tag{3.17}$$

as the metric on M^3 with $\mathring{g}_2$ a metric on M^2 and x^3 a local coordinate coordinate on N. Assuming that $p \in \mathscr{C}^\infty(M^2)$, a short calculation then reveals that

$$\varpi_3 \;=\; \varpi_2 \wedge \mathrm{d}x^3 + \mathrm{vol}_{M^2} \wedge \mathrm{d}q_3 \quad \text{and} \quad \alpha_3 \;=\; \alpha_2 \wedge \mathrm{d}x^3 + \varpi_2 \wedge \mathrm{d}q_3 \;. \tag{3.18}$$

The decomposition for α_3 and the effectiveness $\alpha_2 \wedge \varpi_2 = 0$ imply that

$$\alpha_3 \wedge (X \lrcorner \alpha_3) \;=\; -2\,(\varpi_2 \wedge X \lrcorner \alpha_2)\,\mathrm{d}q_3 \wedge \mathrm{d}x^3 \tag{3.19}$$

for all $X \in \mathfrak{X}(T^*M^2)$.[16] Since $\varepsilon_3 = \varepsilon_2 \wedge \frac{\partial}{\partial x^3} \wedge \frac{\partial}{\partial q_3}$, this then yields

$$\varepsilon_3 \lrcorner (\alpha_3 \wedge X \lrcorner \alpha_3) \;=\; -2\varepsilon_2 \lrcorner (\varpi_2 \wedge X \lrcorner \alpha_2) \;. \tag{3.20}$$

Consequently, combining this result with (3.14) and (3.16), we finally obtain

$$\hat{\mathcal{J}}_3|_{M^2} \;=\; \hat{\mathcal{J}}_2 \;. \tag{3.21}$$

Remark 3.4. The metrics (2.26) and (3.15) on T^*M are in spirit of the rescaled Sasaki metrics studied e.g. in [50]. The main difference here is that our $\hat{f}$ is a function on T^*M rather than on M. This results in a metric (3.15) which is allowed to change type across T^*M. Furthermore, earlier work [51] has focused on constructing almost para-Nordenian manifolds in the case $\hat{f} > 0$, preferentially selecting a structure which is almost para-complex [52], as opposed to almost complex.

Before moving on, we conclude with some remarks concerning the curvatures of the metric (3.15) on T^*M and its pull-back to L, as well as a connection with helicity.

3.3.3. Curvature. In view of our later applications, let us state the curvature scalar for the metric (3.15). The following is derived in appendix C.2 and holds in any dimension. In particular, we have

$$\begin{aligned}\hat{R} \;=\;& \frac{1}{\hat{f}}\mathring{R} - \frac{1}{4\hat{f}^2}\mathring{R}_{ijk}{}^{l}\mathring{R}^{ijkm}q_k q_m - (m-1)\,\hat{\Delta}_{\mathrm{B}}\log\left(|\hat{f}|\right) - \mathring{g}_{ij}\frac{\partial^2}{\partial q_i \partial q_j}\log\left(|\hat{f}|\right) \\ &+ \frac{1}{4\hat{f}}(m-1)(m-2)\,\mathring{g}^{ij}\left(\frac{\partial}{\partial x^i} + \mathring{\Gamma}_{ik}{}^{l}q_l\frac{\partial}{\partial q_k}\right)\log\left(|\hat{f}|\right)\left(\frac{\partial}{\partial x^j} + \mathring{\Gamma}_{jm}{}^{n}q_n\frac{\partial}{\partial q_m}\right)\log\left(|\hat{f}|\right) \\ &+ \frac{1}{4}m(m-3)\,\mathring{g}_{ij}\frac{\partial}{\partial q_i}\log\left(|\hat{f}|\right)\frac{\partial}{\partial q_j}\log\left(|\hat{f}|\right) \;,\end{aligned} \tag{3.22}$$

where $\hat{\Delta}_{\mathrm{B}}$ is the Beltrami Laplacian for $\hat{g}$. The occurrence of the term $\hat{\Delta}_{\mathrm{B}}\log(|\hat{f}|)$ again suggests that the accumulation of $\hat{f}$ will determine the sign of the scalar curvature, as it does in the two-dimensional case.

[16] The horizontal lift of X to T^*M^3 is trivial because of the assumed form of the metric $\mathring{g}_3$.

3.3.4. Pull-back metric. It is a straightforward exercise to check that the pull-back $g := \iota^* \hat{g}$ of (3.15) to the 2-Lagrangian submanifold L via ι given by (3.3) with $i = 1,2,3$ is

$$g \;=\; \frac{1}{2} g_{ij} \mathrm{d}x^i \odot \mathrm{d}x^j \quad \text{with} \quad g_{ij} \;:=\; A^k{}_i A_{kj} - \frac{1}{2} \mathring{g}_{ij} A_{kl} A^{lk} \,. \tag{3.23}$$

Here, we have made use of the velocity-gradient tensor $A_{ij} := \mathring{\nabla}_j v_i$ and noted that

$$f \;:=\; \iota^* \hat{f} \;=\; \frac{1}{2} \left(\zeta_{ij} \zeta^{ij} - S_{ij} S^{ij} \right) \;=\; -\frac{1}{2} A_{ij} A^{ji} \tag{3.24}$$

with ζ_{ij} the vorticity two-form and S_{ij} the rate-of-strain tensor introduced in (2.11), and the indices on ζ_{ij}, S_{ij}, and A_{ij} raised with the background metric. Again, as in the two-dimensional case, the pull-back metric is a quadratic function of the velocity gradient tensor and curvature will be generated by gradients of vorticity and rate-of-strain.

3.3.5. Helicity. In two dimensions, we utilised the local Gauß–Bonnet theorem (2.29) in order to relate the geometry of fluid flows, as described by the curvature scalar (2.33*a*), to a topological invariant, namely the Euler characteristic of a given compact region. In three dimensions, it quickly becomes apparent that this is not a suitable approach and that we require an alternative topological quantity.

Recall that the pull-back of the standard symplectic form ω seen in (3.13), under (3.3), is $\iota^* \omega = \mathrm{d}v = \zeta_{ij} \mathrm{d}x^i \wedge \mathrm{d}x^j$ with ζ_{ij} the vorticity. The pull-back of the associated tautological one-form $\theta := q_i \mathrm{d}x^i$ is simply $v = v_i \mathrm{d}x^i$. It then follows that

$$\iota^* \left(\theta \wedge \mathrm{d}\theta \right) \;=\; v_i \zeta^i \, \mathrm{vol}_{M^3} \quad \text{with} \quad \zeta^i \;:=\; \sqrt{\det(\mathring{g}_3)} \varepsilon^{ijk} \zeta_{jk} \tag{3.25}$$

the vorticity in three dimensions, derived from (2.11). Integrals of quantities of the form (3.25), over a compact region $U \subseteq M^3$, are referred to as helicity [53, 54]. Hence, in our context, $v_i \zeta^i$ may be referred to as the helicity per volume.

Consider an inviscid, incompressible fluid, with kinematics described by the Euler equations, on a compact region $U \subseteq M^3$. Suppose also that U describes the volume contained inside a closed orientable surface, which is moving with the fluid and has (outward) unit normal n with components denoted n_i. It is shown[17] in [53] that, provided the distribution of vorticity is local and continuous, and $n_i \zeta^i = 0$, then the integral of (3.25) is an invariant of the Euler equations and the vorticity field within the volume is conserved. Furthermore, it is shown that for discrete vortex filaments, this quantity can be associated[18] with the topological invariants given by the Gaußlinking number and Călugăreanu invariant [57, 58]. In [59] it was also shown that helicities are isotopy invariants of their volume. Perhaps more significantly, a recent work [60] has managed to demonstrate that, in ideal conditions, helicity-type quantities can be reinterpreted as Abelian Chern–Simons actions and hence can be related to the Jones polynomial.

In addition to the interpretation of the pull-backs of (3.12*b*) under (3.3) as the divergence-free constraint and the pressure equation, we now also have that the corresponding pull-back of the standard symplectic form encodes the helicity. Additionally, previous work relating helicity to various topological invariants suggests that, as in two dimensions, one can relate the topology of fluid flows to our geometric constructions.

[17] In the context of magneto-hydrodynamics, the analogous result was presented in [54].

[18] We point the interested reader towards [55, 56] for elaboration on these associations.

3.4. Examples in three dimensions

In this section, we adopt the notation $x := x^1$, $y := x^2$, and $z := x^3$ and consider some classical examples of flows in $\mathbb{R}^3$ with background metric $\mathring{g}_{ij} = \delta_{ij}$.

3.4.1. Preliminaries. Recall the expressions of the vorticity two-form and the rate-of-strain tensor defined in (2.11). In view of our discussion below, we set

$$\zeta =: \begin{pmatrix} 0 & \zeta_3 & -\zeta_2 \\ -\zeta_3 & 0 & \zeta_1 \\ \zeta_2 & -\zeta_1 & 0 \end{pmatrix} \quad \text{and} \quad S =: \begin{pmatrix} \alpha & \sigma_3 & \sigma_2 \\ \sigma_3 & \beta & \sigma_1 \\ \sigma_2 & \sigma_1 & \gamma \end{pmatrix} \tag{3.26a}$$

and introduce the velocity-gradient matrix

$$A := S - \zeta = \begin{pmatrix} \alpha & \sigma_3 - \zeta_3 & \sigma_2 + \zeta_2 \\ \sigma_3 + \zeta_3 & \beta & \sigma_1 - \zeta_1 \\ \sigma_2 - \zeta_2 & \sigma_1 + \zeta_1 & \gamma \end{pmatrix}. \tag{3.26b}$$

Furthermore, the metric (3.15) in the then takes the form

$$\hat{g} = \begin{pmatrix} \frac{1}{2}\Delta p \mathbb{1}_3 & 0 \\ 0 & \mathbb{1}_3 \end{pmatrix} \quad \text{with} \quad \Delta p = -\operatorname{tr}\left(A^2\right). \tag{3.27}$$

It now follows that the pull-back metric (3.23) is

$$g = A^{\mathsf{T}} A - \frac{1}{2}\operatorname{tr}\left(A^2\right)\mathbb{1}_3 . \tag{3.28}$$

Whilst it is now possible to substitute (3.26*b*) into (3.28), the result would not be particularly helpful. To see the structure of the pull-back metric a little more clearly, we next consider Burgers' canonical model of the vortex, for which the velocity-gradient matrix takes a relatively simple form, and which in turn motivates our work on higher symplectic reduction. Studying this example will show how the signature of the metric depends on relationships between vorticity and rate-of-strain.

3.4.2. Burgers' vortex. Earlier works [7, 9] considered a class of solutions to the three-dimensional incompressible Euler and Navier–Stokes equations, with Euclidean background metric, that can be reduced to solutions to the incompressible equations in two dimensions via the Lundgren transformation [61]. Such solutions, which take the form [62]

$$(\dot{x}, \dot{y}, \dot{z}) := \left(v_x(t,x,y), v_y(t,x,y), z\phi(t,x,y) + W(t,x,y)\right) \tag{3.29}$$

for some functions ϕ and W, where the superposed dot refers to the derivative with respect to the time t, are often referred to as two-and-a-half-dimensional flows [63]. In particular, a geometric description of Burgers' vortex [64] has been presented through this lens.

Consider the following idealised Burgers' vortex [64] with the velocity components be given by

$$u = \alpha x + (\sigma_3 - \zeta_3) y , \quad v = \beta y + (\sigma_3 + \zeta_3) x , \quad \text{and} \quad w = \gamma z \tag{3.30}$$

with α, β, γ, σ_3, and ζ_3 constant in space. Then, the divergence-free constraint is given by $\alpha+\beta+\gamma=0$. In particular, we have chosen $\phi=\gamma(t)$ and $W\equiv 0$ in (3.29).

Next, the velocity-gradient matrix is simply

$$A \;=\; \begin{pmatrix} \alpha & \sigma_3-\zeta_3 & 0 \\ \sigma_3+\zeta_3 & \beta & 0 \\ 0 & 0 & \gamma \end{pmatrix}, \tag{3.31}$$

and using the divergence-free constraint, it follows that

$$\frac{1}{2}\Delta p \;=\; -\frac{1}{2}\mathrm{tr}\left(A^2\right) \;=\; \alpha\beta+\gamma\left(\alpha+\beta\right)+\zeta_3^2-\sigma_3^2\,. \tag{3.32}$$

We can now deduce that the pull-back metric (3.28) is

$$g \;=\; \begin{pmatrix} \gamma\beta+2\zeta_3\left(\sigma_3+\zeta_3\right) & \alpha\left(\sigma_3-\zeta_3\right)+\beta\left(\sigma_3+\zeta_3\right) & 0 \\ \alpha\left(\sigma_3-\zeta_3\right)+\beta\left(\sigma_3+\zeta_3\right) & \gamma\alpha+2\zeta_3\left(\zeta_3-\sigma_3\right) & 0 \\ 0 & 0 & \alpha\beta+\left(\zeta_3-\sigma_3\right)\left(\zeta_3+\sigma_3\right) \end{pmatrix} \tag{3.33}$$

which has eigenvalues

$$E_\pm \;=\; \frac{1}{2}\left\{4\zeta_3^2-\gamma^2\pm\sqrt{\gamma^2\left(\alpha-\beta\right)^2+4\left[4\sigma_3^2\zeta_3^2+\left(\alpha+\beta\right)^2\sigma_3^2+\left(\alpha-\beta\right)^2\zeta_3^2\right]}\right\}, \tag{3.34}$$

$$E_3 \;=\; \alpha\beta-\sigma_3^2+\zeta_3^2\,.$$

The top left (2×2)-block of (3.33), with $\gamma=0$ is precisely the pull-back metric of an incompressible two-dimensional flow with velocity-gradient matrix given by the top left (2×2)-block of (3.31), where $\gamma=-(\alpha+\beta)=0$. Hence, setting $\gamma\neq 0$ produces compressible two-dimensional flows, for example Burgers' vortex after reduction as described in [9]. It follows that when $\Delta p>0$, $E_3>0$. Furthermore, if we assume axi-symmetry by setting $\alpha=\beta=-\frac{1}{2}\gamma$, then with $\Delta p>0$ and $E_3>0$, we have $E_+>0$, while E_- is bounded below by $-\gamma^2$. Further investigation of such criteria might facilitate a classification of conditions under which accumulations of vorticity could constitute 'a vortex'.

With [9] in mind, we now show how higher symplectic geometry and reductions thereof, provide a mechanism for formulating the Monge–Ampère geometry of certain exact solutions to the incompressible Navier–Stokes equations in three dimensions.

3.5. *Higher symplectic reductions*

In the following, we wish to study dimensional reductions from three to two dimensions. In particular, we shall focus on symplectic and higher symplectic reductions. This will enable us to study fluid flows in three dimensions with symmetries that eventually can be analysed as effective two-dimensional problems. As we shall explain, symplectic and higher symplectic reductions yield, to the extent in which we are interested in this paper, essentially the same geometric information in two dimensions; however, the higher symplectic reduction will yield the two-dimensional problem directly in terms of a stream function, thus resolving the lower-dimensional would-be divergence-free constraint automatically. Before analysing examples in section 3.6, including the Arnol'd–Beltrami–Childress flow and Hicks–Moffatt-type vortices, let us set the stage. In particular, we first recall the Marsden–Weinstein reduction process

[65, 66], a well-known tool from symplectic geometry, for reducing spaces with symmetries. Concretely, this reduction process can be summarised as follows.

Theorem 3.5. *Let (M,ω) be a symplectic manifold. Suppose that G is a Lie group acting by symplectomorphisms on (M,ω). Let $\mu : M \to \mathfrak{g}^*$ be the moment map for this action with $\mathfrak{g}$ the Lie algebra of G. Furthermore, let $c \in \mathfrak{g}^*$ be a regular value of μ and $\mathsf{G}_c \subseteq \mathsf{G}$ the (coadjoint) stabiliser group of c. We assume that G_c acts freely and properly on $\mu^{-1}(\{c\})$. Set $M_c := \mu^{-1}(\{c\})/\mathsf{G}_c$ and consider,*

$$\begin{array}{ccc} \mu^{-1}(\{c\}) & \xhookrightarrow{\mathfrak{i}} & M \\ \big\downarrow{\scriptstyle \mathfrak{p}} & & \\ M_c & & \end{array} \tag{3.35}$$

Then, there exists a unique symplectic structure ω_c on M_c such that $\mathfrak{p}^*\omega_c = \mathfrak{i}^*\omega$.

To discuss symmetry reductions of higher-dimensional fluid flows which are described directly in terms of higher Monge–Ampère structures, we would like to generalise this result to the higher symplectic geometry summarised in section 3. Fortunately for us, theorem 3.5 has been generalised to the k-plectic case rather recently as follows [21].

Theorem 3.6. *Let (M,ϖ) be a k-plectic manifold. Suppose that G is a Lie group acting by k-plectomorphisms on (M,ϖ). Let $\mu : M \to \bigwedge^{k-1} T^*M \otimes \mathfrak{g}^*$ be the moment map for this action with $\mathfrak{g}$ the Lie algebra of G. Furthermore, let $c \in \Omega^{k-1}(M,\mathfrak{g}^*)$ be closed and define*

$$\begin{aligned} \mu^{-1}(\{c\}) &:= \{x \in M \,|\, \mu(x) = c_x\}\,, \\ \mathsf{G}_c &:= \{g \in \mathsf{G} \,\big|\, g_*^{-1}X_1 \lrcorner \ldots \lrcorner g_*^{-1}X_{k-1} \lrcorner \mathrm{Ad}^*_g c_{g^{-1}x} = X_1 \lrcorner \ldots \lrcorner X_{k-1} \lrcorner c_x \\ &\qquad \text{for all } x \in M \text{and for all } X_1,\ldots,X_{k-1} \in T_xM\}\,. \end{aligned} \tag{3.36}$$

Suppose that $\mu^{-1}(\{c\})$ is an embedded submanifold of M and that G_c acts freely and properly on $\mu^{-1}(\{c\})$. Set $M_c := \mu^{-1}(\{c\})/\mathsf{G}_c$ and consider,

$$\begin{array}{ccc} \mu^{-1}(\{c\}) & \xhookrightarrow{\mathfrak{i}} & M \\ \big\downarrow{\scriptstyle \mathfrak{p}} & & \\ M_c & & \end{array} \tag{3.37}$$

Then, there exists a unique closed differential form $\varpi_c \in \Omega^{k+1}(M_c)$ on M_c such that $\mathfrak{p}^*\varpi_c = \mathfrak{i}^*\varpi$.

Evidently, for $k = 1$ this result reduces to theorem 3.5. It is important to stress that for $k > 1$, the differential form $\varpi_c \in \Omega^{k+1}(M_c)$ might be degenerate. For full details of the above, see [21].

3.5.1. Setting for dimensional reduction. In remark 3.3, we have already discussed a simple dimensional reduction of the Monge–Ampère structure (3.12*b*) by assuming that the three-dimensional background manifold M^3 is a direct product of a two-dimensional manifold M^2

and a one-dimensional manifold N. Let us now assume it is of warped-product form instead, that is, we take

$$\mathring{g}_3 \;=\; \mathring{g}_2 + \mathrm{e}^{2\varphi}\,\mathrm{d}x^3 \otimes \mathrm{d}x^3 \tag{3.38}$$

with $\varphi \in \mathscr{C}^\infty(M^2)$ as the metric on M^3 where $\mathring{g}_2$ is a metric on M^2 and x^3 local coordinates on N, respectively. Put differently, we assume that there is a one-parameter family of isometries, and we choose adapted coordinates. Now let $i,j,\ldots = 1,2$, such that

$$\mathring{g}_2 \;=\; \frac{1}{2}\mathring{g}_{ij}\mathrm{d}x^i \odot \mathrm{d}x^j\,. \tag{3.39}$$

Hence, the only non-vanishing Christoffel symbols for the metric $\mathring{g}_3$ are $\mathring{\Gamma}_{ij}{}^k$, which are precisely the Christoffel symbols for $\mathring{g}_2$, alongside

$$\mathring{\Gamma}_{33}{}^i \;=\; -\mathrm{e}^{2\varphi}\mathring{g}^{ij}\partial_j\varphi \quad\text{and}\quad \mathring{\Gamma}_{i3}{}^3 \;=\; \partial_i\varphi\,. \tag{3.40}$$

Next, consider the differential forms (3.12*b*) on M^m for $m = 2,3$. As in remark 3.3, let us denote them by ϖ_m and α_m, and let us also use a similar notation for other quantities. Then, under the assumption that $p \in \mathscr{C}^\infty(M^2)$, some algebra reveals that

$$\begin{aligned}\varpi_3 \;&=\; \mathrm{e}^{\varphi}\,\varpi_2 \wedge \mathrm{d}x^3 + \mathrm{e}^{-\varphi}\,\mathrm{vol}_{M^2} \wedge \mathring{\nabla} q_3\,,\\ \alpha_3 \;&=\; \mathrm{e}^{\varphi}(\alpha_2 - \hat{h}_+\mathrm{vol}_{M^2}) \wedge \mathrm{d}x^3 + \mathrm{e}^{-\varphi}\,(\varpi_2 - q_3\mathrm{d}x^3 \wedge \star_{\mathring{g}_2}\mathrm{d}\varphi) \wedge \mathring{\nabla} q_3\end{aligned} \tag{3.41*a*}$$

with

$$\hat{h}_\pm \;:=\; \frac{1}{2}[\mathring{\nabla}^i\varphi\partial_i p - (\mathring{\nabla}^i\mathring{\nabla}^j\varphi \pm \mathring{\nabla}^i\varphi\mathring{\nabla}^j\varphi)q_iq_j - \mathrm{e}^{-2\varphi}(\mathring{\Delta}_{\mathrm{B}}\varphi \pm \mathring{\nabla}^i\varphi\partial_i\varphi)q_3^2]\,, \tag{3.41*b*}$$

where again all differential operators in $\hat{h}_\pm$ are with respect to the metric $\mathring{g}_2$.

Furthermore, we obtain

$$\begin{aligned}\varpi_2' \;&:=\; \frac{\partial}{\partial x^3} \lrcorner\, \varpi_3\\ &=\; \mathrm{e}^{\varphi}(\varpi_2 + q_i\mathring{\nabla}^i\varphi\,\mathrm{vol}_{M^2})\,,\\ \alpha_2' \;&:=\; \frac{\partial}{\partial x^3} \lrcorner\, \alpha_3\\ &=\; \mathrm{e}^{\varphi}[\alpha_2 - (\hat{h}_+ + \mathrm{e}^{-2\varphi}\mathring{\nabla}^i\varphi\partial_i\varphi\, q_3^2)\,\mathrm{vol}_{M^2} + q_i\mathring{\nabla}^i\varphi\,\varpi_2] + \mathrm{e}^{-\varphi}q_3\mathrm{d}q_3 \wedge \star_{\mathring{g}_2}\mathrm{d}\varphi\,.\end{aligned} \tag{3.42}$$

A short calculation then shows that both ϖ_2' and α_2' are closed. In fact, using (3.2*b*), we also have that

$$\varpi_2' \;=\; \mathrm{d}(\star_{\mathring{g}_2}\mathrm{e}^{\varphi}\,q_i\mathrm{d}x^i)\,. \tag{3.43}$$

3.5.2. Symplectic reduction of the higher Monge–Ampère structure. Given that ϖ_2' and α_2' are closed, Cartan's formula for Lie derivatives then immediately yields that $\mathcal{L}_{\frac{\partial}{\partial x^3}}\varpi_3 = 0 = \mathcal{L}_{\frac{\partial}{\partial x^3}}\alpha_3$. Consequently, we can consider a dimensional reduction following theorem 3.5. In particular, we take the symplectic form

$$\omega_3 \;:=\; \mathrm{d}q_i\wedge\mathrm{d}x^i - \mathrm{d}\left(\lambda q_3\right)\wedge\mathrm{d}x^3\;, \tag{3.44}$$

where $\lambda\in\mathscr{C}^\infty(M^2)$ is assumed to be non-vanishing. Evidently, $\frac{\partial}{\partial x^3}\lrcorner\,\omega_3 = \mathrm{d}(\lambda q_3)$, so the corresponding moment map is $\mu(x,q) = \lambda q_3$. Hence,

$$\mu^{-1}\left(\{c\}\right) \;=\; \left\{(x,q)\,|\,q_3 = c\,\lambda^{-1}\right\} \tag{3.45}$$

for any regular value $c\in\mathbb{R}$. Consequently, $\mu^{-1}(\{c\})/\mathsf{G}_c$ is locally given by $(x^i,x^3,q_i,q_3) = (x^i,\mathrm{const},q_i,q_3 = q_3(x^i))$. Next, by virtue of theorem 3.5, we obtain the symplectic form

$$\omega_c \;:=\; \mathrm{d}q_i\wedge\mathrm{d}x^i \tag{3.46}$$

on $\mu^{-1}(\{c\})/\mathsf{G}_c\cong T^*M^2$ which satisfies $\mathfrak{p}^*\omega_c = \mathfrak{i}^*\omega_3$, as well as two closed differential two-forms given by

$$\begin{aligned}\tilde{\varpi}_2 \;&:=\; \mathrm{e}^{\varphi}\left(\varpi_2 + q_i\mathring{\nabla}^i\varphi\,\mathrm{vol}_{M^2}\right)\,,\\ \tilde{\alpha}_2 \;&:=\; \mathrm{e}^{\varphi}\left\{\alpha_2 - \left[\hat{h}_+ + \mathrm{e}^{-2\varphi}\left(\mathring{\nabla}^i\varphi\partial_i\varphi\,q_3^2 - q_3\mathring{\nabla}^i\varphi\partial_i q_3\right)\right]\mathrm{vol}_{M^2} + q_i\mathring{\nabla}^i\varphi\,\varpi_2\right\}\,,\end{aligned} \tag{3.47}$$

which are simply the differential two-forms from (3.42) with q_3 understood as a function of x^1 and x^2. Upon requiring the vanishing of the pull-back of $\tilde{\varpi}_2$ and $\tilde{\alpha}_2$ along (3.3) together with the relabeling the function q_3 by v_3, we obtain

$$\begin{aligned}\mathring{\nabla}_i v^i \;&=\; -v^i\partial_i\varphi\,,\\ \mathring{\Delta}_{\mathrm{B}}p + \mathring{\nabla}_i v^j\mathring{\nabla}_j v^i + \frac{1}{2}|v|^2\mathring{R} \;&=\; -\mathring{g}^{ij}\partial_i\varphi\partial_j p + v^i v^j\mathring{\nabla}_i\partial_j\varphi\\ &\quad + \mathrm{e}^{-2\varphi}\left[\left(\mathring{\Delta}_{\mathrm{B}}\varphi - \mathring{g}^{ij}\partial_i\varphi\partial_j\varphi\right)v_3^2 + 2v_3\mathring{g}^{ij}\partial_i\varphi\partial_j v_3\right]\,.\end{aligned} \tag{3.48}$$

These are precisely the divergence-free constraint (2.4*b*) and the pressure equation (2.10) when adapted to the warped product metric (3.38), under the assumption that p is independent of x^3. Evidently, when $\varphi = 0$, we obtain the standard situation of an incompressible fluid flow in two dimensions from section 2.2, and v_3 is not constrained by (3.48).

Next, let X be a vector field on $\mu^{-1}(\{c\})/\mathsf{G}_c\cong T^*M^2$ and consider its horizontal lift $\tilde{X}$ to T^*M^3 using the Levi–Civita connection for the metric (3.38),

$$\tilde{X} \;:=\; X + X\lrcorner\,\mathrm{d}x^i\mathring{\Gamma}_{i3}{}^3 q_3\frac{\partial}{\partial q_3} \;=\; X + X\lrcorner\,\mathrm{d}\varphi\,q_3\frac{\partial}{\partial q_3}\,. \tag{3.49}$$

Using that

$$\tilde{X}\lrcorner\,\mathring{\nabla}q_3 \;=\; 0 \quad\text{and}\quad \varpi_2\wedge\left(\alpha_2 - \hat{h}_+\,\mathrm{vol}_{M^2}\right) \;=\; 0\,, \tag{3.50}$$

we obtain

$$\alpha_3\wedge\left(\tilde{X}\lrcorner\,\alpha_3\right) \;=\; -2\varpi_2\wedge X\lrcorner\left(\alpha_2 - \hat{h}_+\,\mathrm{vol}_{M^2}\right)\wedge\mathring{\nabla}q_3\wedge\mathrm{d}x^3\,. \tag{3.51}$$

Consequently, the endomorphism (3.14) becomes

$$\hat{\mathcal{J}}_3\tilde{X} \;=\; \frac{1}{\sqrt{|\hat{f}_2+\hat{h}_+|}}\,\varepsilon_2 \lrcorner \left[\varpi_2 \wedge X \lrcorner \left(\alpha_2 - \hat{h}_+\,\mathrm{vol}_{M^2}\right)\right] , \tag{3.52}$$

where ε_2 is the dual to the Liouville volume form on T^*M^2; see also remark 3.3. Hence, we obtain an endomorphism $\hat{\mathcal{J}}_2$ on $\mu^{-1}(\{c\})/\mathsf{G}_c$ that is precisely of the form (3.16) (or, equivalently of the form (3.6)) when using the Monge–Ampère structure $\left(\varpi_2, \alpha_2 - \hat{h}_+\,\mathrm{vol}_{M^2}\right)$. Here, $\hat{h}_+$ is considered to be a function of (x^i, q_i) only, since $\mu^{-1}(\{c\})/\mathsf{G}_c \cong T^*M^2$, with $q_3 = v_3(x^i)$. Note $\alpha_2 - \hat{h}_+\,\mathrm{vol}_{M^2}$ is simply α_2 with $\hat{f}_2$ replaced with $\hat{f}_2 + \hat{h}_+$. Also, whilst ϖ_2 is a symplectic form on T^*M^2, $\alpha_2 - \hat{h}_+\,\mathrm{vol}_{M^2}$ fails to be closed and is degenerate when $\hat{f}_2 + \hat{h}_+ = 0$. Next, we consider (3.7) and set

$$\hat{\mathcal{K}}_2 \;:=\; \sqrt{|\hat{f}_2+\hat{h}_+|}\,\mathring{\nabla} q_i \wedge \mathrm{d}x^i \,. \tag{3.53}$$

Then, as before, $\hat{\mathcal{K}}_2(\hat{\mathcal{J}}_2 X, Y) = -\hat{\mathcal{K}}_2(X, \hat{\mathcal{J}}_2 Y)$ for all vector fields X and Y on $\mu^{-1}(\{c\})/\mathsf{G}_c$ so that $\hat{g}_2(X,Y) := \hat{\mathcal{K}}_2(X, \hat{\mathcal{J}}_2 Y)$ is an almost (para-)Hermitian metric on $\mu^{-1}(\{c\})/\mathsf{G}_c$. Explicitly,

$$\hat{g}_2 \;=\; \frac{1}{2}\left(\hat{f}_2+\hat{h}_+\right)\mathring{g}_{ij}\mathrm{d}x^i \odot \mathrm{d}x^j + \frac{1}{2}\mathring{g}^{ij}\mathring{\nabla} q_i \odot \mathring{\nabla} q_j \,. \tag{3.54}$$

3.5.3. Higher symplectic reduction of the higher Monge–Ampère structure. Let us now discuss the two-plectic reduction of the Monge–Ampère structure (3.12*b*) following theorem 3.6. In particular, by virtue of exactness (3.43), we can take

$$\mu(x,q) \;=\; \star_{\mathring{g}_2}\mathrm{e}^{\varphi}\, q_i \mathrm{d}x^i \tag{3.55}$$

as the moment map which, of course, is defined up to a shift by an exact form. Then, for $\psi \in \mathscr{C}^\infty(M^2)$, it follows the $\mu^{-1}(\{-\mathrm{d}\psi\})$ is non-empty and given by

$$\mu^{-1}\left(\{-\mathrm{d}\psi\}\right) \;=\; \left\{(x,q)\,\middle|\, q_i = -\sqrt{\det(\mathring{g}_2)}\,\mathrm{e}^{-\varphi}\varepsilon_{ij}\mathring{g}^{jk}\partial_k\psi\right\} \,. \tag{3.56}$$

Consequently, the quotient $\mu^{-1}(\{-\mathrm{d}\psi\})/\mathsf{G}_{-\mathrm{d}\psi}$ is locally given by $(x^i, x^3, q_i, q_3) = \left(x^i, \mathrm{const}, -\sqrt{\det(\mathring{g}_2)}\,\mathrm{e}^{-\varphi}\varepsilon_{ij}\mathring{g}^{jk}\partial_k\psi, q_3\right)$. Furthermore, we obtain

$$\varpi_{-\mathrm{d}\psi} \;:=\; \mathrm{e}^{-\varphi}\mathrm{vol}_{M^2} \wedge \mathrm{d}q_3 \tag{3.57}$$

on $\mu^{-1}(\{-\mathrm{d}\psi\})/\mathsf{G}_{-\mathrm{d}\psi}$, which satisfies $\mathfrak{p}^*\varpi_{-\mathrm{d}\psi} = \mathfrak{i}^*\varpi_3$. In addition, whilst the pull-back of ϖ_2' given in (3.42) to $\mu^{-1}(\{-\mathrm{d}\psi\})$ vanishes identically, there is a closed differential two-form $\alpha_{-\mathrm{d}\psi}$ on $\mu^{-1}(\{-\mathrm{d}\psi\})/\mathsf{G}_{-\mathrm{d}\psi}$ given by

$$\alpha_{-\mathrm{d}\psi} \;:=\; \mathrm{e}^{\varphi}\left[\det\left(\mathring{\nabla}^i q_j\right) - \left(\hat{f}_2+\hat{h}_-\right)\right]\Big|_{q_i = -\sqrt{\det(\mathring{g}_2)}\,\mathrm{e}^{-\varphi}\varepsilon_{ij}\mathring{g}^{jk}\partial_k\psi}\mathrm{vol}_{M^2} + \mathrm{e}^{-\varphi}q_3\mathrm{d}q_3 \wedge \star_{\mathring{g}_2}\mathrm{d}\varphi \tag{3.58}$$

and which satisfies $\mathfrak{p}^*\alpha_{-\mathrm{d}\psi} = \mathfrak{i}^*\alpha_2'$. The function $\hat{h}_-$ used here was defined in (3.41*b*). Finally, upon requiring the vanishing of the pull-back of $\alpha_{-\mathrm{d}\psi}$ along

$$\iota : x^i \;\mapsto\; \left(x^i, q_3\right) \;:=\; \left(x^i, v_3\left(x^i\right)\right) \,, \tag{3.59}$$

we obtain the system (3.48) with v_i given by

$$v_i \;=\; -\sqrt{\det(\mathring{g}_2)}\,\mathrm{e}^{-\varphi}\varepsilon_{ij}\mathring{g}^{jk}\partial_k\psi\,. \tag{3.60}$$

Evidently, the first equation of (3.48) can be rewritten as $\mathring{\nabla}^i(\mathrm{e}^{\varphi}v_i)=0$, and by the Poincaré lemma, any solution to $\mathring{\nabla}^i(\mathrm{e}^{\varphi}v_i)=0$ is locally of the form (3.60) for some $\psi\in\mathscr{C}^\infty(M^2)$. Hence, the two-plectic reduction of the Monge–Ampère structure directly yields the two-dimensional fluid flow in terms of the stream function. Indeed, as already indicated, the symplectic reduction provides all of the geometric information that two-plectic reduction does, at least to the extent in which we are interested in this paper, thus enabling the analysis of singularities and curvature scalars as in two-dimensions. However, should one only require a description of the reduced kinematics, k-plectic reduction is certainly a more elegant, compact tool.

Before discussing specific examples, let us close this section by stating that the pull-back of the metric (3.54) along

$$\tilde{\imath}\,:\,x^i\mapsto\left(x^i,q_i,q_3\right)\;:=\;\left(x^i,-\sqrt{\det(\mathring{g}_2)}\,\mathrm{e}^{-\varphi}\varepsilon_{ij}\mathring{g}^{jk}\partial_k\psi,v_3\left(x^j\right)\right) \tag{3.61}$$

given by (3.56) and (3.59), is

$$g_2 \;=\; \frac{1}{2}\left(\mathring{\Delta}_{\mathrm{B}}\psi\mathring{\nabla}_i\partial_j\psi+T_{ij}\right)\mathrm{e}^{-2\varphi}\mathrm{d}x^i\odot\mathrm{d}x^j \tag{3.62a}$$

with

$$\begin{aligned}T_{ij}\;:=\;&\mathring{g}_{ij}\{\mathring{\nabla}^l\varphi\,\partial_l\psi(\mathring{\nabla}^k\varphi\,\partial_k\psi-\mathring{\Delta}_{\mathrm{B}}\psi)-(\mathring{\nabla}^k\varphi\,\partial_k\varphi)(\mathring{\nabla}^l\psi\,\partial_l\psi)\\&+\mathring{\nabla}^k\varphi[\mathring{\nabla}^l\psi\,\mathring{\nabla}_k\partial_l\psi+v_3(\partial_k v_3-v_3\partial_k\varphi)]\}\\&+\partial_i\varphi\,\partial_j\varphi(\mathring{\nabla}^k\psi\,\partial_k\psi)-\mathring{\nabla}^k\psi[\partial_i\varphi\,\mathring{\nabla}_j\partial_k\psi+\partial_j\varphi\,\mathring{\nabla}_i\partial_k\psi]\,.\end{aligned} \tag{3.62b}$$

Evidently, $T_{ij}=0$ when $\varphi=0$, in which case we recover the metric (2.27).

Alternatively, we may write the above formula in such a way that the term $\hat{f}_2+\hat{h}_+$ remains explicit

$$g_2 \;=\; \frac{1}{2}g_{ij}\mathrm{d}x^i\odot\mathrm{d}x^j \tag{3.63a}$$

with

$$\begin{aligned}g_{ij}\;=\;&\tilde{\imath}^*(\hat{f}_2+\hat{h}_+)\mathring{g}_{ij}\\&+\mathrm{e}^{-2\varphi}\{(\mathring{\nabla}^k\partial_i\psi)(\mathring{\nabla}_k\partial_j\psi)+(\partial_i\varphi)(\partial_j\varphi)(\mathring{\nabla}^k\psi)(\partial_k\psi)-2(\partial_k\psi)[(\mathring{\nabla}^k\partial_{(i}\psi)(\partial_{j)}\varphi)]\}\,.\end{aligned} \tag{3.63b}$$

It follows from (3.61) that $\tilde{\imath}^*\hat{f}_2=f_2$ if and only if $\varphi=0$. Again, we note from (3.62a) and (3.62a) that the pull-back metric is a quadratic function of the velocity gradients.

Remark 3.7. Recall that we define

$$\hat{f}_m \;:=\; \frac{1}{2}\left(\mathring{\Delta}_{\mathrm{B}}p+\mathring{R}_{ij}q^i\,q^j\right)\,, \tag{3.64}$$

where the differential operators are taken with respect to the metric $\mathring{g}_m$ and $i,j = 1,2,\ldots,m$, as in (2.23*a*) and (3.12*a*). For fluid flows on three-dimensional background manifolds with warped-product metric (3.38), assuming both $p, v_3 \in \mathscr{C}^\infty(M^2)$, it follows that

$$\hat{f}_3 \;=\; \hat{f}_2 + \hat{h}_+ \,, \tag{3.65}$$

with $\hat{h}_+$ as defined in (3.41*b*). Hence, for three-dimensional flows with symmetry $\frac{\partial}{\partial x^3}$, the function $\hat{f}_2 + \hat{h}_+$ should be interpreted as the diagnostic quantity $\hat{f}_3$, where the former representation highlights the deviation from the diagnostic quantity $\hat{f}_2$ for two-dimensional incompressible fluid flows.

In computing the pull-back of (3.65) along (3.61)[19], similar representations of the traces of the squares of the vorticity two-form and the rate-of-strain tensor (2.11) are also enlightening. Let ζ^m_{ij} and S^m_{ij} respectively denote the vorticity two-form and the rate-of-strain tensor in m dimensions, where $i,j = 1,2,\ldots m$ and the covariant derivatives occurring in (2.11) are understood to be with respect to $\mathring{g}_m$. Then,

$$\zeta^3_{IJ}\zeta_3^{IJ} \;=\; \zeta^2_{ij}\zeta_2^{ij} + \frac{1}{2}\left(\partial_i v_3\right)\left(\mathring{\nabla}^i v_3\right)\mathrm{e}^{-2\varphi} \tag{3.66a}$$

and

$$S^3_{IJ}S_3^{IJ} \;=\; S^2_{ij}S_2^{ij} + \mathrm{e}^{-2\varphi}\left[\frac{1}{2}\left(\partial_i v_3\right)\left(\mathring{\nabla}^i v_3\right) - \left(\partial_i v_3\right)\left(\mathring{\nabla}^i\varphi\right)v_3 + \left(\partial_i\varphi\right)\left(\mathring{\nabla}^i\varphi\right)v_3^2\right] + \left(v_i\mathring{\nabla}^i\varphi\right)^2 \,, \tag{3.66b}$$

where the indices $I,J = 1,2,3$ and $i,j = 1,2$. Like $\hat{f}_2 + \hat{h}_+$, these expressions do not depend on the coordinate x^3, however unlike $\hat{f}_2$, the quantities ζ^2_{ij} and S^2_{ij} retain some dependence on the three-dimensional geometry via φ, since v_i must satisfy (3.48).

Remark 3.8. The reduction presented explicitly in this work assumes a one-dimensional symmetry $\frac{\partial}{\partial x^3}$ of the underlying manifold M^3, dictated by complete x^3 independence of the velocity components. In contrast, by applying the above approach to cases where the symmetry lies in $\mathfrak{X}(T^*M^3)$, flows where $v_3(x)$ depends linearly on x^3 may also be considered. In particular, it was shown in [9] that Burgers' vortex, a flow of the form (3.29) with $W \equiv 0$ and $\phi = \phi(t)$, has a symmetry generated by $\frac{\partial}{\partial x^3} + \phi\frac{\partial}{\partial q_3}$, hence admits a Hamiltonian reduction.

3.6. Examples of higher symplectic reductions

Let us now discuss a few examples of the reduction processes as outlined in section 3.5.

3.6.1. Arnol'd–Beltrami–Childress flow. Let us consider flows on $M_3 := \mathbb{R}^3$ equipped with the standard Euclidean metric

$$\mathring{g}_3 \;:=\; \mathring{g}_2 + \mathrm{d}z\otimes\mathrm{d}z \quad \text{with} \quad \mathring{g}_2 \;:=\; \mathrm{d}x\otimes\mathrm{d}x + \mathrm{d}y\otimes\mathrm{d}y \,, \tag{3.67}$$

which corresponds to the case when $\varphi = 0$. Then, $\hat{h}_\pm = 0$ and our symplectic reduction yields an incompressible fluid flow in two dimensions, on an Euclidean background. In summary, the

[19] This is equivalent to computing (3.24) for flows with symmetry $\frac{\partial}{\partial x^3}$.

equation (3.47) reduce to $\tilde{\varpi}_2 = \varpi_2$, and $\tilde{\alpha}_2 = \alpha_2$, with the divergence-free constraint and the pressure equation (3.48) respectively given by

$$\partial_x v_x + \partial_y v_y \;=\; 0 \tag{3.68a}$$

and

$$\Delta p \;=\; 2\left(\partial_x v_x \partial_y v_y - \partial_x v_y \partial_y v_x\right) \quad \text{with} \quad \Delta \;:=\; \partial_x^2 + \partial_y^2 \,, \tag{3.68b}$$

where v_x and v_y are functions of x and y only.

Additionally, performing the two-plectic reduction to obtain velocity components v_x and v_y satisfying (3.68*a*), in terms of a stream function in two dimensions, yields the same result as applying the Poincaré lemma to (3.68*a*) itself, that is,

$$q_x \;:=\; v_x \;=\; -\partial_y \psi \quad \text{and} \quad q_y \;:=\; v_y \;=\; \partial_x \psi \tag{3.69}$$

for some stream function $\psi = \psi(x,y)$. The corresponding differential form (3.58) is

$$\alpha_{-\mathrm{d}\psi} \;=\; \left[\partial_x^2\psi\,\partial_y^2\psi - \left(\partial_x\partial_y\psi\right)^2 - \frac{1}{2}\Delta p\right] \mathrm{d}x \wedge \mathrm{d}y \,. \tag{3.70}$$

This is unchanged when pulled back along $(x,y) \mapsto (x,y,q_z) := (x,y,v_z(x,y))$, so imposing a vanishing pull-back condition is equivalent to the Monge–Ampère equation

$$\frac{1}{2}\Delta p \;=\; \partial_x^2\psi\,\partial_y^2\psi - \left(\partial_x\partial_y\psi\right)^2 \,, \tag{3.71}$$

which is, in turn, precisely (3.68*b*) with v_x and v_y evaluated as per (3.69). Hence, one is free to choose a pair of z-independent functions ψ and v_z in order to recover an incompressible fluid flow in $\mathbb{R}^3$ that reduces to an incompressible flow on the (x,y)-plane.

Making the choice

$$v_z(x,y) \;=\; \psi(x,y) \;:=\; A\cos(y) + B\sin(x) \tag{3.72}$$

for $A, B \in \mathbb{R}$ some constants, see figure 6(a), and computing (3.69), we recover the velocity field for the integrable case of Arnol'd–Beltrami–Childress flow [67],

$$(v_x, v_y, v_z) \;=\; (\dot{x},\dot{y},\dot{z}) \;=\; \left(A\sin(y), B\cos(x), A\cos(y) + B\sin(x)\right) . \tag{3.73}$$

Next, following [67], upon taking the quotient of v_x and v_y, this system integrates to $v_z = A\cos(y) + B\sin(x) = \text{const}$. Furthermore, (3.71) becomes

$$\hat{f}_2 \;=\; \frac{1}{2}\Delta p \;=\; AB\sin(x)\cos(y) \,, \tag{3.74}$$

and this is displayed in figure 6(b).

Since $\hat{h}_+ = 0$ and $M^2 = \mathbb{R}^2$, it follows that the metric (3.54) on the reduced phase space $\mu^{-1}(\{c\})/\mathsf{G}_c \cong T^*\mathbb{R}^2$ is precisely (2.38). Hence, we may follow exactly the treatment from section 2.3. Therefore, the curvature scalar $\hat{R}_2$ for the metric (3.54) follows directly from (2.39),

$$\hat{R}_2 \;=\; \frac{\sin^2(x) + \cos^2(y)}{AB\sin^3(x)\cos^3(y)} \,, \tag{3.75}$$

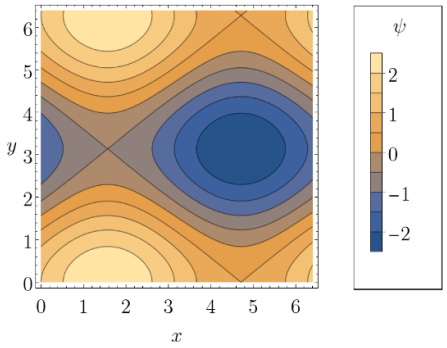

(a) Plot of the streamlines for ψ. The locus $\psi = 0$ defines a shear layer between two homoclinic orbits, corresponding to vanishing vorticity $\zeta := \Delta\psi = -\psi$.

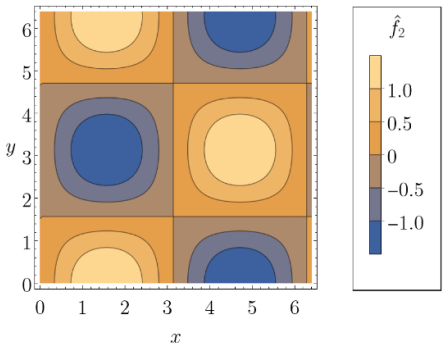

(b) Contour plot for $\hat{f}_2$. The domain is partitioned into squares of side length π, across which the sign of Δp alternates.

Figure 6. Plots of the iso-lines of the stream function (3.72) and reduced Laplacian of pressure (3.74) for an integrable Arnol'd–Beltrami–Childress flow with parameters $A = 1.5$ and $B = 1$.

and as in previous examples, for $\hat{f}_2 \gtrless 0$ the metric $\hat{g}_2$ is Riemannian/Kleinian and the associated curvature is positive/negative. Again, when $\hat{f}_2 = 0$, both the metric and the curvature scalar are singular.

In turn, the pull-back metric (3.62*a*), with v_x and v_y as given in (3.73), is

$$g_2 \;=\; [A\cos(y) + B\sin(x)] \begin{pmatrix} B\sin(x) & 0 \\ 0 & A\cos(y) \end{pmatrix}, \tag{3.76}$$

where the vorticity is $\zeta = -A\cos(y) - B\sin(x)$. This metric is again singular when $\hat{f}_2 = 0$, however it also exhibits a further singularity when $A\cos(y) + B\sin(x) = 0$, which is precisely the shear layer featuring in the streamlines of figure 6(a) and which also corresponds to vanishing vorticity. The curvature scalar R_2 associated with (3.76) is then

$$R_2 \;=\; \frac{B\sin(x)\left[\sin^2(x) + 3\cos^2(y)\right] + A\cos(y)\left[\cos^2(y) + 3\sin^2(x)\right]}{2\sin^2(x)\cos^2(y)\left[B\sin(x) + A\cos(y)\right]^3}\,. \tag{3.77}$$

The lines $x = n\pi$ and $y = \left(n + \frac{1}{2}\right)\pi$ for all $n \in \mathbb{Z}$, along which $f_2 = 0$, are singularities of both the metric g and its curvature R, as was the case for the metric (3.54). Additionally, the presence of $A\cos(y) + B\sin(x)$ in the denominator illustrates that the shear layer is a curvature singularity. See figure 7(b). This curvature singularity arises due to the vanishing vorticity and is otherwise unseen by the pressure criterion. The shear layer is a separatrix between topologically distinct flows and in this case coincides with where the eigenvalues of the pull-back metric (3.76) both change sign, while the signature of the pull-back metric is unchanged. See figure 8.

3.6.2. Hicks–Moffatt vortex. We now discuss another important class of examples—vortices of Hicks–Moffatt type [53, 68]. Consider flows on $M := (\mathbb{R}^+ \times \mathbb{R}) \times_{r^2} S^1$ equipped with

$$\mathring{g}_3 \;:=\; \mathring{g}_2 + r^2 \mathrm{d}\theta \otimes \mathrm{d}\theta \quad \text{with} \quad \mathring{g}_2 \;:=\; \mathrm{d}r \otimes \mathrm{d}r + \mathrm{d}z \otimes \mathrm{d}z\,, \tag{3.78}$$

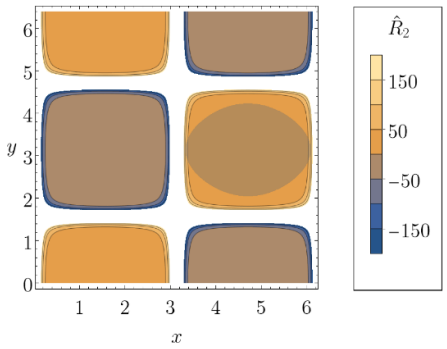

(a) Contour plot for the curvature scalar $\hat{R}_2$. Both $\hat{R}_2$ and $\hat{f}_2$ have the same signs and $\hat{R}_2$ blows up as $\hat{f}_2$ tends to zero.

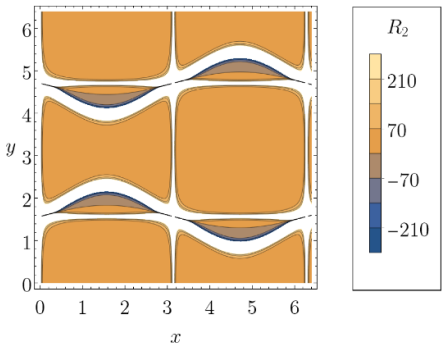

(b) Contour plot for the curvature scalar R_2. Note that curvature singularities occur when $\hat{f}_2 = 0$.

Figure 7. Contour plots of the curvatures (3.75) (left) and (3.77) (right) respectively, for the Arnol'd–Beltrami–Childress flow with parameters $A = 1.5$ and $B = 1$. The ellipse highlighted on the left is the domain bounded by the closed streamline $\psi = -\frac{27}{16}$, which is contained in a region on which the metrics $\hat{g}_2$ and g are Riemannian, and $\hat{f}_2 > 0$.

where $r \in \mathbb{R}^+$, $z \in \mathbb{R}$, and $\theta \in [0, 2\pi)$, that is, standard cylindrical coordinates. Then,

$$\varphi \;=\; \log(r) \quad \text{and} \quad \hat{h}_+ \;=\; \frac{1}{2r}\partial_r p \tag{3.79}$$

with $p = p(r,z)$ in (3.41a). Hence, the equations (3.47) reduce to

$$\begin{aligned} \tilde{\varpi}_2 \;&=\; r\left(\varpi_2 + \frac{1}{r}q_r\,\mathrm{d}r\wedge\mathrm{d}z\right), \\ \tilde{\alpha}_2 \;&=\; r\left\{\alpha_2 - \left[\frac{1}{2r}\partial_r p + \frac{1}{r^2}\left(\frac{1}{r^2}q_\theta^2 - \frac{1}{r}q_\theta\partial_r q_\theta\right)\right]\mathrm{d}r\wedge\mathrm{d}z + \frac{1}{r}q_r\varpi_2\right\}. \end{aligned} \tag{3.80}$$

Furthermore, the requirements that the pull-backs of $\tilde{\varpi}_2$ and $\tilde{\alpha}_2$ under (3.3) vanish become

$$\frac{1}{r}\partial_r(rv_r) + \partial_z v_z \;=\; 0\,, \tag{3.81a}$$

and

$$\frac{1}{r}\partial_r(r\partial_r p) + \partial_z^2 p \;=\; 2\left[\partial_r v_r\partial_z v_z - \partial_r v_z\partial_z v_r - \frac{1}{r^2}v_r^2 - \frac{1}{r^4}\left(v_\theta^2 - \frac{r}{2}\partial_r v_\theta^2\right)\right], \tag{3.81b}$$

which are the equations (3.48) for the metric (3.78), with $v_\theta = v_\theta(r,z)$ arbitrary. Evidently, the first equation is simply the divergence of v for such a v_θ and the left hand side of the second equation is the Laplacian of $p = p(r,z)$, both expressed in cylindrical polar coordinates.

Turning now to the two-plectic reduction, note that we can take the moment map (3.55) to be

$$\mu(x,q) \;=\; rq_r\mathrm{d}z - rq_z\mathrm{d}r\,. \tag{3.82}$$

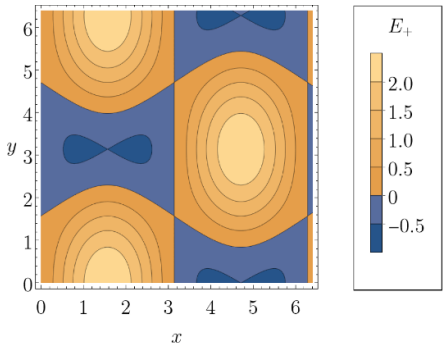

(a) Contour plot for the eigenvalue E_+, which vanishes both along the shear layer and along $x = \pi$.

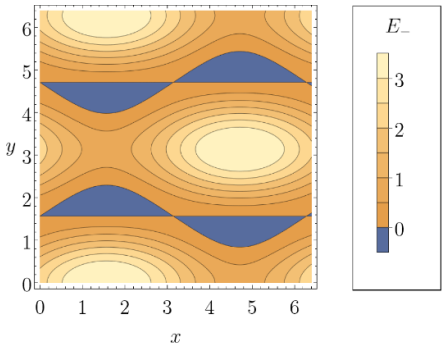

(b) Contour plot for the eigenvalue E_-. In addition to the shear layer, E_- also vanishes along $y = \frac{\pi}{2}$ and $y = \frac{3\pi}{2}$.

Figure 8. Plots of the eigenvalues of the pull-back metric (3.76) with $g_2 = \mathrm{diag}(E_+, E_-)$ of the Arnol'd–Beltrami–Childress flow with parameters $A = 1.5$ and $B = 1$. The signs of both eigenvalues change across the shear layer, where the vorticity prefactor changes sign, hence the signature of the metric is unchanged across this singularity.

It then follows that, locally on $\mu^{-1}(\{-\mathrm{d}\psi\})/\mathsf{G}_{-\mathrm{d}\psi}$, we have

$$q_r := v_r = -\frac{1}{r}\partial_z\psi \quad \text{and} \quad q_z := v_z = \frac{1}{r}\partial_r\psi\,, \tag{3.83}$$

which can be interpreted as expressions for the velocity components in the r and z directions, in terms of a stream function $\psi = \psi(r,z)$ in two dimensions. Consequently, these solve the adapted divergence-free constraint (3.81*a*). In fact, imposing that the pull-back of the closed differential form (3.58) along $(r,z) \mapsto (r,z,q_\theta) := (r,z,v_\theta(r,z))$ vanishes, we find

$$\begin{aligned}\frac{1}{2}\left[\frac{1}{r}\partial_r\left(r\partial_r p\right) + \partial_z^2 p\right] &= \frac{1}{r^2}\left[\partial_r^2\psi\partial_z^2\psi - \left(\partial_r\partial_z\psi\right)^2\right] - \frac{1}{r^4}\left(\partial_z\psi\right)^2 \\ &\quad + \frac{1}{r^3}\left(\partial_z\psi\partial_r\partial_z\psi - \partial_r\psi\partial_z^2\psi\right) - \frac{1}{r^4}\left(v_\theta^2 - \frac{r}{2}\partial_r v_\theta^2\right),\end{aligned} \tag{3.84}$$

that is, (3.81*a*) with v_r and v_z given in terms of ψ as in (3.83). One is free to choose ψ and v_θ, provided they satisfy (3.84). Furthermore, (3.81*a*) is trivially satisfied for any such choices, given (3.83).

In what follows, we fix of ψ and v_θ corresponding to vortices of Hicks–Moffatt type. In particular, we shall discuss a class of spherical vortices with swirl parameter κ, normalising the radius of the sphere to 1 for convenience. For an in-depth review of such vortices, we direct the interested reader to [69].

Firstly, consider a unit sphere in $\mathbb{R}^3$ and set $\sigma(r,z) := \sqrt{r^2+z^2}$ in cylindrical polar coordinates, as above. Fix the angular velocity to be

$$v_{\theta,\kappa}(r,z) = \frac{\kappa\psi}{r}\,, \tag{3.85}$$

on the whole domain. We then fix the stream function on the interior and exterior of the sphere, such that they coincide on the boundary. In particular, on the interior we set

$$\psi_{\text{int},\kappa}(r,z) := \frac{3}{2}r^2\left(b(\kappa) - c(\kappa)\frac{J_{\frac{3}{2}}(\kappa\sigma)}{(\kappa\sigma)^{\frac{3}{2}}}\right), \tag{3.86a}$$

with

$$b(\kappa) := \frac{J_{\frac{3}{2}}(\kappa)}{\kappa J_{\frac{5}{2}}(\kappa)} \quad \text{and} \quad c(\kappa) := \frac{\sqrt{\kappa}}{J_{\frac{5}{2}}(\kappa)}, \tag{3.86b}$$

where $J_n(x)$ is the nth order Bessel function with argument x[20]. See figure 9 for plots of the interior solution. On the exterior of the sphere, one chooses the stream function to be independent of the swirl parameter and to match the interior solution on the boundary of the sphere, given by $\sigma^2 = 1$; for example, we choose

$$\psi_{\text{ext}}(r,z) := \frac{1}{2}r^2\left(1 - \frac{1}{\sigma^3}\right), \tag{3.87}$$

so that the flow far from the sphere is uniform with unit speed directed along the z axis, with non-zero velocity in the θ-direction when $\kappa \neq 0$. It is important to observe that the helicity (3.25) is non-zero if and only if the flow has non-zero swirl [71, 72].

Let us now focus on the limiting case $\kappa = 0$ when the flow has vanishing helicity. This corresponds to Hill's spherical vortex [73]. The θ-component of velocity, (3.85) then becomes $v_{\theta,0}(r,z) = 0$. Firstly, note that for the exterior solution, (3.87) remains the same. Henceforth, we focus our attention on the interior alone. The interior solution, for which the stream function (3.86*a*) is given by

$$\psi_{\text{int},0}(r,z) := \frac{3}{4}r^2\left(r^2 + z^2 - 1\right). \tag{3.88}$$

See figure 10(a).

Upon applying (3.81*a*), we obtain the velocity components

$$v_r = -\frac{3}{2}rz \quad \text{and} \quad v_z = \frac{3}{2}\left(2r^2 + z^2 - 1\right), \tag{3.89}$$

Then, it follows from (3.84) that the Laplacian of pressure is given by

$$\hat{f}_2 + \hat{h}_+ = \frac{1}{2}\left(\partial_r^2 p + \partial_z^2 p + \frac{1}{r}\partial_r p\right) = \frac{9}{4}\left(4r^2 - 3z^2\right). \tag{3.90}$$

See figure 10(b).

The metric (3.54) takes the form

$$\hat{g}_2 = \begin{pmatrix} \left(\hat{f}_2 + \hat{h}_+\right)\mathbb{1}_2 & 0 \\ 0 & \mathbb{1}_2 \end{pmatrix}. \tag{3.91}$$

[20] Such an explicit solution was found in the context of magneto-hydrodynamics [70]. In the context of Navier–Stokes, solutions to this type are also referred to as Hill's spherical vortex with swirl.

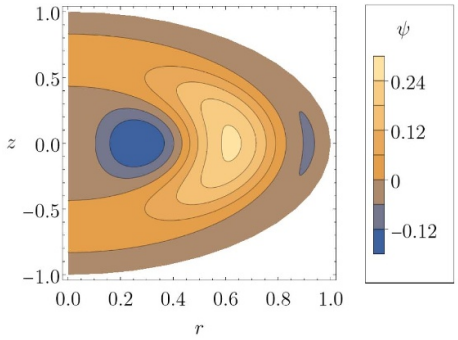

(a) A plot of the streamlines for (3.86). The increased helicity (knotting) of the vortex lines results in layers of closed contours of alternating sign.

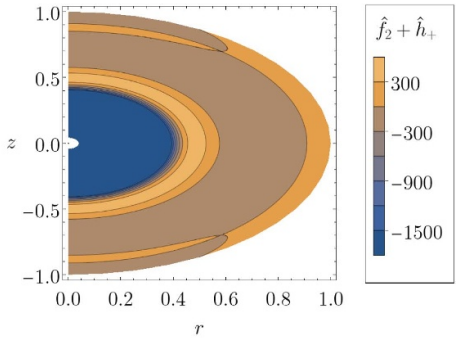

(b) A plot of the Laplacian of pressure function $\hat{f}_2 + \hat{h}_+$, as discussed in Remark 3.7, for the stream function $\psi_{\text{int},10}$.

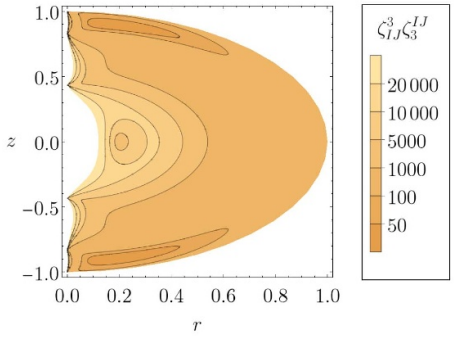

(c) A plot of the iso-lines of (3.66a), for the Hicks–Moffatt vortex with $\kappa = 10$. Note that this quantity is independent of θ.

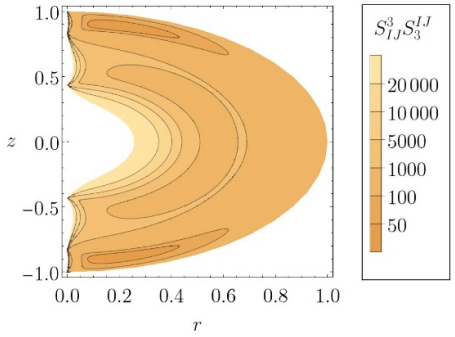

(d) A plot of the iso-lines of (3.66b) for the Hicks–Moffatt vortex with $\kappa = 10$. Note that this quantity is independent of θ.

Figure 9. A selection of plots for the Hicks–Moffatt vortex interior solution with swirl parameter $\kappa = 10$. Since $\hat{f}_3 = \hat{f}_2 + \hat{h}_+$ in this case, the quantity shown in (b) is precisely the difference between those shown in (c) and (d).

and $\hat{R}_2$ is given by (2.39), with f replaced by $\hat{f}_2 + \hat{h}_+$. Namely

$$\hat{R}_2 = \frac{56\left(4r^2 + 3z^2\right)}{9\left(4r^2 - 3z^2\right)^3}, \tag{3.92}$$

which is plotted in figure 11(a). When $4r^2 > 3z^2$, then $\hat{f}_2 + \hat{h}_+ > 0$, the metric is Riemannian, and the curvature scalar is positive. Similarly, the metric is Kleinian and the curvature scalar negative when $\hat{f}_2 + \hat{h}_+ < 0$ and $4r^2 < 3z^2$. Furthermore, the metric is singular when $4r^2 = 3z^2$, that is, when $\hat{f}_2 + \hat{h}_+ = 0$ and it is clear that this singularity is also one for the curvature.

The pull-back metric (3.62*a*) becomes

$$g_2 = \frac{9}{4}\begin{pmatrix} 20r^2 - 2z^2 & 9rz \\ 9rz & 5r^2 + z^2 \end{pmatrix}. \tag{3.93}$$

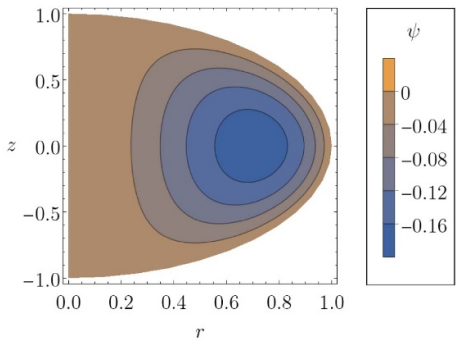

(a) Contours for $\psi_{\text{int},0}$ (3.88). The contours are closed and concentric, forming toroidal vortex tubes when rotated around the z axis to form our three-dimensional flow.

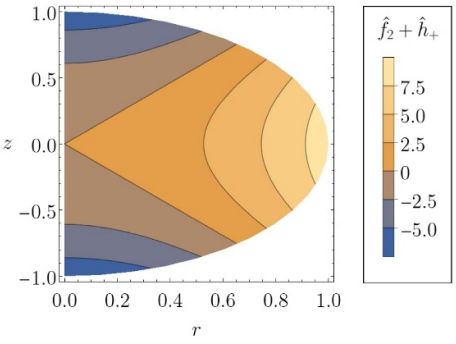

(b) $\hat{f}_2 + \hat{h}_+$ on the interior of the unit sphere, with stream function (3.88). The function vanishes along $4r^2 = 3z^2$, is positive between these curves and negative outside of them.

Figure 10. Plots of the iso-lines of the stream function (3.88) and the function (3.90) respectively, for the interior of Hill's spherical vortex.

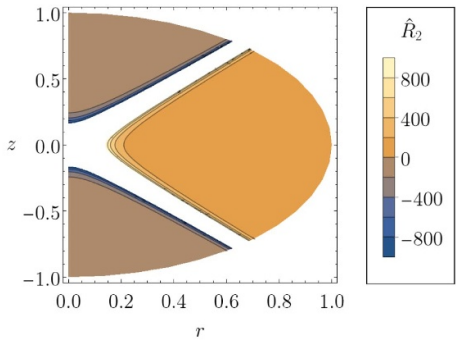

(a) A plot of $\hat{R}_2$ for the stream function (3.88). The curvature decreases in magnitude towards the boundary of the sphere and is singular along $4r^2 = 3z^2$.

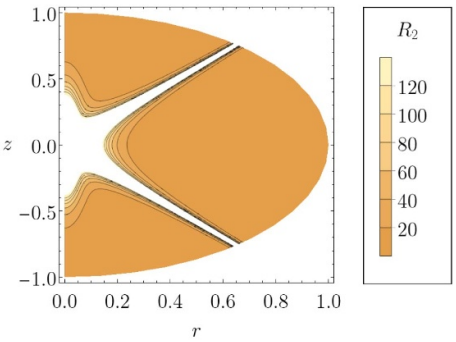

(b) A plot of R_2 for the stream function (3.88). This is singular along $100r^4 - 71r^2z^2 - 2z^4 = 0$ where $E_- = 0$ and hence where the metric g_2 is degenerate.

Figure 11. Contour plots of the curvatures (3.92) (left) and (3.95) (right) respectively, for the interior of Hill's spherical vortex. Note that the curvature singularities in these two plots do not coincide, in contrast to earlier examples.

Its eigenvalues, displayed in figure 12, are given by

$$E_\pm = \frac{9}{8}\left(25r^2 - z^2 \pm 3\sigma\sqrt{(25r^2+z^2)}\right). \tag{3.94}$$

Furthermore, the curvature scalar R_2 associated with (3.93) is

$$R_2 = \frac{28\left(50r^4+z^4\right)}{9\left(100r^4-71r^2z^2-2z^4\right)^2}. \tag{3.95}$$

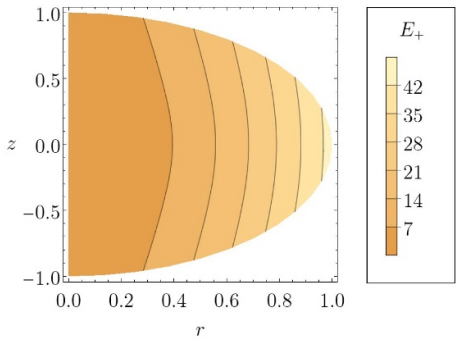

(a) A contour plot for the eigenvalue E_+. This eigenvalue is always positive and increases in magnitude with z. Hence, the signature of g_2 is determined by E_-.

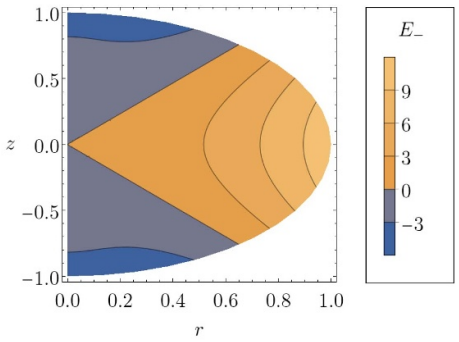

(b) A contour plot for the eigenvalue E_-. This eigenvalue vanishes along $100r^4 - 71r^2z^2 - 2z^4 = 0$, is positive between these lines and negative outside of them.

Figure 12. Plots of the eigenvalues (3.94) of the pull-back metric (3.93) for the interior solution of Hill's spherical vortex.

Both the curvature R_2 and eigenvalue E_+ are non-negative, with E_+ vanishing only at the origin. Additionally, R_2 is singular precisely when E_- vanishes, that is, where the metric is singular. See figure 11(b).

4. Summary and conclusions

We have developed a framework for studying the Poisson equation for the pressure, for incompressible flows, by formulating the concept of higher Monge–Ampère geometry. Earlier work has been revisited and the definition of Monge–Ampère structures extended, using higher symplectic geometry, to facilitate a study of equations in three (or more) independent variables that are not necessarily of explicit Monge–Ampère type.

In contrast to the earlier work, the focal point of our investigations has shifted from the perspective of symplectic geometry to that of Riemannian and Kleinian geometries, as defined by a metric and its pull-back to higher Lagrangian submanifolds. This change of viewpoint has illuminated some seemingly important connections between fluid flows dominated by either vorticity or strain and the geometry of Lagrangian submanifolds. From the examples studied thus far, regions of the flow one might label 'a vortex' are characterised by Monge–Ampère structures with Riemannian metrics, whereas those regions in which strain dominates, are characterised by Kleinian metrics. Where vorticity or strain accumulate, the higher Lagrangian submanifold develops curvature, and the singular behaviour of the pull-back metric and the scalar curvature arising from (1.6) appears to delineate regions of the flow with distinct topological characteristics. Furthermore, where vorticity dominates over the strain, the metric is typically Riemannian with positive curvature scalar.

We have focused on the Ricci scalar curvature, simply because, as an invariant, it is a natural starting point for attempting to identify the salient connections between the characteristics of the fluid flow and the geometry of the Lagrangian submanifolds. However, the Ricci curvature itself may reveal further insights.

We have also noted that there is typically a one-parameter family of metrics, with time t acting as the parameter. The evolution of the metrics, as the parameter t increases, will depend

on whether the evolution of the dynamics is governed by the incompressible Euler or by the incompressible Navier–Stokes equations. It is through such a time evolution that the geometry we have introduced will reflect the differences in the solutions to these two sets of equations. It is therefore intriguing to speculate as to whether Monge–Ampère structures may reveal information on the existence and/or regularity of solutions to the Euler and Navier–Stokes equations, via a notional geometric flow. A connection between Monge–Ampère geometry and optimal transport [74], in terms of a metric whose properties relate to regularity of solutions to Monge–Ampère equations has been made in [46].

Possible future directions include a systematic study of the fully three-dimensional solutions to the Navier–Stokes equations and the associated metrics, with particular emphasis on topological properties of the higher Lagrangian submanifolds that might be characterised by the metrics and their curvature.

A recent companion study to this paper, [33], has also explored the connections between Monge–Ampère structures and the geometry of Lagrangian submanifolds arising in a more conventional application of Monge–Ampère geometry, in which a fully non-linear Monge–Ampère equation lies at the heart of a model used in the study of geophysical flows. Emphasis in that paper is placed on the projection between M and L, and singularities thereof. This is an important issue to follow up in the context of the results presented here.

Data availability statement

No additional research data beyond the data presented and cited in this work are needed to validate the research findings in this work. For the purpose of open access, the authors have applied a Creative Commons Attribution (CC BY) licence to any Author Accepted Manuscript version arising. All data that support the findings of this study are included within the article (and any supplementary files). Data will be available from 31 March 2023.

Acknowledgments

We gratefully acknowledge stimulating conversations with Jonathan Bevan, Thomas Bridges, Roberto D'Onofrio, Jan Gutowski, Giovanni Ortenzi, Christian Saemann, and Paul Skerritt. We are particularly grateful to Jan Gutowski and Paul Skerritt for comments on the first version of this paper. L N was supported by the STFC grant ST/V507118/1. V R thanks IHES for hospitality during the final stage of this work as well as the Centre Henri Lebesgue, Programme ANR-11-LABX-0020-0.

Appendix A. Lagrangian submanifolds

Let M be an m-dimensional manifold and $\pi : T^*M \to M$ its cotangent bundle. We call a submanifold $\iota : L \hookrightarrow T^*M$ locally a section if and only if, for each $y \in L$, there exists a neighbourhood $V_y \subseteq L$ of y, an open and contractible set $U_y \subseteq M$, and a function $\psi_y \in \mathscr{C}^\infty(U_y)$ such that $\iota(V_y) = \mathrm{d}\psi_y(U_y)$. Next, let $U_M \subseteq M$ be open and contractible and let (x^i, q_i) with $i,j,\ldots = 1,\ldots,m$ be local coordinates on $\pi^{-1}(U_M) \subseteq T^*M$ with x^i local coordinates on M and q_i local fibre coordinates, respectively. Consider a Lagrangian submanifold $\iota : L \hookrightarrow T^*M$ with respect to the standard symplectic form $\omega := \mathrm{d}q_i \wedge \mathrm{d}x^i$.

Proposition A.1. *The Lagrangian submanifold L is locally a section $d\psi : U_M \to T^*M$ for some $\psi \in \mathscr{C}^\infty(U_M)$ if and only if $\pi|_L := \pi \circ \iota : L \to M$ is a local diffeomorphism.*

Proof. Suppose that L is locally a section and consider a point $y \in L$. Evidently, V_y and $\iota(V_y)$ are diffeomorphic. Furthermore, as the restriction $\pi|_{\mathrm{d}\psi_y(U_y)}$ is the inverse of $\mathrm{d}\psi_y : U_y \to \mathrm{d}\psi_y(U_y) \subseteq T^*M$, it follows that U_y and $\mathrm{d}\psi_y(U_y)$ are diffeomorphic. As $\mathrm{d}\psi_y(U_y) = \iota(V_y)$, it then follows that U_y and V_y are diffeomorphic, with diffeomorphism given by $\pi|_L|_{V_y} : V_y \to U_y$ and $\iota^{-1} \circ \mathrm{d}\psi_y : U_y \to V_y$. Since this holds for all $y \in L$, it follows that $\pi|_L : L \to M$ is a local diffeomorphism.

Conversely, suppose that $\pi|_L : L \to M$ is a local diffeomorphism and let $y \in L$ be arbitrary. By the local diffeomorphism property of $\pi|_L : L \to M$, there exists a neighbourhood $V_y \subseteq L$ of y such that $\pi|_L(V_y) =: U_y$ is open and contractible in M and $\pi|_L|_{V_y}$ is a diffeomorphism onto its image. Let y^i be local coordinates on V_y. Then, $V_y \ni y^i \overset{\pi|_L}{\mapsto} x^i(y) \in U_y$. Again by the local diffeomorphism properties of $\pi|_L$, we have locally the invertibility of the Jacobian $\frac{\partial x^i}{\partial y^j}$ and the inverse relation $y^i = y^i(x)$. Hence, the embedding $\iota : L \hookrightarrow T^*M$ becomes

$$\iota : y^i \mapsto \big(x^i(y), q_i(y)\big) = \big(x^i, q_i(y(x))\big) =: \big(x^i, p_i(x)\big) \tag{A.1}$$

in local coordinates. Furthermore, since L is Lagrangian with respect to $\omega = \mathrm{d}q_i \wedge \mathrm{d}x^i$, we find

$$\frac{\partial x^i}{\partial y^j}\frac{\partial q_i}{\partial y^k} = \frac{\partial x^i}{\partial y^k}\frac{\partial q_i}{\partial y^j} \tag{A.2}$$

upon computing $\iota^*\omega = 0$.[21] Hence,

$$\begin{aligned}
\frac{\partial x^i}{\partial y^l}\left(\frac{\partial p_j}{\partial x^i} - \frac{\partial p_i}{\partial x^j}\right) &= \frac{\partial x^i}{\partial y^l}\left(\frac{\partial y^k}{\partial x^i}\frac{\partial q_j}{\partial y^k} - \frac{\partial y^k}{\partial x^j}\frac{\partial q_i}{\partial y^k}\right) \\
&= \frac{\partial q_j}{\partial y^l} - \frac{\partial y^k}{\partial x^j}\frac{\partial x^i}{\partial y^l}\frac{\partial q_i}{\partial y^k} \\
&= \frac{\partial q_j}{\partial y^l} - \frac{\partial y^k}{\partial x^j}\frac{\partial x^i}{\partial y^k}\frac{\partial q_i}{\partial y^l} \\
&= \frac{\partial q_j}{\partial y^l} - \frac{\partial q_j}{\partial y^l} \\
&= 0\,.
\end{aligned} \tag{A.3}$$

Therefore,

$$\frac{\partial p_j}{\partial x^i} - \frac{\partial p_i}{\partial x^j} = 0\,, \tag{A.4}$$

that is, the one-form $\eta := p_i \mathrm{d}x^i$ is closed. Consequently, by the Poincaré lemma, there is a function $\psi_y \in \mathscr{C}^\infty(U_y)$ so that $\eta = \mathrm{d}\psi_y$ (and therefore $p_i = \partial_i \psi_y$). It follows that $\mathrm{d}\psi_y(U_y) = \iota(V_y)$. As this holds for any $y \in L$, it follows that L is locally a section. □

When $\pi|_L : L \to M$ is a local diffeomorphism, we may choose coordinates on L so that $\pi|_L$ becomes locally the identity in those coordinates. Put differently, we may take the x^i as local coordinates on L in that case.

[21] Note that $\iota_*\left(\frac{\partial}{\partial y^i}\right) = \frac{\partial x^j}{\partial y^i}\frac{\partial}{\partial x^j} + \frac{\partial q_j}{\partial y^i}\frac{\partial}{\partial q_j}$.

Appendix B. Non-degenerate Monge–Ampère structures

Let (M,ω) be a $2m$-dimensional almost symplectic manifold. Following [28], a differential p-form is called ω-effective if and only if $\omega^{-1}\lrcorner\alpha = 0$. Whenever $p = m$ this is equivalent to requiring $\alpha\wedge\omega = 0$. Then, we have the Hodge–Lepage–Lychagin theorem [28] (see also the text book [8] for a comprehensive treatment):

Theorem B.1. *Let (M,ω) be an almost symplectic manifold. Then, any differential p-form $\alpha\in\Omega^p(M)$ has a unique decomposition*

$$\alpha \;=\; \alpha_0+\alpha_1\wedge\omega+\alpha_2\wedge\omega\wedge\omega+\cdots \tag{B.1}$$

into ω-effective differential $(p-2k)$-forms $\alpha_k\in\Omega^{p-2k}(M)$. Furthermore, if two ω-effective p-forms vanish on the same p-dimensional isotropic submanifolds, they must be proportional.

Let now M be four-dimensional and (ω,α) a Monge–Ampère structure on M, that is, $\alpha\in\Omega^2(M)$ with $\alpha\wedge\omega=0$ and suppose that the Pfaffian $\mathsf{Pf}(\alpha)\in\mathscr{C}^\infty(M)$, defined by $\alpha\wedge\alpha = \mathsf{Pf}(\alpha)\omega\wedge\omega$, is non-zero. We then set [14]

$$\frac{\alpha}{\sqrt{|\mathsf{Pf}(\alpha)|}} =: J_\alpha\lrcorner\omega\ , \tag{B.2}$$

for J_α an endomorphism of the tangent bundle. This yields the identity

$$J_\alpha\lrcorner(\alpha\wedge\omega) = \sqrt{|\mathsf{Pf}(\alpha)|}\left(J_\alpha^2\lrcorner\omega+\frac{\mathsf{Pf}(\alpha)}{|\mathsf{Pf}(\alpha)|}\omega\right)\wedge\omega\ . \tag{B.3}$$

Upon combining this identity with the ω-effectiveness of α and the non-degeneracy of ω, we immediately see that J_α is an almost complex (respectively, para-complex) structure when $\mathsf{Pf}(\alpha)>0$ (respectively, $\mathsf{Pf}(\alpha)<0$). The differential forms ω and $J_\alpha\lrcorner\omega$ define the non-degenerate differential $(2,0)$- and $(0,2)$-forms with respect to J_α. Then, we have the following result:

Proposition B.2. *For J_α as defined in (B.2) there exists a differential $(1,1)$-form K on M such that $K\wedge K\neq 0$, $K\wedge\omega=0$, and $K\wedge(J_\alpha\lrcorner\omega)=0$.*

Proof. Note that ω and $J_\alpha\lrcorner\omega$ are linearly independent. Next, let $\rho\in\Omega^2(M)$ be such that $\{\omega, J_\alpha\lrcorner\omega,\rho\}$ is linearly independent. By theorem B.1, we have a unique decomposition $\rho=\rho_0+\lambda_0\omega$ with $\rho_0\wedge\omega=0$ and $\lambda_0\in\mathscr{C}^\infty(M)$. Since $(J_\alpha\lrcorner\omega)\wedge(J_\alpha\lrcorner\omega)\neq 0$, we may again apply theorem B.1 to obtain the unique decomposition $\rho_0=\rho_1+\lambda_1(J_\alpha\lrcorner\omega)$ with $\lambda_1\in\mathscr{C}^\infty(M)$ such that $\rho_1\wedge(J_\alpha\lrcorner\omega)=0$. Since $(J_\alpha\lrcorner\omega)\wedge\omega=0$, we also have $\rho_1\wedge\omega=0$. Hence, $\{\omega, J_\alpha\lrcorner\omega,\rho_1\}$ is linearly independent, and we must also have that $\rho_1\wedge\rho_1\neq 0$ since the exterior product yields a non-degenerate metric on $\bigwedge^2 T^*M$. In summary, we have thus obtained a $K:=\rho_1$ such that $K\wedge K\neq 0$, $K\wedge\omega=0$, and $K\wedge(J_\alpha\lrcorner\omega)=0$.

Finally, since ω and $J_\alpha\lrcorner\omega$ combine to give non-degenerate differential $(2,0)$- and $(0,2)$-form, $\Omega^{(2,0)}$ and $\Omega^{(0,2)}$, and since $K\wedge\omega=0$ and $K\wedge(J_\alpha\lrcorner\omega)=0$, we conclude that $K\wedge\Omega^{(2,0)}=0$ and $K\wedge\Omega^{(0,2)}=0$. Since $\Omega^{(2,0)}\wedge\Omega^{(0,2)}\neq 0$, K must be of type $(1,1)$ with respect to J_α. □

Appendix C. Connections and curvatures

C.1. Pull-back metric in two dimensions

In what follows, we shall provide some more details on the computation of the Levi–Civita connection and curvature scalar associated with the metric (2.27) from section 2.2. Firstly, recall that using (2.22), the metric (2.27) can be written in the form

$$g_{ij} \;=\; \zeta\tilde{g}_{ij} \quad \text{with} \quad \tilde{g}_{ij} \;=\; \psi_{ij}\,, \tag{C.1}$$

where the indices on $\psi \in \mathscr{C}^{\infty}(M)$ are interpreted via (2.30). As g is, up to a sign, a conformal scaling of the Hessian metric with respect to ψ when $\zeta \neq 0$, we wish to exploit this to write the connection and curvature scalar of g in terms of those for $\tilde{g}$.

C.1.1. Connection. We begin by observing that

$$\mathring{\nabla}_i\psi_{jk} \;=\; \psi_{ijk} + \frac{1}{3}\left(\left[\mathring{\nabla}_i,\mathring{\nabla}_j\right]\psi_k + \left[\mathring{\nabla}_i,\mathring{\nabla}_k\right]\psi_j\right) \;=\; \psi_{ijk} - \frac{1}{3}\left(\mathring{R}_{ijk}{}^{l} + \mathring{R}_{ikj}{}^{l}\right)\psi_l \tag{C.2}$$

and so,

$$\mathring{\nabla}_i\psi_{jk} + \mathring{\nabla}_j\psi_{ik} - \mathring{\nabla}_k\psi_{ij} \;=\; \psi_{ijk} + \frac{4}{3}\mathring{R}_{k(ij)}{}^{l}\psi_l\,. \tag{C.3}$$

Consequently, the Christoffel symbols for $\tilde{g}$ are given by

$$\begin{aligned}\tilde{\Gamma}_{ij}{}^{k} \;&=\; \frac{1}{2}\tilde{g}^{kl}\left(\partial_i\tilde{g}_{jl} + \partial_j\tilde{g}_{il} - \partial_l\tilde{g}_{ij}\right)\\ &=\; \mathring{\Gamma}_{ij}{}^{k} + \frac{1}{2}\tilde{g}^{kl}\left(\mathring{\nabla}_i\psi_{jl} + \mathring{\nabla}_j\psi_{il} - \mathring{\nabla}_l\psi_{ij}\right)\\ &=\; \mathring{\Gamma}_{ij}{}^{k} + \frac{1}{2}\Upsilon_{ijl}\tilde{g}^{lk}\,,\end{aligned} \tag{C.4}$$

where we have used (C.3) and introduced the notation

$$\Upsilon_{ijk} \;:=\; \psi_{ijk} + \frac{4}{3}\mathring{R}_{k(ij)}{}^{l}\psi_l\,. \tag{C.5}$$

This thus verifies (2.32*b*). The Christoffel symbols (2.32*a*) then follow from the usual argument for conformal rescalings (see e.g. [75]).

C.1.2. Curvature. Let us now compute the curvature scalar for (2.27). Firstly, we note that

$$\begin{aligned}\tilde{R}_{ijk}{}^{l} \;&=\; \partial_i\tilde{\Gamma}_{jk}{}^{l} - \partial_j\tilde{\Gamma}_{ik}{}^{l} - \tilde{\Gamma}_{ik}{}^{m}\tilde{\Gamma}_{jm}{}^{l} + \tilde{\Gamma}_{jk}{}^{m}\tilde{\Gamma}_{im}{}^{l}\\ &=\; \mathring{R}_{ijk}{}^{l} + \frac{1}{2}\left(\mathring{\nabla}_i\Upsilon_{jk}{}^{l} - \mathring{\nabla}_j\Upsilon_{ik}{}^{l} - \frac{1}{2}\Upsilon_{ik}{}^{m}\Upsilon_{jm}{}^{l} + \frac{1}{2}\Upsilon_{jk}{}^{m}\Upsilon_{im}{}^{l}\right),\end{aligned} \tag{C.6}$$

where we have used (C.4) and set $\Upsilon_{ij}{}^{k} := \Upsilon_{ijl}\tilde{g}^{lk}$. Next, it is not too difficult to see that

$$\mathring{\nabla}_i\tilde{g}^{jk} \;=\; -\tilde{g}^{jl}\tilde{g}^{km}\left(\psi_{ilm} - \frac{2}{3}\mathring{R}_{i(lm)}{}^{n}\psi_n\right). \tag{C.7}$$

and

$$\mathring{\nabla}_i\psi_{jkl} \;=\; \psi_{ijkl} - 2\mathring{R}_{i(jk}{}^m\psi_{l)m} - \frac{1}{2}\psi_m\mathring{\nabla}_{(j}\mathring{R}_{|i|kl)}{}^m \,. \tag{C.8}$$

Using these two relations, we find that $\Upsilon_{jk}{}^l = \tilde{g}^{lm}\Upsilon_{jkm}$,

$$\begin{aligned}\mathring{\nabla}_i\Upsilon_{jk}{}^l \;=\; &-\tilde{g}^{lr}(\psi_{irs} - \frac{2}{3}\mathring{R}_{i(rs)}{}^n\psi_n)\Upsilon_{jk}{}^s + \frac{4}{3}\tilde{g}^{lm}(\mathring{R}_{m(jk)}{}^n\psi_{in} + \psi_n\mathring{\nabla}_i\mathring{R}_{m(jk)}{}^n)\\ &+\tilde{g}^{lm}(\psi_{ijkm} - \frac{1}{2}\psi_n\mathring{\nabla}_{(j}\mathring{R}_{|i|km)}{}^n - 2\mathring{R}_{i(jk}{}^n\psi_{m)n})\,.\end{aligned} \tag{C.9}$$

Upon substituting this expression and (C.5) into (C.6), the curvature scalar (2.33*b*) then follows directly from the traces $\tilde{R} = \tilde{g}^{ij}\tilde{R}_{kij}{}^k$. Finally, the curvature scalar (2.33*a*) then follows from the usual argument for conformal rescalings (see e.g. [75]).

C.2. Phase space curvature

We now compute the curvature of the metric (2.26). Before we do so, however, let us recap the vielbein formalism as it is more efficient than working in a coordinate basis.

C.2.1. Vielbein formalism. Let (M,g) be an m-dimensional (semi-)Riemannian manifold coordinatised by x^i with $i,j,\ldots = 1,\ldots,m$. Then

$$g \;=\; \frac{1}{2}g_{ij}\mathrm{d}x^i\odot\mathrm{d}x^j \,. \tag{C.10}$$

We denote the vielbeins by $E_a = E_a{}^i\partial_i \in \mathfrak{X}(M)$ for $a,b,\ldots = 1,\ldots,m$, with $(E_a{}^i) \in \mathscr{C}^\infty(M,\mathsf{GL}(m))$. Dually, we have $e^a = \mathrm{d}x^i e_i{}^a \in \Omega^1(M)$, with $(e_i{}^a) \in \mathscr{C}^\infty(M,\mathsf{GL}(m))$, satisfying $E_a \rightharpoonup e^b = \delta_a{}^b$. Consequently, we have

$$E_a{}^i e_i{}^b \;=\; \delta_a{}^b \quad\text{and}\quad e_i{}^a E_a{}^j \;=\; \delta_i^j \,, \tag{C.11}$$

and therefore

$$g \;=\; \frac{1}{2}e^b\odot e^a\eta_{ab} \,, \tag{C.12}$$

with $\eta_{ab} = \mathrm{diag}(-1,\ldots,-1,1,\ldots,1)$.

The structure functions $C_{ab}{}^c \in \mathscr{C}^\infty(M)$ are given by

$$[E_a,E_b] \;=\; C_{ab}{}^cE_c \,, \tag{C.13}$$

or, dually,

$$\mathrm{d}e^a \;=\; \frac{1}{2}e^c\wedge e^bC_{bc}{}^a \,. \tag{C.14}$$

The torsion and curvature two-forms,

$$T^a \;=\; \frac{1}{2}e^c\wedge e^bT_{bc}{}^a \quad\text{and}\quad R_a{}^b \;=\; \frac{1}{2}e^d\wedge e^cR_{cda}{}^b \,, \tag{C.15}$$

are defined by the Cartan structure equations

$$\mathrm{d}e^a - e^b \wedge \omega_b{}^a =: -T^a \quad \text{and} \quad \mathrm{d}\omega_a{}^b - \omega_a{}^c \wedge \omega_c{}^b =: -R_a{}^b \,, \tag{C.16}$$

where $\omega_a{}^b = e^c \omega_{ca}{}^b$ is the connection one-form. The associated Ricci tensor and the curvature scalar are then given by

$$R_{ab} := R_{cab}{}^c \quad \text{and} \quad R := \eta^{ba} R_{ab} \,. \tag{C.17}$$

Furthermore, metric compatibility amounts to requiring

$$\omega_{ab} = -\omega_{ba} \quad \text{with} \quad \omega_{ab} := \omega_a{}^c \eta_{cb} \,. \tag{C.18}$$

Imposing (C.18) and the torsion freeness constraint $T^a = 0$ yields the Levi-Civita connection and a short calculation shows that this connection is given by

$$\omega_{ab}{}^c = \frac{1}{2}\left(C^c{}_{ab} + C^c{}_{ba} + C_{ab}{}^c\right) \tag{C.19}$$

with indices raised and lowered using η_{ab}. In this case, the curvature scalar (C.17) is

$$R = 2E_a C^a{}_b{}^b - C_{ab}{}^b C^a{}_c{}^c - \frac{1}{2} C_{abc} C^{acb} - \frac{1}{4} C_{abc} C^{abc} \,. \tag{C.20}$$

C.2.2. Connection. Let now $(M, \mathring{g})$ be a Riemannian manifold, and consider the metric (3.15) on T^*M now assumed to be in $2m$ dimensions. Furthermore, let

$$\mathring{E}_a := \mathring{E}_a{}^i \frac{\partial}{\partial x^i} \quad \text{and} \quad \mathring{e}^a := \mathrm{d}x^i \mathring{e}_i{}^a \tag{C.21}$$

be the vielbeins and dual vielbeins on $(M, \mathring{g})$ with structure functions $\mathring{C}_{ab}{}^c$, and set

$$\begin{aligned} (\hat{e}^A) &= (\hat{e}^a, \hat{e}_a) := \left(\sqrt{|\hat{f}|}\, \mathrm{d}x^i \mathring{e}_i{}^a, \mathring{E}_a{}^i \mathring{\nabla} q_i\right) , \\ (\hat{\eta}_{AB}) &= \begin{pmatrix} \hat{\eta}_{ab} & \hat{\eta}_a{}^b \\ \hat{\eta}^a{}_b & \hat{\eta}^{ab} \end{pmatrix} := \begin{pmatrix} \operatorname{sgn}\left(\hat{f}\right) \mathbb{1}_m & 0 \\ 0 & \mathbb{1}_m \end{pmatrix} \end{aligned} \tag{C.22}$$

for multi-indices $A, B, \ldots$. Then, the metric (3.15) becomes

$$\hat{g} = \frac{1}{2} \hat{e}^B \odot \hat{e}^A \hat{\eta}_{AB} \,. \tag{C.23}$$

Note that $\mathring{e}_i{}^a$ and $\mathring{E}_a{}^i$ only depend on the base manifold coordinates x^i and not on the fibre coordinates q_i.

Next, dually, we have $\hat{E}_A \lrcorner \hat{e}^B = \delta_A{}^B$ with $(\hat{E}_A) = (\hat{E}_a, \hat{E}^a)$ and

$$\hat{E}_a := \frac{1}{\sqrt{|\hat{f}|}} \mathring{E}_a{}^i \left(\frac{\partial}{\partial x^i} + \mathring{\Gamma}_{ij}{}^k q_k \frac{\partial}{\partial q_j}\right) \quad \text{and} \quad \hat{E}^a := \mathring{e}_i{}^a \frac{\partial}{\partial q_i} \,. \tag{C.24}$$

After a straightforward calculation, we obtain for $[\hat{E}_A, \hat{E}_B] = \hat{C}_{AB}{}^C \hat{E}_C$ the relations

$$\begin{aligned}
[\hat{E}_a, \hat{E}_b] &= \frac{1}{\sqrt{|\hat{f}|}} \mathring{C}_{ab}{}^c \hat{E}_c - \hat{E}_{[a} \log(|\hat{f}|) \hat{E}_{b]} + \frac{1}{|\hat{f}|} \mathring{R}_{abc}{}^d q_d \hat{E}^c \,, \\
[\hat{E}_a, \hat{E}^b] &= \frac{1}{2} \hat{E}^b \log(|\hat{f}|) \hat{E}_a - \frac{1}{\sqrt{|\hat{f}|}} \mathring{\omega}_{ac}{}^b \hat{E}^c \,, \\
[\hat{E}^a, \hat{E}^b] &= 0 \,,
\end{aligned} \tag{C.25}$$

where we have set $q_a := \mathring{E}_a{}^i q_i$ and used the identities

$$\mathring{\omega}_{ab}{}^c = \mathring{E}_a{}^i \mathring{E}_b{}^j \left(\mathring{\Gamma}_{ij}{}^k \mathring{e}_k{}^c - \frac{\partial}{\partial x^i} \mathring{e}_j{}^c \right) \quad \text{and} \quad \mathring{R}_{abc}{}^d = \mathring{E}_a{}^i \mathring{E}_b{}^j \mathring{E}_c{}^k \mathring{R}_{ijk}{}^l \mathring{e}_l{}^d \,. \tag{C.26}$$

Reading off the structure functions $\hat{C}_{AB}{}^C$ from these relations and using the formula (C.19), the Levi-Civita connection $\hat{\omega}_{AB}{}^C$ for the metric (3.15) can be written in terms of the Levi-Civita connection $\mathring{\omega}_{ab}{}^c$ for the background metric $\mathring{g}$ as

$$\hat{\omega}_{AB}{}^C = \frac{1}{2} (\hat{C}^C{}_{AB} + \hat{C}^C{}_{BA} + \hat{C}_{AB}{}^C) \,. \tag{C.27}$$

C.2.3. Curvature. Upon combining (C.25) and (C.27) with (C.20), the curvature scalar of the metric (3.15) is given by

$$\begin{aligned}
\hat{R} = {} & \frac{1}{\hat{f}} \mathring{R} - \frac{1}{4\hat{f}^2} \mathring{R}_{abc}{}^d \mathring{R}^{abce} q_d q_e - (m-1) \hat{\Delta}_{\mathrm{B}} \log(|\hat{f}|) - \delta_{ab} \hat{E}^a \hat{E}^b \log(|\hat{f}|) \\
& + \frac{\mathrm{sgn}(\hat{f})}{4} (m-1)(m-2) \delta^{ab} \hat{E}_a \log(|\hat{f}|) \hat{E}_b \log(|\hat{f}|) \\
& + \frac{1}{4} m(m-3) \delta_{ab} \hat{E}^a \log(|\hat{f}|) \hat{E}^b \log(|\hat{f}|) \,,
\end{aligned} \tag{C.28}$$

where $\hat{\Delta}_{\mathrm{B}}$ is the Beltrami Laplacian for $\hat{g}$. Here, $\mathring{R}_{abc}{}^d$ is the Riemann curvature tensor for the background metric $\mathring{g}$ and $\mathring{R}$ the associated curvature scalar. In our coordinate basis, this becomes

$$\begin{aligned}
\hat{R} = {} & \frac{1}{\hat{f}} \mathring{R} - \frac{1}{4\hat{f}^2} \mathring{R}_{ijk}{}^l \mathring{R}^{ijkm} q_k q_m - (m-1) \hat{\Delta}_{\mathrm{B}} \log(|\hat{f}|) - \mathring{g}_{ij} \frac{\partial^2}{\partial q_i \partial q_j} \log(|\hat{f}|) \\
& + \frac{1}{4\hat{f}} (m-1)(m-2) \mathring{g}^{ij} \left(\frac{\partial}{\partial x^i} + \mathring{\Gamma}_{ik}{}^l q_l \frac{\partial}{\partial q_k} \right) \log(|\hat{f}|) \left(\frac{\partial}{\partial x^j} + \mathring{\Gamma}_{jm}{}^n q_n \frac{\partial}{\partial q_m} \right) \log(|\hat{f}|) \\
& + \frac{1}{4} m(m-3) \mathring{g}_{ij} \frac{\partial}{\partial q_i} \log(|\hat{f}|) \frac{\partial}{\partial q_j} \log(|\hat{f}|) \,,
\end{aligned} \tag{C.29}$$

where we have used (C.24). This verifies (3.22).

Finally, we note that in the case of the flat background metric $\mathring{g}_{ij} = \delta_{ij}$, we have $\hat{f} = f = \frac{1}{2} \Delta p$ with Δ the standard Laplacian on $\mathbb{R}^m$ and so, the formula (C.29) simplifies to

$$\hat{R} = \frac{m-1}{4f^3} [(6-m) \partial_i f \partial^i f - 4f \Delta f] \,. \tag{C.30}$$

References

[1] Gibbon J D 2008 The three-dimensional Euler equations: where do we stand? *Physica* D **237** 1894
[2] Larchevêque M 1990 Equation de Monge–Ampère et écoulements incompressibles bidimensionnels *C. R. Acad. Sci., Paris* II **311** 33
[3] Larchevêque M 1993 Pressure field, vorticity field and coherent structures in two-dimensional incompressible turbulent flows *Theor. Comp. Fluid Dyn.* **5** 215
[4] Weiss J 1991 The dynamics of enstrophy transfer in two-dimensional hydrodynamics *Physica* D **48** 273
[5] Jeong J and Hussian F 1995 On the identification of a vortex *J. Fluid Mech.* **285** 69
[6] Dubief Y and Delcayre F 2000 On coherent-vortex identification in turbulence *J. Turbulence* **1** N11
[7] Roulstone I, Banos B, Gibbon J D and Roubtsov V N 2009 Kähler geometry and Burgers' vortices *Proc. Ukrain. Natl. Acad. Sci.* **16** 303 (arXiv:nlin/0509023)
[8] Kushner A, Lychagin V V and Rubtsov V N 2007 *Contact Geometry and non-Linear Differential Equations* (Cambridge University Press) (https://doi.org/10.1017/CBO9780511735141)
[9] Banos B, Roubtsov V N and Roulstone I 2016 Monge–Ampère structures and the geometry of incompressible flows *J. Phys. A: Math. Theor.* **49** 244003
[10] Roulstone I, Banos B, Gibbon J D and Roubtsov V N 2009 A geometric interpretation of coherent structures in Navier–Stokes flows *Proc. R. Soc.* A **465** 2015
[11] Cantrijn F, Ibort A and De León M 1999 On the geometry of multisymplectic manifolds *J. Austr. Math. Soc.* **66** 303
[12] Baez J C, Hoffnung A E and Rogers C L 2010 Categorified symplectic geometry and the classical string *Commun. Math. Phys.* **293** 701
[13] Rogers C L 2011 Higher symplectic geometry *PhD Thesis* University of California (arXiv:1106.4068)
[14] Lychagin V V, Rubtsov V N and Chekalov I V 1993 A classification of Monge–Ampère equations *Ann. Sci. Ec. Norm. Sup.* **26** 281
[15] Vinogradov A M 1973 Multivalued solutions and a principle of classification of non-linear differential equations *Dokl. Akad. Nauk* **210** 11
[16] Vinogradov A M and Krasil'shchik I S 1975 What is the Hamiltonian formalism? *Uspekhi Mat. Nauk* **30** 173
[17] Vinogradov A M and Kupershmidt B A 1977 The structures of Hamiltonian mechanics *Uspekhi Mat. Nauk* **32** 175
[18] Douady S, Couder Y and Brachet M E 1991 Direct observation of the intermittency of intense vorticity filaments in turbulence *Phys. Rev. Lett.* **67** 983
[19] Moffatt H K, Kida S and Ohkitani K 1994 Stretched vortices – the sinews of turbulence; large-Reynolds-number asymptotics *J. Fluid Mech.* **259** 241
[20] Enciso A and Paralta-Salas D 2015 Knotted vortex lines and vortex tubes in stationary fluid flows *Newslett. Eur. Math. Soc.* **96** 26
[21] Blacker C 2021 Reduction of multisymplectic manifolds *Lett. Math. Phys.* **111** 31
[22] Ebin D G and Marsden J 1970 Groups of diffeomorphisms and the motion of an incompressible fluid *Ann. Math.* **92** 102
[23] Cao C, Rammaha M A and Titi E S 1999 The Navier–Stokes equations on the rotating 2-D sphere: Gevrey regularity and asymptotic degrees of freedom *Z. Angew. Math. Phys.* **50** 341
[24] Kobayashi M H 2008 On the Navier–Stokes equations on manifolds with curvature *J. Eng. Math.* **60** 55
[25] Pierfelice V 2017 The incompressible Navier–Stokes equations on non-compact manifolds *J. Geom. Anal.* **27** 577
[26] Chan C H, Czubak M and Disconzi M M 2017 The formulation of the Navier–Stokes equations on Riemannian manifolds *J. Geom. Phys.* **121** 335
[27] Samavaki M and Tuomela J 2020 Navier–Stokes equations on Riemannian manifolds *J. Geom. Phys.* **148** 103543
[28] Lychagin V V 1979 Contact geometry and non-linear second-order differential equations *Russ. Math. Surv.* **34** 149
[29] Banos B 2002 Non-degenerate Monge–Ampère structures in dimension 6 *Lett. Math. Phys.* **62** 1
[30] Ishikawa G and Machida Y 2006 Extra singularities of geometric solutions to Monge–Ampère equation of three variables RIMS 1502: *Developments of Cartan Geometry and Related Mathematical Problems* (*Research Institute for Mathematical Sciences, Kyoto University, Kyoto,*

Japan, *October 2005*) vol 1502, ed T Morimoto p 41 (available at: https://www.kurims.kyoto-u.ac.jp/~kyodo/kokyuroku/contents/1502.html)
[31] Ishikawa G and Machida Y 2015 Monge–Ampère systems with Lagrangian pairs *SIGMA* **11** 32
[32] Lychagin V V 1985 Singularities of multivalued solutions of nonlinear differential equations and nonlinear phenomena *Acta Appl. Math.* **3** 135
[33] D'Onofrio R, Ortenzi G, Roulstone I and Rubtsov V N 2023 Solutions and singularities of the semigeostrophic equations via the geometry of Lagrangian submanifolds *Proc. R. Soc.* A **479** 20220682
[34] Kruglikov B 1999 Classification of Monge–Ampère equations with two variables *Banach Center Publ.* **50** 179
[35] Rotskoff G 2010 The Gauss–Bonnet theorem *Master Thesis* University of Chicago
[36] Birman G S and Nomizu K 1984 The Gauss–Bonnet theorem for 2-dimensional space-times *Michigan Math. J.* **31** 77
[37] Steller M 2006 A Gauss–Bonnet formula for metrics with varying signature *Z. Anal. Anwend.* **45** 143
[38] Moffatt H K 2001 The topology of scalar fields in 2D and 3D turbulence *IUTAM Symposium on Geometry and Statistics of Turbulence T* Kambe, T Nakano and T Miyuchi (*Fluid Dynamics and its Applications* vol 59)(Springer) p 13
[39] Roulstone I, White A A and Clough S A 2014 Geometric invariants of the horizontal velocity gradient tensor and their dynamics in shallow water flow *Q. J. R. Meteorol. Soc.* **140** 2527
[40] Landau L D and Lifshitz E M 1987 *Fluid Mechanics* (*Course of Theoretical Physics* vol 6) (Pergamon) (https://doi.org/10.1016/C2013-0-03779-1)
[41] Sewell M J 1987 *Maximum and Minimum Principles: A Unified Approach With Applications* (Cambridge University Press) (https://doi.org/10.1017/CBO9780511569234)
[42] Sewell M J and Roulstone I 1994 Families of lift and contact transformations *Proc. R. Soc.* A **447** 1931
[43] Taylor G I and Green A E 1937 Mechanism of the production of small eddies from large ones *Proc. R. Soc.* A **158** 499
[44] Roubtsov V N and Roulstone I 2001 Holomorphic structures in hydrodynamical models of nearly geostrophic flow *Proc. R. Soc.* A **457** 1519
[45] Kossowski M 1992 Prescribing invariants of Lagrangian surfaces *Topology* **31** 337
[46] D'Onofrio R 2023 A note on optimal transport and Monge–Ampère geometry *J. Geom. Phys.* **186** 104771
[47] Hitchin N J 2000 The geometry of three-forms in six dimensions *J. Differ. Geom.* **55** 547
[48] Xu F 2006 SU(3)-structures and special Lagrangian geometries (arXiv:math/0610532)
[49] Xu F 2008 Geometry of SU(3) manifolds *PhD Thesis* Duke University
[50] Wang J and Wang Y 2011 On the geometry of tangent bundles with rescaled metric (arXiv:1104.5584 [math.DG])
[51] Gezer A and Altunbas M 2014 Notes on the rescaled Sasaki type metric on the cotangent bundle *Acta Math. Sci.* **34** 162
[52] Cruceanu V 1993 Une classe de structures géométriques sur le fibré cotangent *Tensor* **53** 196
[53] Moffatt H K 1969 The degree of knottedness of tangled vortex lines *J. Fluid Mech.* **35** 117
[54] Woltjer L 1958 A theorem on force-free magnetic fields *Proc. Natl Acad. Sci.* **44** 489
[55] Moffatt H K and Ricca R L 1992 Helicity and the Călugăreanu invariant *Proc. R. Soc.* A **439** 1906
[56] Ricca R L and Moffatt H K 1992 Helicity of a Knotted Vortex Filament *Topological Aspects of the Dynamics of Fluids and Plasmas H K* Moffatt, G M Zaslavsky, P Comte and M Tabor (*NATO ASI Series* vol 218) (Springer) p 225
[57] Călugăreanu G 1959 L'intégral de Gauss et l'analyse des noeuds tridimensionnels *Rev. Math. Pures Appl.* **4** 5
[58] Călugăreanu G 1961 Sur les classes d'isotopie des noeuds tridimensionnels et leurs invariants *Czech. Math. J.* **11** 588
[59] Whitehead J H C 1947 An expression of Hopf's invariant as an integral *Proc. Natl Acad. Sci.* **33** 117
[60] Liu X and Ricca R L 2012 The Jones polynomial for fluid knots from helicity *J. Phys. A: Math. Theor.* **45** 205501
[61] Lundgren T S 1982 Strained spiral vortex model for turbulent fine structure *Phys. Fluids* **25** 2193
[62] Ohkitani K and Gibbon J D 2000 Numerical study of singularity formulation in a class of Euler and Navier–Stokes flows *Phys. Fluids* **12** 3181

[63] Gibbon J D, Fokas A S and Doering C R 1999 Dynamically stretched vortices as solutions of the 3d Navier–Stokes equations *Physica* D **132** 497
[64] Burgers J M 1948 A mathematical model illustrating the theory of turbulence *Adv. Appl. Mech.* **1** 171
[65] Marsden J and Weinstein A 1974 Reduction of symplectic manifolds with symmetry *Rep. Math. Phys.* **5** 121
[66] Meyer K R 1973 Symmetries and integrals in mechanics *Dyn. Syst.* **5** 259
[67] Dombre T, Frisch U, Greene J M, Hénon M, Mehr A and Soward A 1986 Chaotic streamlines in the ABC flows *J. Fluid Mech.* **31** 353
[68] Hicks W M 1899 Researches in vortex motion—part III: on spiral or gyrostatic vortex aggregates *Phil. Trans. R. Soc.* A **192** 33
[69] Abe K 2022 Existence of vortex rings in Beltrami flows *Commun. Math. Phys.* **391** 873
[70] Prendergast K H 1956 The equilibrium of a self-gravitating incompressible fluid sphere with a magnetic field *Astrophys. J.* **123** 498
[71] Bannikova E Y, Kontorovich V M and Poslavsky S A 2016 Helicity of a toroidal vortex with swirl *J. Exp. Theor. Phys.* **122** 769
[72] Moffatt H K and Tsinober A 1992 Helicity in laminar and turbulent flow *Ann. Rev. Fluid Mech.* **24** 281
[73] Hill M J M 1894 On a spherical vortex *Phil. Trans. R. Soc.* A **185** 185
[74] Kim Y-H, McCann R J and Warren M 2010 Pseudo-Riemannian geometry calibrates optimal transportation *Math. Res. Lett.* **17** 1183
[75] Besse A L 1987 *Einstein Manifolds* (*Classics in Mathematics*) (Springer) (https://doi.org/10.1007/978-3-540-74311-8)